The Preparation and Characterization of PEK/TEOS Glasses by the Sol-Gel Method

by

John Lee W. Noell

Thesis submitted to the Faculty of the

Virginia Polytechnic Institute and State University

in partial fulfillment of the requirements for the degree of

Master of Science

in

Chemical Engineering

APPROVED:

Dr. Garth L. Wilkes, Chairman

Dr. Harry W. Gibson

Dr. William L. Conger

July, 1987

Blacksburg, Virginia

The Preparation and Characterization of PEK/TEOS Glasses by the Sol-Gel Method

by

John Lee W. Noell

Dr. Garth L. Wilkes, Chairman

Chemical Engineering

(ABSTRACT)

Over the last twenty years, substantial emphasis has been placed on the development of a new class of inorganic glasses using the sol-gel approach. This technique utilizes metal alkoxide precursors such as tetraethylorthosilcate (TEOS) to build an inorganic glass matrix out of solution by a two step poly(hydrolysis-condensation) reaction mechanism. The benefits of making ceramics by this method include considerable energy savings due to the lower sintering temperatures required to form the densified glass and the ability to produce multi-component amorphous materials that can not be made through the traditional firing processes. As a result of this last possibility, polymer researchers have sought to develop spin-off hybrid inorganic-organic network systems that can be prepared by the sol-gel method using reactively functionalized oligomers and/or monomers along with the metal alkoxide precursors. These types of organically modified multicomponent glasses could have enormous potential from an applications standpoint because the system's mechanical and physical features can be tailored in accordance to the organic and polymeric materials chosen.

One such inorganic-organic system prepared by this procedure is the new PEK/TEOS glasses. The PEK represents the bisphenol-A polyarylene ether ether ketone thermoplastic polymer endcapped with triethoxysilane functional groups. By mixing the PEK and TEOS components at different weight compositions in the starting sol-gel reaction solution, a notable change in the mechanical properties is observed as the TEOS content is increased for the final thin film glasses. Also, a poor extent of reaction or degree of incorporation of the PEK oligomer is revealed which has been attributed to the vitrification of the glass before the PEK endgroups have a chance to react. To alleviate this problem, thermal treatments are employed to further the sol-gel reaction and to complete the network formation in the PEK/TEOS

glasses. After the thermal treatments, the change in the mechanical and physical properties are monitored, and the data reflects systematic trends in regards to the TEOS content and the temperature of the thermal treatment utilized. In addition to these results, some speculative information is provided on the temperature sensitivity and the rate of curing of the PEK/TEOS glasses during the thermal treatments.

Acknowledgements

The pursuance of the Masters degree in Chemical Engineering has seemed to have progressed through several stages during my graduate career, and I am very grateful to those who helped me along the way. Specifically, I would like to thank Dr. Garth L. Wilkes, my research advisor, for his guidance and professional approach that has allowed my expertise in the polymer field to grow. Furthermore, his investigative strategies and manner of overcoming experimental obstacles has left an invaluable impression on my academic career that will be remembered long into the future. Also, I would like to thank Dr. Dillip Mohanty, a post doctoral fellow in Chemistry, for his help, cooperation, and beneficial advice during the course of my research. To and , I appreciate their taking time to introduce me to the Sol-Gel field and their additional insight on the problems I encountered. I am also grateful to and for teaching me the in's and out's of the GML SCRIPT word processing program on which this document was produced.

Besides those people directly involved in my academic adventure, I would like to thank my parents and grandmother for their support in both my undergraduate and graduate studies. When the times were rough, they were always there to help me emotionally and financially. In addition to my family, I would especially like to thank who has endured as I have through the good and bad times of the masters program and has remained at my side through all.

Lastly, I thank the 3M Corporation for providing the financial funding necessary to make this research project possible.

Table of Contents

List of Illustrations

List of Tables

1.0 Introduction

In the past, the worlds of ceramics and polymer science have grown and developed independently from one another without much overlap between the two areas. Generally, the field of ceramics concerns itself with the preparation of inorganic matrix glass materials through a sintering or firing process while the area of polymers relates to the synthesis, characterization, and processing of linear, nonlinear, and network forming organic high molecular weight molecules. Products of both of these areas have similar and dissimilar features, but on the whole the ceramic materials strongly differ in chemistry and mechanical properties from the organic polymers (still there are a few exceptions). Even though this fact remains evident, advancing science and technology has sought to combine the beneficial physical properties of the polymer and ceramic systems to invent a new class of materials for futuristic applications. Thus, by incorporating the hardness of a ceramic glass and the elasticity of a polymer into one material, the resulting hybrid inorganic-organic network may display the properties of both sciences. For instance, a polymeric glass might be prepared that has good impact resistance , characteristic of certain polymers, and the transparency and scratch resistance of an inorganic glass. Materials of this nature could be much lighter and stronger than the traditional silicate bulk glasses which could be a very important in the future of the automotive industry.

The only shortcoming of this idea which presents a major problem is in order to produce a glass with desirable physical properties, a high temperature sintering process (i.e., $\sim 1300^{0}C$) is required. Temperatures of this magnitude would ,realistically, burn up any organic component in the hybrid glass, and consequently would rule out any hopes of develop-

ing an inorganic-organic network material. However, one new area of research, which was spawned in the ceramics field, has emerged as a viable technique for developing these hybrid systems. The new method has been termed the sol-gel process, and its name refers to the a evolution of a network glass out of solution. The actual reaction mechanism is a two step poly(hydrolysis-condensation) process in which first a metal or silicon alkoxide ($M(OR)_4$ or $Si(OR)_4$) is hydrolyzed to form a $\equiv$M-OH functionality (where M is a metal species) that can subsequently condense in the second step to form a metal network site ($\equiv$M-O-M$\equiv$). In the ceramics area, this technique has generated considerable enthusiasm because of the process's potential to make multicomponent homogeneous glasses out of solution at low temperatures. From a polymer perspective, if an oligomer or polymer can be functionally modified to have sol-gel reactive components located in at least two positions (preferably terminal placement) on the polymer chain, then the organic material can be used as a precursor in the poly(hydrolysis-condensation) reaction as long as the solubility problems of the inorganic and organic species can be overcome. Therefore, this last development offers one possible avenue of systematically obtaining the polymer modified inorganic glasses. The chief advantage and objective of this experimental procedure is that the inorganic-organic materials produced can be tailor made with specific physical properties depending on the nature of the organics employed.

However before this final goal can be achieved, a better understanding of the basic principles of the sol-gel process must be attained through both theoretical and experimental approaches. The characterization of the development of an inorganic network in the solution state of the sol-gel reaction has challenged many scientists working in the field as to how the random growth process proceeds to form the matrix structure. At this point in time, all the researchers agree that a variety of reaction parameters such as the water content, temperature, solution pH, and solvent medium significantly influence the development of the final network structure. For example, under one extreme of conditions a highly condensed network with a particulate nature is formed, while at the other extreme a more linear, lightly branched matrix is produced. Some authors have used chemical arguments and physical models to

explain the development of the drastically different structures in respect to the reaction variables studied. Their desire has been to obtain a more complete understanding of the principles involved in the sol-gel process so that they may be able to predict its structural growth more conclusively. Only then when this point is reached will the development of the polymer modified inorganic system have success on a commercial and industrial scale. In the following pages, one such polymer modified inorganic system is exclusively covered; the reveals some very interesting phenomena that may hopefully in the future help those whose pursue the development of this field further.

2.0 Literature Review

2.1 Introduction

In the past twenty years, many advances have been made concerning the preparation of inorganic glasses by the sol-gel technique. The driving force behind this science stems from its ability to produce low temperature homogeneous gels with multiple compositions and properties that may be used in many different applications. Another important aspect is the relative ease by which these materials can be made. The gelled network glasses, depending on the preparation procedure, may be 'polymeric' in nature as one extreme or colloidal particulates on the other. Sakka and Summino have shown that by altering the reaction recipes that fibers, thin glass sheets, film glasses, and bulk glasses can be obtained with high purity (1-3). In other work done by Yoldas, certain conditions produce gels that are suitable for ceramic precursors which can undergo sintering (4-7).

The basic 'sol-gel' reaction process is described by the poly(hydrolysis-condensation) of a metal alkoxide, $M(OR)_4$, in the presence of water, a host solvent, and a catalyst. A wide variety of metal alkoxides exist with the most commons ones being composed of silicon, titanium, aluminum, boron, and zirconium. The R group of the alkoxide is preferably a methyl, ethyl or isopropyl functionality. Generally when the sol-gel chemistry is used in conjunction with an inorganic or organic species, a silicon alkoxide in the form of tetraethyl orthosilicate (TEOS, $Si(OEt)_4$) is the primary constituent employed, and the following discussion is centered

around its use in this area. The reaction of the silicon alkoxide precursor proceeds by a two step reaction mechanism consisting of a hydrolysis step first and secondly a condensation or a dehydration reaction (8).

$$nSi(OR)_4 + 4nH_2O \overset{cat.}{\rightarrow} nSi(OH)_4 + 4nROH \qquad [2.1]$$

$$nSi(OH)_4 \overset{cat.}{\rightarrow} (SiO_2)_n + 2nH_2O \qquad [2.2]$$

The poly(hydrolysis condesation) reaction results on near completion in the formation of an oxide network via a chemical polymerization that is similar to quartz (4).

During the gelation process, many of the physical properties associated with the glasses may be determined. According to Aelion, the extents of the reaction of (2.1) and (2.2) are a strong determinant in the final properties of the glass (8). A glass with unhydrolyzed R groups can inhibit the condensation reaction and a more linear or polymeric structure develops. The actual kinetic effects on the final product throughout the course of the reaction cannot so simply be explained by the preceding example. More often, the final product properties are explained in terms of the relative rates and the extents of the hydrolysis and condensation mechanisms. The rates shown by Brinker and co-workers are dependent on the reactant concentrations of TEOS and water, and the solution pH (9-10). In brief, a relatively slow hydrolysis in comparison with the condensation reaction promotes the silicon alkoxide to polymerize in an extended linear fashion whereas in a fast hydrolysis and a slow condensation situation a more condensed species is formed.

Optimally, the relative rates of the hydrolysis and condensation reaction can be manipulated through various reaction parameters. Yoldas has suggested that the final product formation can be altered through the H_2O/TEOS ratio, catalyst type and its concentration, hydrolysis medium (solvent), dilution ratio, and temperature of the reaction (4). The H_2O/TEOS ratio and the catalyst are the strongest factors affecting the sol-gel reaction while the tem-

perature and solvent type produce only secondary effects (8). By fixing the experimental conditions appropriately, the final gel structure can be modified for use in various applications. For example, Pouxviel developed three different experimental outlines designed for specific applications (11). (1) The first experimental procedure slows the hydrolysis reaction down by restricting the availability of water to form polymeric glasses that have potential applications as coatings and/or fibers. (2) Secondly through a partial hydrolysis or 'prehydrolysis' of different alkoxide components and subsequent mixing, a multicomponent glass can be made without the presence of microheterogeneities. (3) Third, a starting mixture can be rapidly hydrolyzed by an excess of water to prepare gel precursors for ceramic sintering processes.

Another avenue of current interest is the modification of inorganic sol-gel networks by the addition of organic species. A variety of authors such as Mark et al. (12-15), Schmidt and coworkers (16-19), and Wilkes et al. (20-22) have taken this approach and have produced new materials. Schmidt, a front runner in the area, has developed a material that is composed of a silicon-titanium matrix with methacrylate organic bridges randomly dispersed within the network. This material has been expected to possibly have considerable promise in the contact lens area. Meanwhile, Mark and Wilkes have both been working with poly(dimethylsiloxane) oligomers and have incorporated these components into a TEOS based network through the sol-gel mechanism to achieve a rubber modified glass. Even though Wilkes and Mark have used similar materials, their experimental approaches are significantly different. The field of organically modified silicates, termed 'Ormosils' by Schmidt, has sparked widespread interest in the scientific community because of its enormous commercial potential (16). This innovative approach eventually may lead to development of glasses with specific properties which can be tailored according to the organics present.

In the remainder of this review, the topics that have been briefly outlined are discussed in more detail. The first subject is based on the kinetics of the sol-gel reaction using the TEOS precursor. Both structural and chemical aspects through the use of models are surveyed and the results provide a strong insight of how the growth of the network evolves. Secondly, the author focuses on how the kinetics of the reaction are shaped through the effects of the H_2O/

silicon alkoxide ratio (R), pH of the system, solvent medium, and temperature and gel time. Once this background has been established, specific reaction conditions can be used to develop desired product properties that can be applied to certain applications. Finally, experimental approaches are reviewed on the synthesis of organically modified inorganic networks using polymeric and oligomeric species.

2.2 *Reaction Kinetics*

2.2.1 Overview

In the development of a network glass through the sol-gel reaction mechanism, the overall structure is determined by the kinetic effects on both the hydrolysis and condensation steps. As mentioned earlier, the relative rates of these reactions in comparison with another and their extents have a controlling effect on the connectivity of the ≡Si-O-Si≡ matrix. Gels prepared under conditions where the hydrolsis is slow with respect to the condensation exhibit extremely fine features, experience large shrinkage, and dry to a high bulk density. In situations where the hydrolysis is fast with respect to the condensation, the gels are particulate and dry to a low bulk density without large sample shrinkage (10). These two extreme cases can be used as guidelines for developing experimental criteria even though under certain conditions these rules do not always hold true.

The evolution of a ≡Si-O-Si≡ network has been suggested to develop along one of two lines. Kelts and co-workers believe that the formation of the network occurs either by (1) the production of linear oligomers that connect through branching and networking or by (2) the formations of cyclic oligomers which are incorporated into the network as the glass approaches the gel point (23). The most consistent interpretation follows the linear growth model and has found substantial backing in the literature. Yoldas supports this representation with

his 'growth' and 'recombination' model (5). In the first step, monomers grow to form dimers and trimers (monomer-cluster growth), and then in second step the larger clusters combine to form large network molecules at the expense of the smaller clusters (cluster-cluster growth). Experimental work using gel permeation chromatography (GPC) reveals a bimodal distribution of molecular sizes in the later stages of the reaction which tends to further support the model (5). Although the cyclic mechanism is not as popular, it is probable under certain conditions. Brinker has concluded that in a reaction in which the condensation is rapid compared to hydrolysis, polysiloxane three and four membered rings can be formed (9). Pouxviel further characterized this process through nuclear magnetic resonance (NMR) studies showing that the hydrolyzed monomers and dimers led to trimer and tetramer cyclics in the early stages of the condensation reaction.

The rates of the condensation and hydrolysis steps ultimately depend on the concentration of Si-OH groups present on the monomer and/or oligomeric components. For both reactions, the rate constants are higher when the intermediate species have a larger number of Si-OH present (11). In the hydrolysis reaction, the removal of the first R group is the slowest compared to the remaining groups as long as the monomer remains unattached and their is sufficient water water present (i.e., > 100%). For example, the rates constants of k_1, k_2, k_3, and k_4 in a TEOS acid catalyzed hydrolysis (pH $\cong$2.5) have the following ratios of 1:5:12:5 (11).

$$Si(OEt)_4 + H_2O \xrightarrow{k_1} HOSi(OEt)_3 + EtOH \qquad [2.3]$$

$$(HO)Si(OEt)_3 + H_2O \xrightarrow{k_2} (HO)_2Si(OEt)_2 + EtOH \qquad [2.4]$$

$$(HO)_2Si(OEt)_2 + H_2O \xrightarrow{k_3} (HO)_3Si(OEt) + EtOH \qquad [2.5]$$

$$(HO)_3Si(OEt) + H_2O \xrightarrow{k_4} Si(OH)_4 + EtOH \qquad [2.6]$$

If the monomer attaches to another monomer or oligomer before the completion of hydrolysis, then the hydrolysis rate may increase or decrease depending on the catalyst type. Total hydrolysis of $Si(OEt)_4$ to $Si(OH)_4$ requires that interaction with any other species during the course of the reaction be precluded. NMR results of a TEOS hydrolysis reveal that in the initial stages of the polymerization that $Si(OEt)_4$, $(HO)Si(OEt)_3$, and $Si(OH)_4$ are the predominant species present (11). High concentrations of $Si(OEt)_4$ and $Si(OH)_4$ show that once the hydrolysis is initiated, the extent of reaction normally proceeds to greater than 75% or more as long as condensation has not occurred. Another factor that can affect the rate of hydrolysis is the size of the alkyl R groups. As the size of the alkyl group increases, the overall rate of hydrolysis decreases chiefly due to steric considerations (ie methyl > ethyl > propyl > etc.)

Since hydrolysis precedes the condensation mechanism, the extent of the first reaction step has a strong influence on the degree of network formation achieved. Under any conditions, the hydrolysis product contains a mixture of various polymeric structures (monomers, dimers, trimers, etc.) whose random statistical interactions during condensation shape the final glass structure (6). Generally, growth of the network during the condensation sequence occurs by the formation of ≡Si-O-Si≡ bridging bonds at the expense of Si-OH and Si-OR functionalities. The presence of the intermediate Si-OH groups tends to accelerate the condensation rates in comparison with Si-OR species (11). Therefore, the degree of network formation of the glass is inversely related to the residual amounts of the silanol and alkoxy groups present. Furthermore, Kelts and co-workers using the NMR technique have revealed that the condensation reaction continues long after gelation to give a more tetrasubstituted network (23).

Up to this point, the kinetics of the poly(hydrolysis-condensation) reaction have been discussed in terms of only the relatives rates of each reaction and their extents, but nothing has been said on what causes these effects. A survey of the literature shows that the H_2O

/TEOS ratio (R), solution pH or catalyst type, solvent medium and dilution ratio, and temperature all have a strong influence on the rates and the extent of the hydrolysis and condensation mechanisms. Much thought has been expressed on what factors cause the most dramatic changes in the kinetics of these reactions, but it remains to be seen which one factor has the most significant effect.

2.2.2 Reaction Models

Before the actual chemistry of the polymerization of silicon alkoxide is discussed, it is informative to approach the subject from a structural standpoint using growth models. Keefer and co-workers, who are largely responsible for this type of analogy, have suggested several different growth processes that can predict some of the polymerization behavior of the sol-gel technique (24). They divided these processes into two areas. The first area suggests that in the early stages of the reaction the growth occurs through either monomer-cluster or cluster-cluster interactions while the second area refers to the later stages where growth may proceed by a reaction limited versus a diffusion limited behavior (24).

Furthermore, Keefer and co-workers (24) have concluded that the polymerization of silica can be described by fractal geometry in some cases. A fractal object is an object that has dilation symmetry which means the object has self-similarity on many length scales. In simple terms, if an object is looked at over several increasing magnifications and the structural appearance remains the same at each stopping point, then the object has a fractal nature. The dimensionality of the fractal objects is consistent with the common dimensional relation, $M \sim R^D$ where M is representative of the molecular weight or mass, R the radius of the object, and D the fractal dimension. The fractal dimension is often a non integer value, and its magnitude may be interpreted using the following guidelines. Interger dimensions of 1, 2, and 3 correspond to the shapes of a compact rod, disc, and sphere respectively. Thus, fractal objects with dimensions existing between two of the boundary objects may be described as having

characteristics of both shapes. In short, objects that conform to the $M \sim R^D$ relationship (which may have non-interger values) have been termed mass fractals as long as $D \leq 3$ (see Figure 1).

By using scattering techniques (small angle X-ray scattering (SAXS) is the most common) during the course of the polymerization, the dimensionality of the fractal structure evolving can be found by monitoring the scattering intensity as a function of the scattering angle (θ). The weak scattering limit of a SAXS experiment for a mass fractal object yields an intensity distribution which is power law.

$$I(K) \sim K^{-D} \qquad [2.7]$$

The D corresponds to the dimensionality and the K is related to the radial scattering angle, θ, through the following relation.(24)

$$K = (4\pi/\lambda) \sin(\theta/2) \qquad [2.8]$$

Also K is inversely related to the spatial correlation. That is, at larger K smaller length scales are probed and vice versa. The low angle region of the scattering curves (where $K << R_g^{-1}$), the Guinier region, reveals information on the mean radius of gyration, R_g , while between the region of $KR_g >> 1$ and $Ka << 1$ (where a is the size of the silica monomer) can predict the dimensionality of the fractal (10). This last region is usually referred to as the intermediate or Porod region.

The utility of the scattering experiment lies in its ability to monitor the dimensionality of the growth process with time and to establish particle sizes at each point. By plotting a log-log plot of the scattered intensity, I(K), versus the scattering vector, K, the slope in the Porod region represents the dimensionality of the structure. A slope of -2 corresponds to a random walk polymer chain or a randomly branched chain, and a slope of -4 signifies a particle with sharp and well defined boundaries (9). At slopes less than -3, the scattering objects have

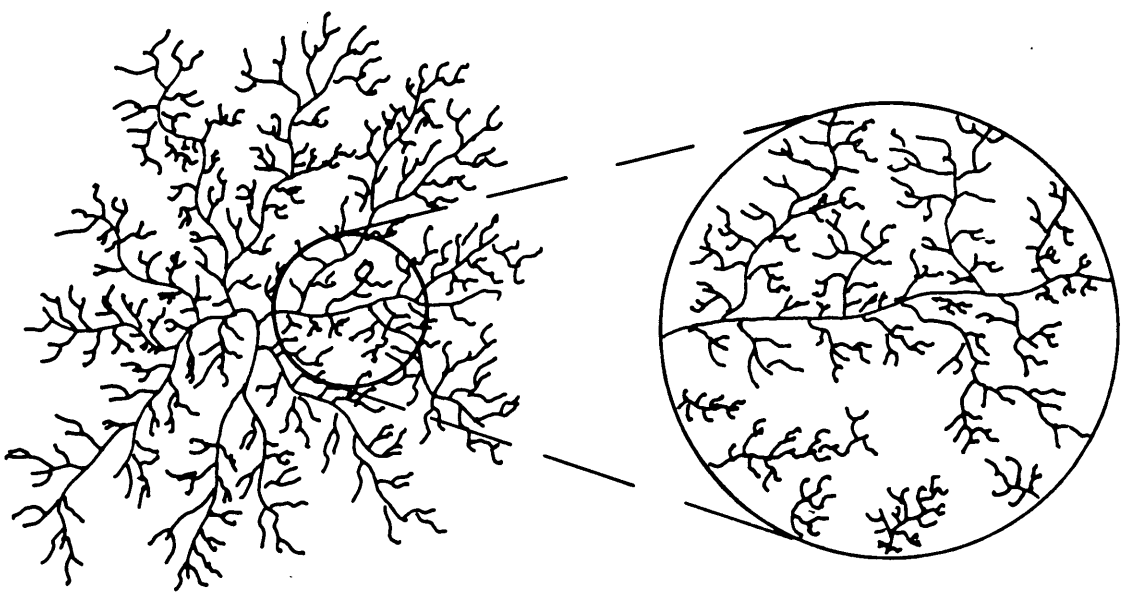

$$M \sim R^{D}$$

$$I \sim K^{-D}$$

Figure 1. Schematic representation of a mass fractal.

distinct surfaces that coincide with the fractal relationship and have dilational symmetry. Objects that fall into this category are called surface fractals, and the surface area follows the mathematic relation of $S \sim R^{Ds}$, where S is a measure of length and Ds is the surface fractal dimension (see Figure 2) (24). Ds ranges between 2 and 3 with 2 representing a Euclidian three dimensional object since the surface of a 3-D object is two dimensional (24).

The scattering curve for the surface fractal shown by Keefer and Schaefer corresponds to the following relation (24).

$$I(K) \sim K^{Ds-6} \qquad [2.9]$$

When the log-log relationship is applied to the Porod region, slopes between -3 and -4 can be expected. Objects with smooth surfaces yield slopes of -4 (Porods law) while the slopes of fractally rough surfaces are found between -3 and -4. At slopes less than -4, the objects are either sub-fractal or have a broad interface (24). However, Craevich has noted that the SAXS method suffers from an inherent ambiguity since Keefer et al. have claimed that the surface fractal's dimension lies between $2 \leq Ds \leq 3$ and for $D=2$ and $D=3$, the limiting cases, the situation reduces to Porods law (25). If this is true, then the scattering method is incapable of distinguishing between a classic smooth surface and a fractal surface with $D=3$ at the limiting cases (25). This last artifact may produce some complicated arguments, but overall the fractal approach provides a fairly consistent means of monitoring the growth process of fractal objects such as in a silica polymerization whether it be a mass or surface fractal.

Now that the topic of fractal geometry has been covered, the next step is to use this theory to distinguish between the various growth models. The first model is based on the nucleation and growth concept in which molecules grow from point sources to form compact structures. These structures tend to have a Porod slope of -4. Schaefer and co-workers have termed this manner of growth as 'Eden Growth' (24). This type of growth occurs when a particle is nucleated from a seed, and the monomers grow from this point until all vacant sites are filled. Characteristics of Eden grown objects are that they have smooth surfaces relative

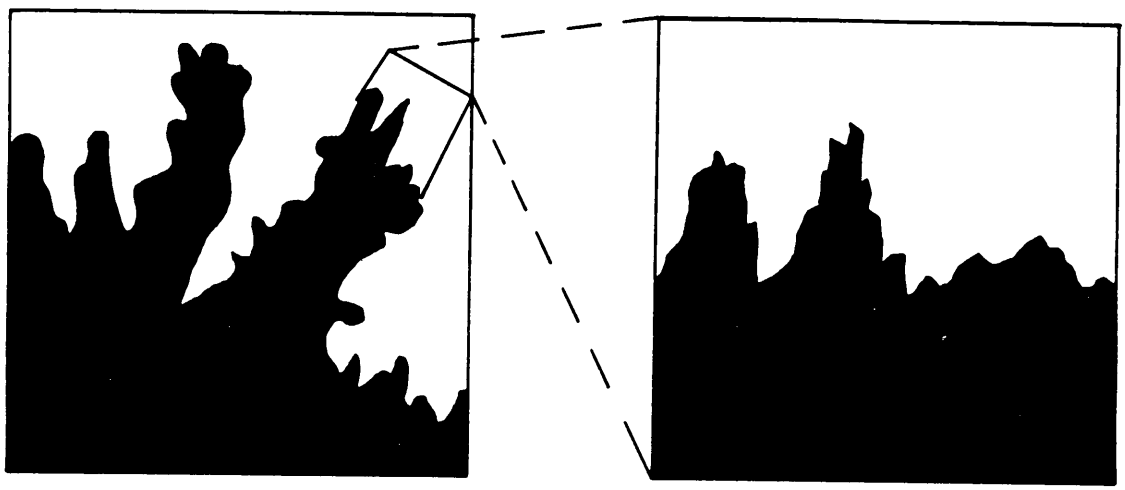

$$S \sim K^{Ds}$$

$$I \sim K^{Ds-6}$$

Figure 2. Schmatic representation of surface fractal.

to their radius and the interiors are uniform (24). Growth by the Eden model produces partilces with compact clusters.

Eden type growth is expected when (1) growth occurs from monomers, and (2) the functionallity of the momomer is large. This growth pattern falls into the category of monomer-cluster growth which results in a high degree of internal condensation. One conditions that promotes Eden growth is the base catalyzed polymerization of silicic acid ($Si(OH)_4$). Keefer has suggested that this reaction proceeds by a S_N2 nucleophilic substitution mechanism in which one of the reacting species undergoes an inversion (24). Since the adding monomer is the only monomer that can invert easily, monomer-cluster growth is favorable while cluster-cluster interactions are inhibited because of the apparent problem of inverting a large species. Thus Eden type growth always builds particles with compact cores, but sometimes ,however, they may not have smooth surfaces.

The case in which Eden growth is observed, but fractally rough surfaces are obtained, can be explained according to the poisoned Eden model. The only important modification of this model in comparison with the previous Eden model is that the momomer functionallity is not constant (24). That is, growth can occur through tetra-, tri-, and difunctional monomers. This model seems more plausible since steric considerations and incomplete hydrolysis of a TEOS precursor may poison the reaction of some active sites between the monomer and the cluster. The net result of this method of growth is a particle with a uniform core and a fractally rough surface that has a value for Ds between 2 and 3.

In the event of cluster-cluster growth, the percolation model provides a simple representation of a development of the silica network with a more ramified structure. Percolation growth starts with a seed located at one site on a lattice and propagates by randomly picking growth sites with a probability p on the surrounding perimeter of the newly born seed. After the selection of the growth sites around the seed, all non-growth sites on the perimeter are dead forever and all growth sites are filled (24). In the following stages, a new perimeter is defined after each growth process as the cluster plus dead sites where further random growth occurs with a probability p through the new neighboring growth sites. This process continues

until all growth sites are occupied. If percolation growth occurs with a probability of $p < p_c$ where p_c is the percolation threshold at which infinite growth is achieved, then the percolation cluster's growth is terminated at some point because of the unavailability of growth sites. In the case of $p > p_c$, the percolation growth can continue forever and this results in the growth of large clusters. At $p = p_c$, a percolation cluster is formed that has fractal dimension of 2.5, while below the percolation threshold large clusters called lattice animals are sometimes found having a fractal dimension of 2.0 (24).

The general difference occurring between percolation and Eden growth is that percolation can generate ramified polymeric structures in which growth from monomers is precluded. Furthermore, percolation primarily proceeds by cluster-cluster interactions. In particular, Keefer has shown that in the later states of an acid catalyzed polymerization of TEOS the scattering data reveals a fractal dimension of 2.0 which suggests a more branched structure and a percolation type growth (24). Another difference between the two models is that in percolation for a lattice animal (a large cluster formed at just below $p = p_c$), the final structure can be one of many configurations since all isomers of the same mass are equally probable. In the Eden case, the probability of attaining a specific structure is not dependent on the isomeric considerations, but only the number of events leading up to the final structure (see Figure 3).

Realistically, the polymerization of silica may posses characteristics of both monomer-cluster and cluster-cluster growth during different stages of the reaction. Also these specific reaction schemes may be further altered by reaction limited and diffusion limited situations. For example in an acid catalyzed reaction where the hydrolysis reaction is rapid, the initial stages of the polymerization promote growth from monomers to form clusters. At the later stages however, the monomer-cluster growth pattern is inhibited because of the removal of all monomers, and the final polymerization proceeds by cluster-cluster interactions. Keefer and co-workers have pointed out this complexity using scattering experiments (24). At the smaller length scales, the SAXS data yield Porod slopes consistent with the Eden model while at larger scales the slopes changes to fit the percolation model. In the final growth stages,

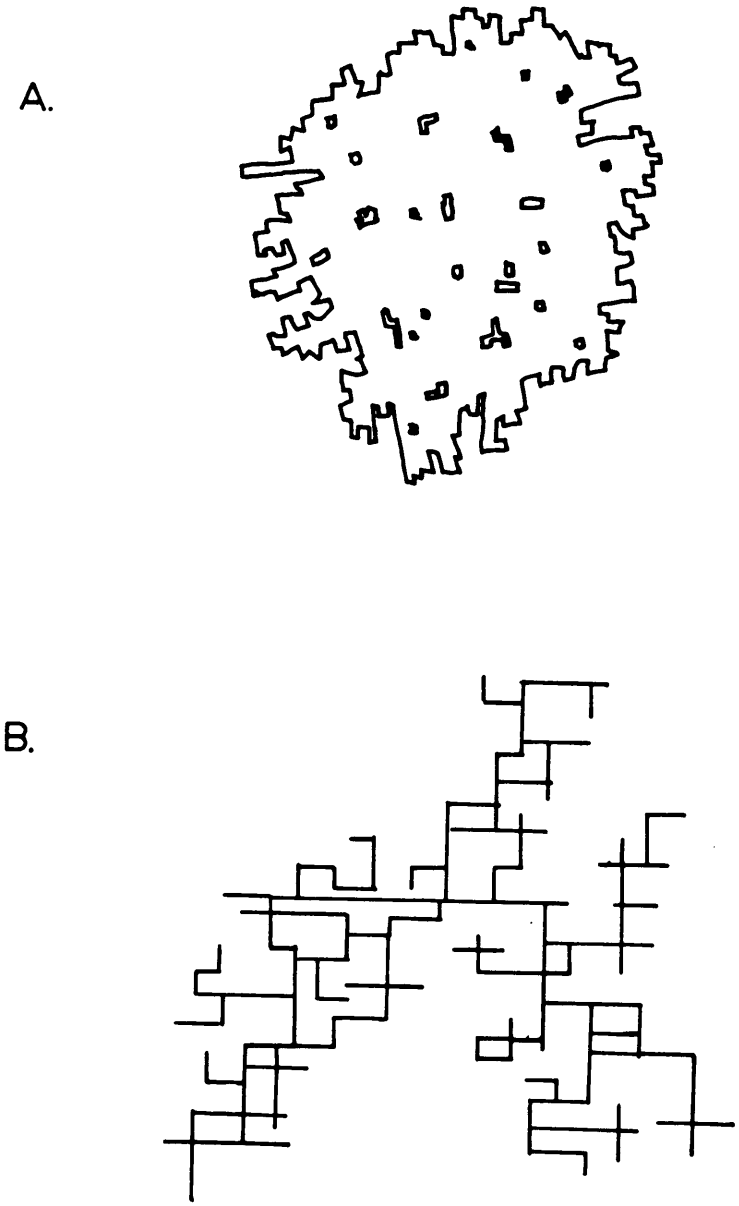

Figure 3. Comparison of Eden and Percolation models: (a) Eden model; (b) Percolation model.

reaction limited versus diffusion limited reaction can alter the final fractal dimension of the silica network. In a reaction limited case in which steric restrictions are a factor in the cluster-cluster interactions, a percolation structure similar to a lattice animal with a fractal dimension of 2 is expected. On the other hand, the diffusion limited situation in which the reactions are exceedingly rapid may have diffusion problems in the later stages and a slightly lower fractal dimension of 1.7 develops (26,27).

Even though the growth models of monomer-cluster and cluster-cluster growth have many shortcomings in predicting the exact polymerization structure of a silica network, the theoretical framework is very helpful when considering the effect of certain reaction conditions on the dimensionality of the structure. These models offer a tangible representation in some instances of the actual chemistry involved.

2.2.3 pH Dependence

In a sol-gel reaction using a silicone alkoxy precursor, the pH and/or catalyst type strongly affects the kinetics of the hydrolysis and condensation reactions. The net result is that different gel structures are obtained depending whether the reaction is catalyzed by an acid or base. Aelion ,back as early as the 1950's, was one of the first authors to report this unique effect (8). The physical difference between the two systems is revealed in their respective structures. The acid catalyzed system forms a gel with extended polymeric chains that are weakly crosslinked, whereas the base system develops gels that are composed of highly compact clusters. From a microscopic point of view, the gels prepared under strongly acidic conditions reveal a very fine microstructure with particle sizes of about 50 Å, and the base prepared gels appear to have two separate structures (10). One of which are large dense clusters having sizes about 900 Å, and the other are fine particles of about 100 Å. The larger particles are composed of the smaller finer particles which give it a particulate nature.

Even though the basic system gels reveal a more compact structure, the bulk density of these glasses is less than the acid system's because of the presence of large voids.

The large change in the physical properties occurring between the low and high pH prepared gels suggests that the two reaction situations proceed by different mechanisms. Indeed this is the case and Okkerse (28), Aelion (8), and Iler (29) are a few of the first authors to study this phenomena. Mutual consent is that at a pH of 2.2, the isoelectric point of silicic acid ($Si(OH)_4$), the polymerization mechanism changes. Below a pH of 2.2, the rate of disappearance of the monomer is third order, while above the isoelectric point its disappearance is second order (29). Okkerse suggests that this difference results from a shift in the silicon coordination number from three to six of the intermediate species in the high and low pH systems. The suggested mechanism of the low pH system is schematically shown below using the silicic acid monomer (30).

$$\equiv Si - \overset{H^+}{O} - H + Si(OH)_4 \rightarrow \equiv Si - \overset{H^+}{O} - Si(OH)_3 + H_2O \qquad [2.10]$$

In this reaction, an equilibrium condition exists between the excess H^+ ions and the silanol groups resulting in a temporarily positively charged complex. This charged species can attract an uncharged silanol functional grouping and can condense to form a $\equiv$Si-O-Si$\equiv$ bond. The remaining positive charge on the product then can be removed by a free water molecule or another $Si(OH)_4$. This model indicates that the condensation mechanism proceeds by an electrophilic means.

Charge considerations force the positively charged $\equiv Si - OH_2^+$ species to preferentially attack the least acidic silanol sites. Since the acidity of the silanol group generally increases with the number of substituents attached to the silicon, the silicon atoms most likely to participate in the polymerization reaction are those bonded to the least condensed end groups. Thus, the polymerization under these conditions promotes the formation of linear chains or

weakly branched structures of a relatively small size (~20 Å) with a low degree of internal condensation (30).

From a hydrolysis perspective, similar arguments can be applied. The mechanism of hydrolysis proceeds by an electrophilic attack on an alkoxide oxygen in which for the most part are unaffected by the electronic effects of the alkyl silicon substituents. However, sterically this mechanism is very sensitive to the size of these groups. As a result, the monomers are more rapidly hydrolyzed than the end groups of chains, which in turn are more easily hydrolyzed than the middle groups of the chains. According to Aelion, the acidic hydrolysis is directed toward the ends of the chains which leads to condensation at these points developing a more linear polymer (8).

At low pH conditions, the hydrolysis step goes to completion within minutes to produce largely monosilicic and disilicic acid. These initial species serve as nuclei for further growth during the condensation step. Consequently, the particles or nucleation centers are large in number, but small in size. As the polymerization continues through cluster-cluster interactions, the weakly crosslinked monomers, dimers, and trimers begin to condense at the terminal ends without a high degree of internal condensation. In the final stages of the reaction, internal condensation sometimes reported as an 'aging' effect occurs during solvent evaporation long after the gel point has been reached (30). This 'aging' reaction results in the development of a fine microporous microstructure without the presence of larger voids and can be attributed to the gel's higher density.

Above the isoelectric point and in high pH conditions the polymerization process is catalyzed by hydroxyl ions and proceeds by the following reaction scheme (30).

$$\equiv Si - O^- + HO - Si\equiv \rightarrow \equiv Si - O - Si\equiv + OH^- \qquad [2.11]$$

Depending on the pH of the reaction medium, an equilibrium is established to deprotonate the silanol groups to siloxanolate anions. The anions then can condense with the remaining silanol groups to form ≡Si-O-Si≡ bonds.

The nucleophilic nature of the basic condensation mechanism requires that the negatively charged deprotonated silanols preferentially attack the most acidic silanols which normally are located on the silicon atom with the highest degree of substitution. That is, under these conditions, the condensation reaction is directed towards the middle of the polymeric chains instead of the end groups. Also, the rate of condensation increases with pH due to the lower ionization potential of the hydroxyl ions (i.e., the rate is proportional to the $[OH]^-$)

In a high pH environment, the effectiveness of the hydrolysis mechansism is diminished significantly, and as a result the reaction becomes the rate determining step. The direct consequence of these conditions is the development of fewer nucleation centers. The molecules that do hydrolyze attach to preexisting structures rather than nucleating into new particles. This type of growth benefits the formation of larger particles, but fewer in number. Kelts and co-workers have confirmed this method of growth in their NMR studies (23). Their results reveal that only a low percentage of low molecular weight oligomers are present throughout the course of the polymerization and that the silicon network evolved is highly substituted.

The extent of the hydrolysis reaction like the condensation mechanism increases with the acidity of the silanol proton the $(RO)_3Si(OH)$ (10). As the acidity of the proton increases, the basicity of the other groups bonded to the silicon decreases. In short, this means the hydrolysis rate increases as the silicon atom becomes more substituted and/or crosslinked because the inductive effects of the adjacent silicon atoms decrease the electron density around the silicon atom, which improve the abstractability of the silanol proton. Thus, as the silicate molecules crosslink more, the hydrolysis rate increases which then further promotes the condensation mechanism. This type of reaction mechanism facilitates internal condensation of the silicate polymer through monomer-cluster interactions that result in the formation of large particles with a particulate nature.

One point of exception is apparent in the base catalyzed case. At a pH greater than 7, depolymerization begins to occur due to the silicon monomer's enhanced solubility, and the rate of condensation is no longer proportional to the $[OH]^-$ (30). As a result, more spherical

particles are grown through the dissolution of the smaller particles and their subsequent deposition on the larger structures (Ostwald ripening).

Comparing the acid and base catalyzed polymerizations of silicon alkoxides, they can be summarized from several different standpoints. Kinetically, the basic media promotes a faster hydrolysis that proceeds by a nucleophilic attack, while the acid system proceeds by an electrophilic mechanism. Also under the basic conditions, the hydrolysis is directed toward the center of the chains or clusters, while the acid hydrolysis is directed more toward the chain ends and/or the monomeric species. Generally, the same rules apply for the acid and base catalyzed condensation mechanisms. The first is characterized by an electrophilic mechanism while the later has a more nucleophilic nature and occurs at a faster rate. The overall effect of the pH on the kinetics of the two step hydrolysis condensation reaction is reflected in the final structure of the gelled glass. In the basic situation, the faster hydrolysis and condensation mechanisms promote a monomer-cluster type growth process that leads to the formation of dense colloidal particulates. In the acid catalyzed reaction, the hydrolysis and condensation mechanisms are directed toward the chain ends and/or monomers that result in a cluster-cluster growth process which produces weakly crosslinked polymeric species.

The molecular arguments pertaining to the pH kinetics of the alkoxy silane polymerization have been confirmed by monitoring certain aspects of the two step reaction through the use of instrumental techniques. NMR, Infrared (IR), and Raman spectroscopies along with SAXS and intrinsic viscosity measurements are useful methods for following the reaction mechanisms. Each approach has specific advantages and disadvantages depending on the polymerization conditions involved. NMR, IR, and Raman techniques commonly are used to monitor the extent of the sol-gel reaction with time while the SAXS and intrinsic viscosity measurements reveal information on the type of structure that is evolving during the polymerization. By surveying the evidence drawn from these methods, a more complete understanding of the complexities of the sol-gel process can be attained.

By far the most useful information describing pH dependence of the kinetics of the sol-gel reaction is derived from silicon and proton NMR studies. Much of the data is obtained through

following the chemical shifts of the different substituted silicon species in Si-NMR and following the alkoxy hydrolysis in H-NMR. Kelts et al. have used these methods to help understand the unique characteristics of the TEOS sol-gel polymerization as a function of the reaction pH (23). For example, their results show that the relative amount of the tetrasubstituted material (-110 ppm Si-NMR) decreases as the pH is lowered with the trisubstituted material being the predominant species at low pH. These findings follow in line with that predicted by the nucleophilic and electrophilic principles. Another interesting observation is that at the gel point for a high pH situation approximately 70% of the gel is unreacted starting material while at low pH none of the starting monomer is remaining (23). These results tend to conflict with the early statement that the hydrolysis and condensation mechanisms of the basic system are faster than those of the acidic system. This phenomena can be explained by considering the relative activation energies of the first hydrolysis step. The acid hydrolysis has a lower initial activation energy which leads to the hydrolysis of most of the monomers while the basic system has a higher initial activation energy. However once the basic hydrolysis has overcome this first rate determining step, then both the condensation and hydrolysis mechanisms proceed much more rapidly than those of the acid catalyzed systems (i.e., basic systems have a much shorter gel time). Further evidence by Kelts and co-workers supports this reasoning (23). In the high pH situation, NMR data reveals that of the 26% of the polymerized TEOS 59% is tetrasubtitued, whereas in the low pH system only 26% of the 100% polymerized material is tetrasubstituted (see Figure 4). Thus, as the pH is increased less starting material is polymerized at the gel point, but the degree of substitution of the network is much greater.

In addition to the NMR characterization of the TEOS polymerization, SAXS experiments can be used to follow the structural development of the network through both dimensionality and particle sizes with respect to the solution pH. Brinker and co-workers have used this approach and have shown that a strong pH dependence or catalyst type (acid vs. base) exists with the dimensionality of the developing network structure (9,10). As explained previously, the dimensionality of the silica polymerization can be attained from the Porod slope of a SAXS scan during the course of the reaction. In the acid catalyzed case, the slopes are found to be

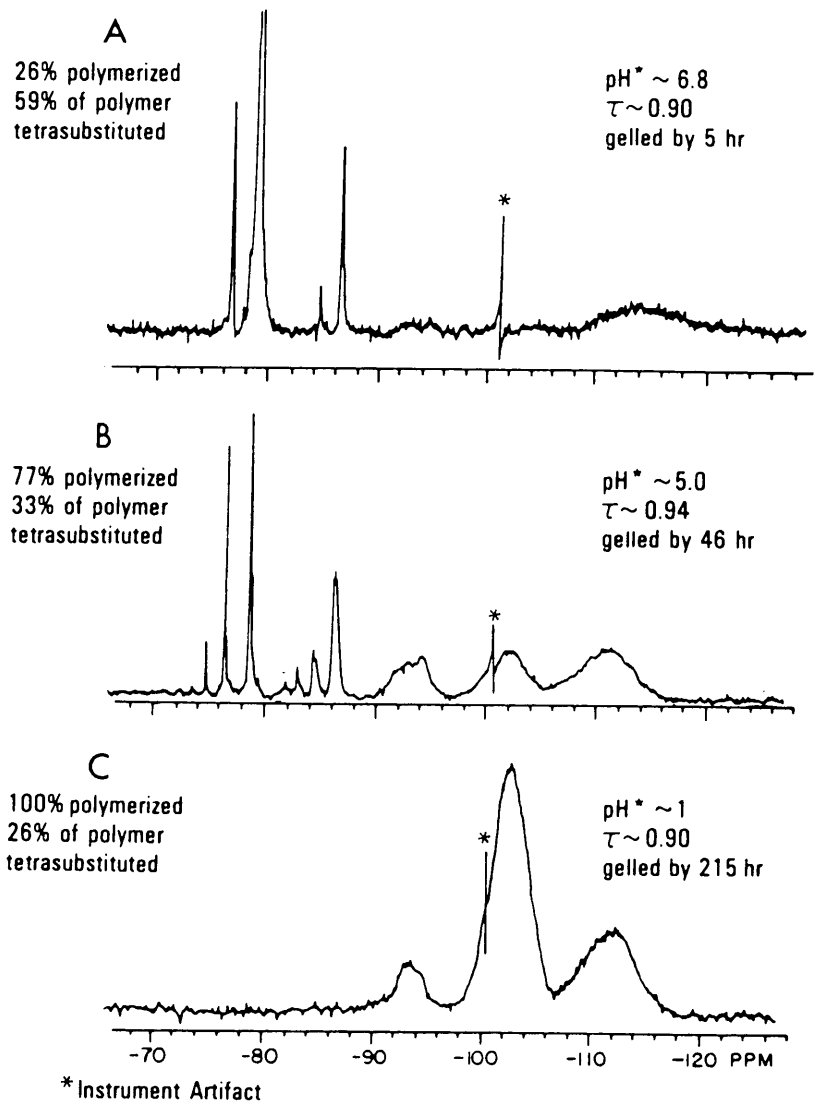

Figure 4. Si-NMR spectra from three sol-gel reactions at different pH's with a τ=.90-.94: (a) 26% polymerized TEOS with 59% of the polymer tetrasubsituted, (b) 77% polymerized with 33% of the polymer tetrasubstituted, and (c) 100% polymerized with 26% of the polymer tetrasubstituted (23).

normally greater than -2.0 (i.e., $D < 2.0$), while those of the base system fall below -2.0 (i.e., $D > 2.0$). This result suggests that the acid catalyzed polymerization develops molecules that are slightly branched and have molecular sizes comparable to K^{-1} (9). Deviations towards more negative slopes in the basic polymerization indicate a more branched or more collapsed structure relative to an ideal random linear polymer (9).

Furthermore, SAXS scattering experiments can also be used to study the effects of the pH on the particle sizes during the polymerization. Brinker et al. have revealed that the radius of gyration, R_g, is significantly influenced by the catalyst type used (9). For the acid catalyzed system, the R_g did not change considerably during the reaction. The size of the particle remains approximately 15-17 Å which indicates a narrow distribution of molecular sizes. This further suggests that the final stages of gelation is characterized by a cluster-cluster growth pattern that forms a gel with a uniform microstructure. Also, Brinker has shown that the R_g of the acid catalyzed system is concentration dependent which supports the early conclusion that the polymers are extended, weakly-branched chains (9).

In the base catalyzed polymerization of TEOS, the R_g increased during the reaction with sizes beginning at 20 Å and ending at 44 Å. The Guinier plots show concavity under these conditions which Keefer has interpreted as either resulting from polydispersity and/or molecular separations (10). Also, the R_g is independent of concentration. This suggests that the growing particles are well separated and have little overlap prior to gelation. Thus, the base catalyzed system forms silica with discrete, more highly branched clusters developed from monomer-cluster interactions.

Zerda (30) and Sakka (2) have also reported that distinguishing differences in particles sizes occur under different catalyst conditions. Zerda has used the Raman technique by monitoring intensity of the ≡Si-O-Si≡ stretching vibration to show that the particle sizes increase with the pH of the reaction solution. Sakka and Sumino have also found through their intrinsic viscosity measurements that a strong dependence is associated with the catalyst type (2). These results support the findings of Brinker and Keefer from their SAXS experiments (9,10). In the acid catalyzed reaction of TEOS, a linear dependence of the reduced viscosity,

η_{sp}/C and the intrinsic viscosity, $[\eta]$, becomes appreciable after $\tau/\tau_g = 0.5$ (where τ_g is the time to gelation). The concentration dependence of η_{sp}/C and $[\eta]$ increases as the the poly(hydrolysis-condensation) reaction approaches the gelation point. This evidence suggests that chain-like polymers are being developed under these conditions. For the base catalyzed system, the concentration dependence for η_{sp}/C and $[\eta]$ is absent until the final stages of gelation. At this point, an abrupt change in the $[\eta]$ occurs and is attributed to the aggregation of spherical SiO_2 particles to form a three dimensional network structure. Again these results further confirm that the base catalyzed systems form gels that are more particulate (i.e., powders) while acid catalyzed systems form networks that are more polymeric (i.e., thin films)

2.2.4 Effect of Water Content

Another important variable that affects the kinetics of the hydrolysis and condensation mechanisms is the availability of water in the reaction medium. According to eqns. [2.1] and [2.2] , a complete hydrolysis requires 4 moles of H_2O/mole silicon alkoxide, while the overall reaction process only requires 2 moles H_2O/mole silicon alkoxide. Normally, the H_2O/TEOS ratio (R) ranges from 1 to 50 for the silica polymerization. At low water concentrations, the hydrolysis reaction is starved and a significant percentage of the alkoxy groups remain apart of the gel structure limiting the connectivity of the network. A TEOS polymerization carried out under these conditions would have a more linear network and would have better low temperature properties (i.e., more flexible). At high water concentrations ($R > 10$), the hydrolysis reaction proceeds nearly to 100%, resulting in a more efficient condensation step which produces a higher degree of network formation. These conditions generally promote the formation of spherical particles that can be used as ceramic precursors.

Thus, the extent of the conversion of a silica network relies heavily on the amount of H_2O used as a reactant. This result makes it possible to introduce structural modifications via the H_2O/alkoxide ratio. The kinetics of the hydrolysis and the condensation mechanisms are

affected by this R ratio, but not as strongly as those influenced by the acid and base catalysts. For example at low H_2O concentrations and mildly acidic conditions, the condensation rate is much more rapid than the hydrolysis rate (10). As a consequence, the hydrolysis step controls the final form of the polymer and not the condensation reaction. In the high H_2O content situation, the rates of the reaction mechanisms are reversed, and now the condensation step becomes the controlling factor in the final gelled-glass structure. Pouxviel and co-workers have confirmed these kinetic effects through the use of Si-NMR (11).

In other studies, Yoldas links the kinetic effects of the R ratio to the structural modifications occurring in the glass (5). This author has shown that as the R values increase, the overall connectivity (bonds per silicon) of the network is increased along with increasing molecular particle sizes and the SiO_2 character or oxide content. For instance, the R ratio's of 1, 2, & 15 produced oxide contents of 70%, 78%, and 93% and connectivities of 1.1, 2.2 and 3.5 respectively (5).

Work by Duran et al. arrives at similar conclusions for the effect of the R ratio on the final gelled-glass structure (31). For a low H_2O content ($R=1.0$), the hydrolysis is incomplete and gelation occurs by a linear chain formation with residual organic groups (i.e., lower connectivity). With excess H_2O, cyclization of the initially formed chains occurs and promotes siloxane bond formation within the particle. Condensation then results from the packing of these cyclic species in orderly fashion to evolve a 3-D network of high matrix density with large interstitial voids between particles (31). This cyclic pattern of condensation has been found to occur in the polymerization of TEOS with a high concentration of H_2O present, but Pouxviel shows that this mechanism is not the predominant condensation method (11). Their NMR results reveal that only 20% of the silicon present is representative of the cyclic species.

2.2.5 *Solvent Effects*

A common participant in the sol-gel reaction whose effects are sometimes overlooked in the literature is the solvent. The primary role of the solvent is to provide a compatible medium between the immiscible water and silicon alkoxide mixture. Thus, the proper selection of a solvent is imperative to forming a homogeneous reaction condition. Some of the more common solvents used are of the lower alcohol family (i.e., methanol, ethanol, isopropanol) because of their ability to solvate the components easily and due to their relatively high volatility. Other solvents and solvent mixtures beside the alcohols have been used, especially when organic material has been introduced into the reaction scheme (20). Even though the solvent is not directly involved in the polymerization, its presence has a considerable effect on the kinetics of the hydrolysis and condensation reactions. Solvent properties, the dilution ratio, the evaporation rates, and ester interchanges are all phenomena that can affect the kinetics of the sol-gel reaction.

The solvent properties whether polar or non-polar and/or protic or aprotic have a remarkable effect on the sol-gel reaction and can be shown to alter the course of the silica polymerization resulting in different structural modifications of the gelled-glass. In a polymerization proceeding by nucleophilic substitution, hydrogen bonding and electrostatic interactions between the solvent and the nucleophile ($\equiv Si\text{-}O^-$) can stabilize the intermediate stage of the bimolecular reaction (see eqn. 2.11). For example, highly polar protic solvents can decelerate the condensation rate by deactivating the nucleophile through hydrogen and/or electrostatic interactions. Also due to a strong dipole momment, the solvent can stabilize the negative charge localized on the silicon intermediate to a greater extent by increasing the activation energy necessary to initiate the condensation step (32). On the other hand, a non-polar aprotic solvent lacks the ability to interact both electrostatically and though hydrogen bonding to either the reactants or the activated complex. This results in the most efficient condensation mechanism producing a highly condensed species. A protic polar or dipolar solvent where hydrogen bonding is absent still can interact electrostatically to stabilize

the reactants with respect to the activated complex through dipole interactions, but cannot deactivate the nucleophile. Thus, a solvent of this nature only moderately reduces the condensation rate.

Zerda and co-workers have published results that closely support these suggested hypotheses (32). Their work focuses on three solvent groups: (1) polar protic (methanol, formamide), (2) dipolar aprotic (acetonitrile, dimethyformamide), and (3) non-polar aprotic (dioxane). According to the theory, the less the solvent can stabilize the reacting species through hydrogen bonding and dipole interactions, the faster the condensation rates, and the larger and more crosslinked the particles. This trend is reflected in the Raman intensities of the ≡Si-O-Si≡ stretch and the TEM grain sizes for the different solvent systems. The solvent's ability to stabilize the reactants and the intermediate complex follows in the order of formamide> methanol> dimethylformamide> acetonitrile> dioxane. The ≡Si-O-Si≡ intensities and particle sizes increase with decreasing solvent stability (more efficient condensation) which is consistent with the earlier stated assumptions.

The subtle differences in the polar aprotic class of solvents can be attributed to the unusual properties of the formamide. This solvent has a large dielectric constant and has the ability to form strong hydrogen bonds by both donating and accepting electrons. The hydrogen bonds of this solvent can form a shielding network around the silicon atoms. However, the methanol solvent is also capable of forming a hydrogen bonded network cage, but formamide's greater steric hindrance can inhibit the condensation reaction more effectively (32). It is these types of properties that has led to the use of formamide as a chemical additive to help shape the final properties of the network gel (33). The addition of this solvent to a silicon alkoxide polymerization has resulted in a drastic reduction in the rate of hydrolysis and promoted the development of extremely branched gel network with a high porosity and a reduced density (32).

The structural modifications occurring from the formamide additions can be explained in terms of the hydrogen bonding ability to form network shields or cages around the silicon reaction centers. A solvent with a strong shielding ability promotes the formation of branched

structures with a more uniform microstructure. That is, a silica polymerization run in a hydrogen bonding medium tends to develop larger and more uniformly distributed micropores that are indicative of polymeric structures. Solvents that have poor shielding capabilities (no hydrogen bonding or electrostatic interactions) produce gelled-glasses with a finer morphology and smaller pores sizes that are representative of spherical condensed particles. For example, Zerda and co-workers have shown through Raman spectroscopy and TEM techniques that the polymerization of TEOS in dioxane under neutral conditions develops large compact spherical particles (32).

Another factor that affects the kinetics of the sol-gel reaction is the relative dilution ratio of the solvent to the reactant species. Based upon diffusion principles, a high dilution ratio shifts the hydrolysis reaction to favorable conditions and decreases the probability of the condensation reaction. As a result, Yoldas has reported that a lower oxide gel is formed with higher dilution ratios and low water concentrations (6). When the hydrolysis and condensation reactions are not well separated, ≡Si-OR groups are localized on the polymeric species and a large decrease in hydrolysis is noticed (11). The actual structural effects of the dilution ratio on the polymerized species are not well documented in the literature. However, postulating from the kinetic observations of Yoldas (6) and Pouxviel (11) on the hydrolysis extents, it seems that the higher dilution ratios would promote a more condensed species in the final gelation stages after a large amount of solvent has evaporated. This assumption tends to conflict with the Yoldas results presented earlier which leaves one to believe that the dilution ratio may have a complex effect depending on the reaction conditions used. Nevertheless, the overall effect of the dilution ratio on the kinetics of the polymerization mechanism is relatively minor in comparison with the pH, the H_2O concentration, and the other solvent effects.

One novel point of interest involving a silicon alkoxide-solvent interaction is the phenomena of ester interchange or transesterification. The mechanism of ester interchange occurs by the substitution of a solvent molecule for an alkoxy group attached to the silicon. This type of mechanism is commonplace in a lower alcohol solution and can be depicted by the following reaction scheme of TEOS in isopropanol.

$$Si(OEt)_4 + niPrOH \rightarrow (iPrO)_nSi(OEt)_{4-n} + (4 - n)EtOH \qquad [2.12]$$

Pouxviel through NMR analysis has observed the presence of five different species in the ratios of 2:9:13:7:1 with $Si(OEt)_4$ on the far left and pure $Si(OiPr)_4$ on the far right (11). It appears that the disubstituted species of the (EtO) and the (iPrO) forms is the most favorable configuration. The transesterification mechanism has yet to be reported as to cause significant problems with the kinetics of the poly(hydrolysis-condensation) reaction of a silicon alkoxide. However, it does tend to confuse the monitoring of some results when using certain instrumentation such as NMR, IR, and Raman spectroscopies.

2.2.6 *Temperature Dependence*

From a ceramics perspective, the effect of temperature on the sol-gel reaction and the gelled glass structure is deemed an extremely important aspect of this science. Normally in the ceramics field, the sol-gel process is completed by a sintering process that densifies the network. The advantage of using the sol-gel techniques stems from its ability to produce amorphous densified glasses at considerably lower temperatures (i.e., 800-900 °C vs. 1100-1300 °C) which offers substantial energy savings. However in the area of organically modified silicates, the temperature effects on the gelled glass are somewhat limited because of the poor thermal stability of the organic materials. This artifact restricts the temperature treatment to much lower temperatures (< 300 °) at which significant sintering does not occur.

In any event, the effect of temperature has been shown both to alter the kinetics of the sol-gel reaction in the solution and beyond the gel point. Aelion has reported that by raising the temperature from 20 to 45.5 °C of the reaction solution, the hydrolysis rate is increased by ten fold (10). However at temperatures above 50 °C, the condensation or dehydration re-

action is no longer complete. Thus, an overall increase in temperature promotes the probability of establishing more network points as the polymerization approaches the gel-point.

After the reaction has reached the gel-point, continued thermal treatment of the glass facilitates the furthering of the underlying poly-condensation reaction. Bertoluzza has pointed out this occurrence qualitatively by showing the intensification of the ≡Si-O-Si≡ related bands as the temperature is increased with IR and Raman spectroscopies (34). In other related work, Duran and co-workers have reported similar findings using IR spectroscopy (24). For example, their results indicate that the asymmetric ≡Si-O-Si≡ stretch (1082 & 1100 cm^{-1}) tends to shift to higher frequencies with increasing temperature for samples prepared with a R ratio lower than 4. This shift as does the intensification of the ≡Si-O-Si≡ bands is due to the strengthening of the silicon matrix by the sintering process by developing more interparticle bonds. In summary, thermal treatment of the gelled-glasses results in a progressive evolution toward v-SiO_2 with increasing temperature.

2.2.7 Gel Time

The time for a silicon alkoxide polymerization to reach the gel point has been shown not to be an influence on the kinetics of the reactions, but more often a direct result of the kinetic effects of the other variables involved. For example, the pH, the water content, and temperature of the reaction all have a bearing on the gelation time. In the case of the pH, Okkerse has revealed that at a pH of 2, approximately the isoelectric point, the gel is the most stable and a long gelation time occurs (24). Above and below this pH, the gelation times decreases with the exception of the pH's above 8 where the gel time begins to increase again due to the enhanced solubility of the silica. At pH's lower than the isoelectric point, the polymerization rate is directly proportional to the $[H]^+$ while above pH 2.2 the rate is proportional to the $[OH]^-$ (30). In addition to the pH, the temperature and the water content also effect the gel time. Gottardi and co-workers have reported that the gelation time is inversely related to the

water content for the acid catalyzed TEOS polymerization (35). Similar results are observed for increasing the temperature of the reaction solution. In both cases by increasing the water content and/or temperature of the solution medium, the hydrolysis rate and extent is increased which in turn further promotes the condensation mechanism reducing the gel time.

The significance of the gelation time is not important from a kinetic consideration, but more from a processing perspective. The gel time corresponds to the window of processability that a particular material may possess. Ultimately, this time span has a direct bearing on what type of applications this material may be developed for.

2.3 *Sol-Gel Applications*

The investigation of the sol-gel technique through the manipulation of the reaction variables of pH, H_2O/silicon alkoxide ratio (R), solvent type, and temperature has preempted a challenging atmosphere to find suitable product applications. In a recent sol-gel colloquium celebrating Professor Norbeit Kreidl's 80th year of life and his achievements in the field, Dislich presented a varying account of the development of the sol-gel method for practical applications (36). Based on past and present research trends, Dislich expects that in the next twenty years this technique may find a small niche in the commercial and industrial market. Even though this process is not economically feasible for the production of large quantities of materials and is not intended in the future to replace any of the 'heavy industrial' procedures (i.e., production of plate glass by sintering), the sol-gel method due to its innovativeness may develop products with very desirable properties that are hard to come by or unattainable by other techniques.

The chief advantage of the sol-gel process is that it offers considerable energy savings over the conventional firing methods in the ceramics industry. Glass materials can be prepared without the necessity of high melt temperatures and in some cases up to 1000°C less

than the normal procedures require (36). However in order to make glasses by the sol-gel method, silicon or metal alkoxides are employed rather than silicon or metal oxides. The alkoxide starting materials at the present time are more costly that the traditional oxides. Thus in the future, the balance between energy savings and material costs may result in a diminished or spurred activity in this field, depending on the economic barriers at the current time.

As mentioned earlier, four potential areas of applications research are currently being conducted. The first is the development of multicomponent bulk glasses through prehydrolysis steps to mediate the reaction rates of the different species. This area of research is of great interest to the ceramics group because of the possible use of these materials as semiconductors. Secondly, the dip coating of substrates for glass glazing has been one of the most promising application areas and has achieved the most success. Thirdly, Sakka and Kamiya (3) have suggested several methods for preparing glass sheets, and the final area deals with the spinning of glass fibers. This last area has aroused much interest in the sol-gel field due to its complexity. Since the topic of the thesis research encompasses mostly the preparation of polymeric thin films, the applications discussion is confined to the latter three areas which have some relevance to the work under study.

The dip coat method devised by Sakka and co-worker uses the reaction variables of the sol-gel reaction to develop a suitable medium for the coating of a substrate (3). The authors indicate that the sol-gel solution should be partially hydrolyzed with a small amount of H_2O and a acid catalyst which promotes the formation of a polymeric species. Once the solution has attained a desirable viscosity (representative of the extent of the reaction), the substrate is dipped into the medium and then is placed in a humidified environment to further the network formation of the gelled silicon glass. In the final stage, the sample is heat treated to improve the adhesion between the glass film and the material. This last step is the most important concern in this application. Normally, 400-500°C is required to develop good adhesion properties through the formation of chemical bonds between the substrate and the glass film. This artifact may perceivably limit its use in the plastics area due to their tendency to degrade

at these higher temperatures. Nevertheless, the dip coat method could significantly enhance the physical properties of some materials such as improving the scratch resistance and may even provide a protective coating to others that reduces fouling.

Another area of application involves the use of the sol-gel process to produce thin film glass sheets. In this application, the sol-gel medium must be partially hydrolyzed with a low water content and under acidic conditions to promote the formation of linear alkoxide polymers that may further condense upon drying to produce monolithic glass sheets. Three processes have been imagined by Sakka et al. (3) for the preparation of these materials: (1) by skimming off a viscous partially reacted sol-gel solution with a wire ring, (2) by drawing the same viscous solution through a slit die, and (3) by molding a thin sheet from the viscous solution on a plastic plate that can removed after film has dried. As one might foresee, these proposed processes for the production of thin glass sheets play host to a variety of problems and are by far the most difficult application to implement successfully. The major difficulty of these techniques arises during the drying process when an enormous shrinkage in volume occurs due to the further condensation of the glass. As result, deleterious warping or cracking of the sheets may develop.

A final area of application of considerable interest is the preparation of silicon and multicomponent glass fibers. This unique application is the most complicated, but already breakthroughs have been reported in actually producing usable glass fibers (3). Typically, the reaction conditions prescribed evoke a very slow hydrolysis so the fibers may be spun from the reaction medium over a fairly long period of time. As in the other applications, the formation of linear polymers in the alkoxide solution is a prerequisite for achieving a spinnable material. Thus, an acid catalyst and low H_2O content ($R < 2$) are mandatory. Sakka and Kamiya have shown experimentally that under basic conditions and/or H_2O/alkoxide ratios greater than 4, the solution is not spinnable (3). In the spinning of the glass fibers, an optimum viscosity range occurs between ten and several hundred poises at which the fibers may be produced efficiently. After the spinning is completed, the gelled material is converted to densified glass fiber by a slow heating program. These types of fibers have promise in the

fiber optics industry because of the possibility of developing multicomponent fibers with superior conducting properties.

Besides the applications discussed here, there exists a multitude of other probable areas the sol-gel technique may be employed. The 'sol-gel tree' of Dislich best summarizes many of the current areas of interest (see Figure 5) (36). As one can see, the suggested applications show a large diversity covering several different scientific fields. One other area that has not been mentioned thus far concerns itself with organically modified silicates where the sol-gel derived glass consists of an inorganic-organic matrix. In the remaining section, this topic will be covered exclusively due to its ability to form materials with tailor made properties.

2.4 *Organically Modified Silicates*

Up to this point, the discussion has been centered on the preparation, characterization, and application of the sol-gel derived inorganic glasses using silicon and/or metal alkoxide precursors. Primarily in the past two decades, this topic of research has received widespread attention in the physics and ceramics sectors, but over the last few years a new area in the sol-gel field has emerged and has sparked interest in the polymer science area. This new aspect concerns itself with the incorporation of organic species of a polymeric nature into the inorganic glass network through the sol-gel process. Several authors have used this approach and have prepared new hybrid materials with unique properties (12-22). The chief advantage of the organic modified silicates, termed 'ormosils', is that the properties of these materials can be tailored according to the organic components present (note that the reaction conditions discussed earlier also play an important role). In most instances, this technique can form monolithic and dense materials at low temperatures. As a result, a sporadic increase in sol-gel research has occurred focusing on the systematic development of new ormosil materials that have potential commercial and industrial applications.

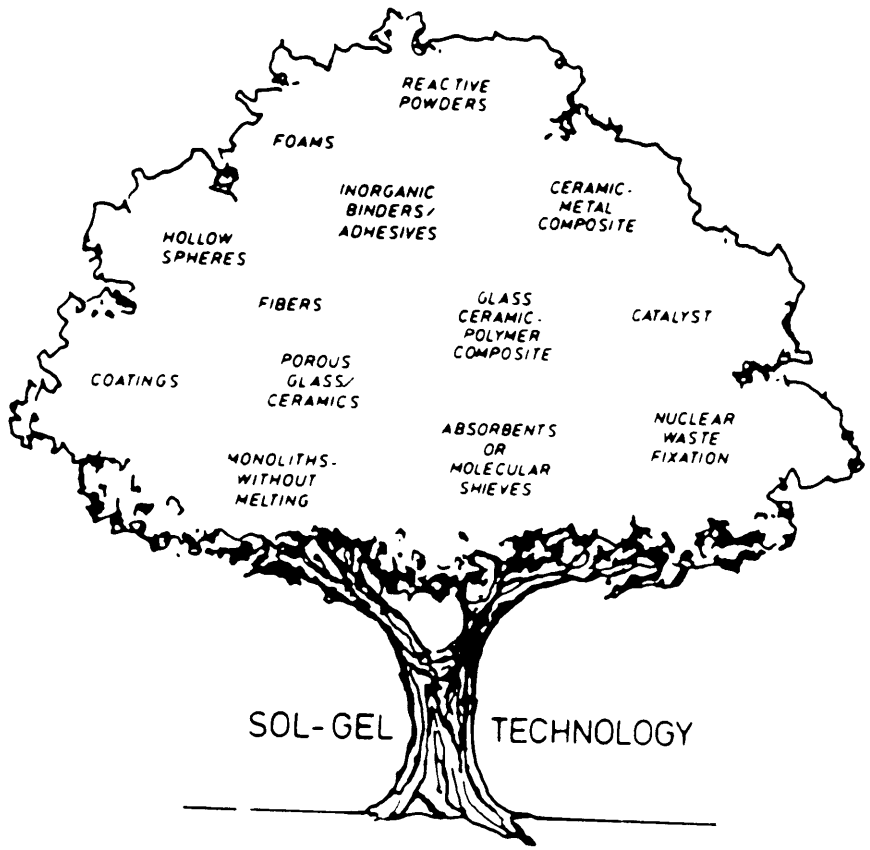

Figure 5. The sol-gel technology tree from Dislich (36).

The development of the ormosil glasses can be directed along one of two lines. The first one involves the use of organic modifiers that can alter the network structure by their presence, but are not actually connected with the inorganic matrix. For example, if a silicon alkoxide precursor has a sol-gel unreactive R group located on the central atom, this R group will limit the connectivity of the matrix and thereby modify the glass's network structure. In the other approach, both inorganic and organic matrixes are formed either simultaneously or sequentially and are intermixed with covalent bonds bridging the two different phases. This latter technique most often requires very specific and sometimes very tedious reaction chemistry to achieve a truly combined inorganic-organic network. The creation of the organic bridges within the network can be developed through several different routes: (1) the polymerization of vinyl side groups on the silicon alkoxide, (2) the addition of vinyl side groups to an adjacent alkyl function group on another matrix site, or (3) a condensation type mechanism during the second step of the sol-gel reaction (see Figure 6) (17). This last reaction scheme is by far the most lucrative approach since the organic constituents can be directly crosslinked into the inorganic network using the same sol-gel mechanism.

However one constraint must be viewed when constructing the organic bridges using any of the proposed crosslinking mechanisms (most importantly the condensation mechanism). A strong ≡Si-C≡ bond which is thermally and hydrolyticly very stable must serve as the connecting interface between the inorganic and organic regions. Even though the ≡Si-O-C≡ bond is thermally stable up to 500°C, this particular bond arrangement is susceptible to hydrolysis during the sol-gel reaction and would not result in the development of an inorganic-organic network structure. Thus by combining the good properties of the ≡Si-O- and the ≡S-C≡ bonds common to the siloxane polymers, one can achieve a ≡Si-O-Si-C≡ bond which, principally, is the most stable bond configuration that can be procured for an inorganic-organic interface.

One other point that deserves noting is when an organic component is linked to a silicon precursor as either an endcapped oligomer or an unreactive R functional group. In this environment, the hydrolysis and condensation rates of the inorganic-organic starting material

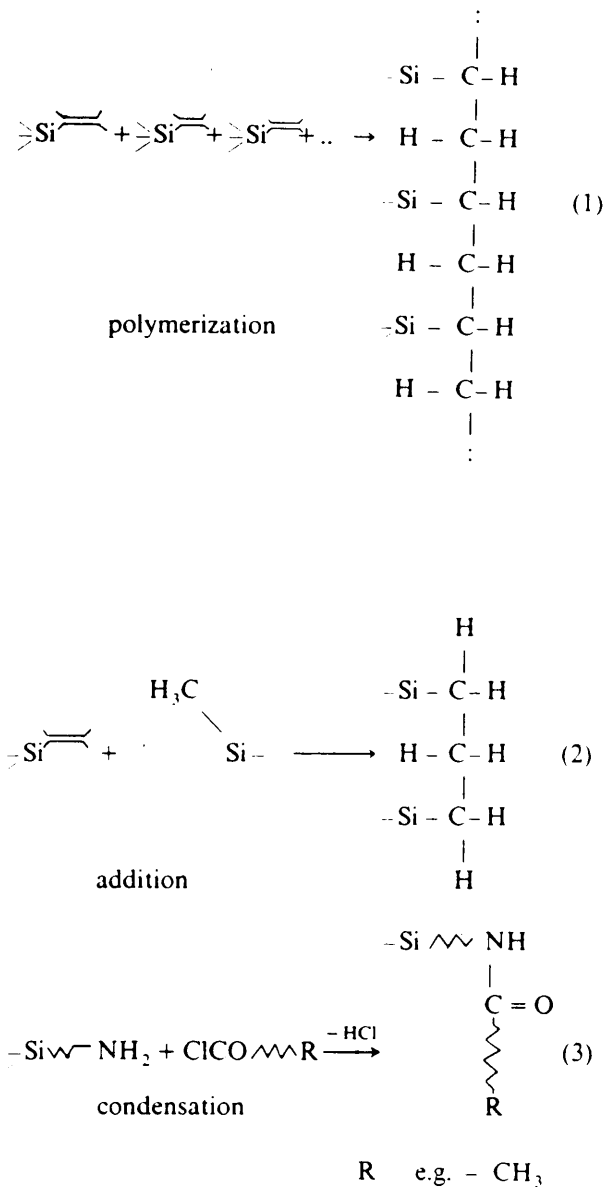

Figure 6. Probable reaction mechanisms for the development of organic bridges (17): (a) polymerization, (b) addition, and (c) condensation.

are typically different than those of a silicon alkoxide precursor. For example, the presence of a R alkyl on a R-Si$(OEt)_3$ species results in a much more rapid hydrolysis than what occurs for TEOS while the presence of a R amine group has just the opposite effect (17). In addition to the rate effects, steric considerations also may play an important role in the degree of network formation attained. Large bulky side groups such as a n-butyl functionality located on the silicon precursor can inhibit the condensation of neighboring network points limiting the connectivity of the final gel structure. In short, not only does the physical nature of the organic present shape the properties of the ormosil material, but also the organic's effect on the reaction rates and steric implications may introduce subtleties into the final glass state.

As previously mentioned, several authors have put forth considerable effort in devising methods to achieve beneficial properties using the ormosils approach. Schmidt and co-workers (16-19), Mark and co-workers (12-14), and Wilkes and co-workers (20-22) are cuurrently the most noted in the area. Each group of these authors have designed their own unique methods for obtaining the organically modified inorganic glass. Schmidt et al, the most published in the field, has undertaken a pragmatic study for the sole purpose of preparing new materials that have specific commercial applications. This author's success has been derived through the use of complex chemistry schemes which have been consequently patented. In other works, Mark et al. and Wilkes et al. have reported the incorporation of polydimethylsiloxane (PDMS) into a TEOS matrix to produce a rubber modified glass by the sol-gel technique. Mark and co-workers have focused on enhancing the existing mechanical properties of the PDMS by crosslinking the chain ends with TEOS endcaps, while Wilkes' research group has primarily sought to understand the structure-property relationship between the TEOS and PDMS components and the effect of the reaction conditions on them (20-21). In addition to this work, Huang, Glaser, and Wilkes have also directed a similar approach in trying to understand a polytetramethylene oxide (PTMO)/TEOS system prepared using the sol-gel method which overall has better mechanical properties than the PDMS/TEOS materials.

Close inspection of Schmidt and co-workers findings (16-19) reveals that the authors have developed patentable materials in three product areas. Specifically, Schmidt et al. have designed suitable procedures for the preparation of ormosils for (1) contact lens, (2) functional and scratch resistant coatings, and (3) hot melt adhesives. Out of the three product areas, the contact lens ormosil is the most interesting and promising which is due to both its unique properties and the novel chemistry used to produce the flexible glass.

In order for the ormosil to be deemed useful in the contact lens area, it must have good wettability, O_2 permeability, non-absorbance of the lachrymal eye fluids, and structural integrity (i.e., a flexible material with sufficient tear and scratch resistance). As one might imagine, to develop or even find a material that meets all these criteria presents a formidable challenge. Schmidt's approach relies on a specific reaction procedure utilizing a multicomponent mixture of several organic and inorganic starting materials (16). The initial reaction begins with a two step condensation procedure of expoxysilane 1, methacryloxysilane, and titanium alkoxide in a molar ratio of 90:5:5 ,respectively, to form a viscous liquid using a minimal amount of H_2O. In the second stage of the reaction, 20-30 mole % of methyl methacrylate (MMA) or 2-hydroxyethyl methacrylate (HEMA) monomer is added to the solution along with a peroxide catalyst, and then thermally cured at 150°C to form transparent and dense solids with only a minor shrinkage. In short, Schmidt and co-worker have figured out a reaction scheme that incorporates both a sol-gel and free radical mechanism occurring sequentially to produce an ormosil lens material (see Figure 7).

Each constituent in the multicomponent glass serves a specific function to meet the combined objective of attaining a suitable lens material. The $Ti(OR))_4$ is used to catalyze the formation of the inorganic network and also improves the hardness or scratch resistance of the glass at the expense of flexibility. In the methacrylate polymerization, the HEMA or MMA builds organic bridges between the inorganic network through the methacryloxysilane vinyl sites which enhance the tensile strength and add the flexibility that is removed by the titanium component. Furthermore, the HEMA when employed has $\equiv$C-OH groups that increase the wettability of the lens material without detrimental absorption of the the lachrymal fluid, unlike

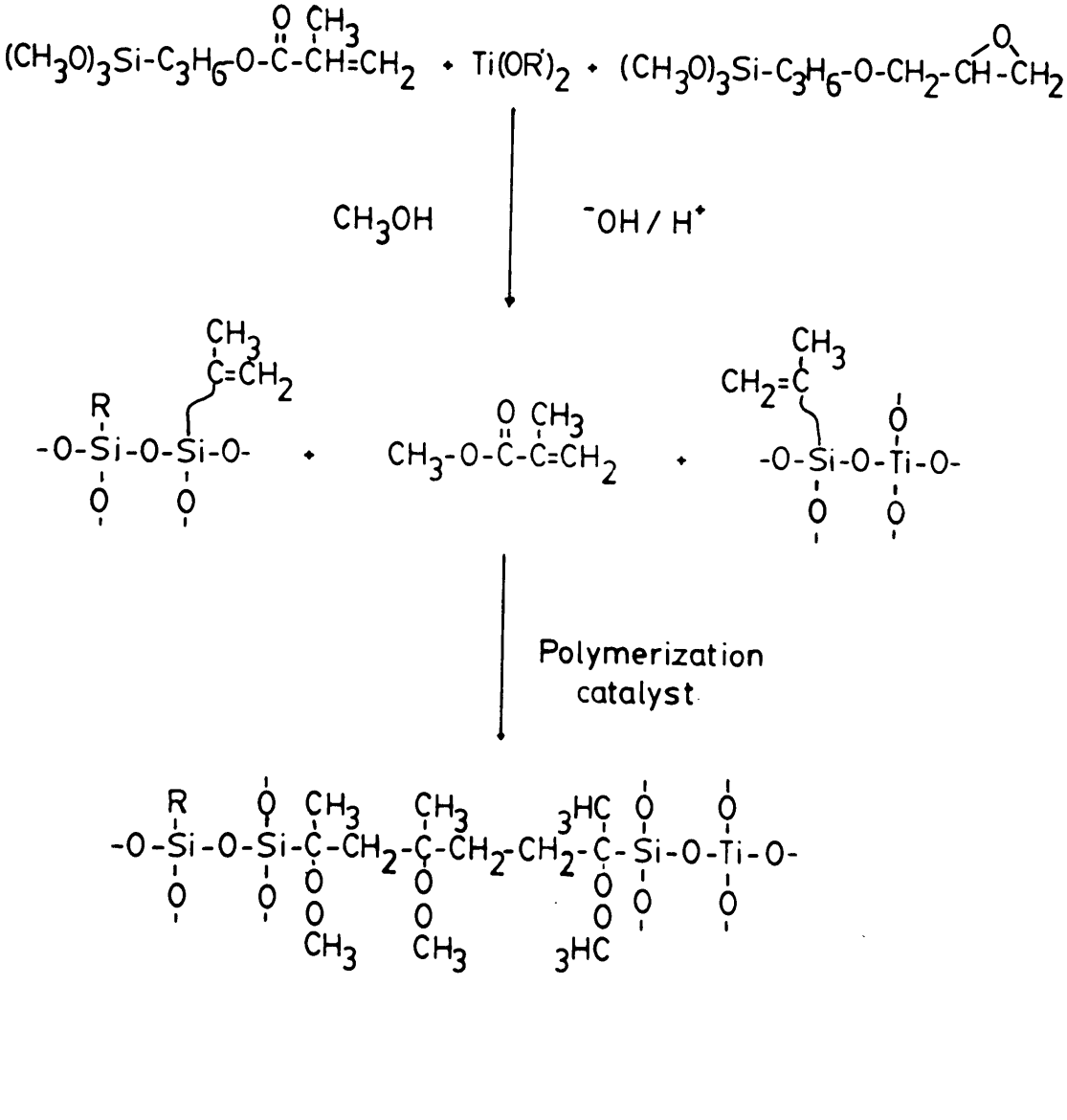

R= glycol group containing organic radical

Figure 7. Simplified reaction schematic of the synthesis of the proposed contact lens ormosil.

the similar ≡Si-OH functionalities. The major purpose of the epoxysilane 1 is to improve the wettability of the ormosil through the hydrolysis of the expoxide linkages to form free ≡C-OH acid groups. A quick perusal of the reaction recipe reveals the expoxysilane 1 is the primary component of the contact lens material which indicates that the criteria of wettability is one of the most important. One other critical factor is the O_2 permeability, and since the ormosil has a remotely similar structure to the very permeable siloxane rubber, this material also satisfies the minimum requirements. Thus, Schmidt and co-workers have developed a material that is suitable for use as a contact lens. However, the complex chemistry required may limit its application from both a processing and economical standpoint.

Another area of application investigated by Schmidt et al. (17-18) deals with functional and scratch resistant coatings. Both the functional and scratch resistant coatings rely on the presence of a chemically active group located on the silicon atom. This reactive group then can participate in a chemical reaction aside from the occurring sol-gel mechanism. In the scratch resistant coating application, Schmidt and Phillip proposed a method of using an expoxysilane precursor as a means of developing organic bridges in $Si(OR)_4$, $Ti(OR)_4$, or $Zr(OR)_4$ based inorganic networks. They found that both the $Zr(OR)_4$ and $Ti(OR)_4$ species catalyzed the polymerization of the epoxy linkages into polyethylene oxide organic bridges in addition to forming the inorganic network (see equation 2.13). Both the $Zr(OR)_4$ and $Ti(OR)_4$ formed hard infusible resins while the $Si(OR)_4$ based matrix did not. This suggests that the $Si(OR)_4$ species could not polymerize the epoxy linkages.

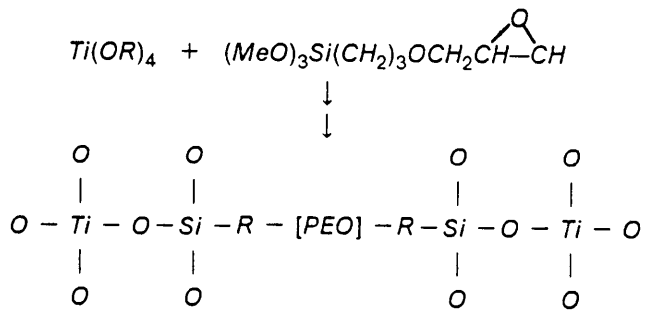

[2.13]

In the functional coating application , Schmidt and co-workers bound chemically active 'Y' groups on the silicon atom. This 'Y' group can react with certain organic functionalities and form covalent bonds to modify the network surface structure (i.e., an adhesion mechanism in a coating application). For example when 'Y' is a amine ($-NH_2$), it has been shown that the amino group acts as a surface modifier in coatings and porous materials (37). In other studies, the amino groups have been used as coupling agents with enzymes and/or antibodies in the biomedical field (38).

The final ormosils application Schmidt and co-workers have looked into involves the use of the sol-gel reaction to produce hot-melt adhesives that can form chemical bonds between a glass substrate and another surface. Their endeavors focus on solving the difficulties that arise when adhering hydrophobic organic polymers to hydrophilic glass surfaces. Since an ormosil can be manipulated through the starting materials to have components with a hydrophobic and hydrophilic nature, this approach may provide a tangible solution to the adhesion problems encountered. After a cumbersome trial and error survey of the silane precursors available, the authors discovered a multicomponent ormosil mixture and the appropriate reaction conditions necessary to form a hot-melt adhesive that delivers a sealing strength of 7 to 8 N/cm and is fairly moisture resistant. Thus, the ormosil mixture possesses adhesion properties that are suitable for many practical applications.

The multicomponent mixture contains the silane monmers of TEOS, $(C_6H_5)_2Si(OH)_2)$, $Ti(OEt)_4$, and $(CH_3=CH)(CH_3Si(OEt)_2$ in the molar ratio of 5:60:5:30 respectively. Once again the author's procedure requires a complex chemistry scheme to produce the hot-melt adhesive material. Summarizing the turn of a events, the reaction starting mixture is first hydrolyzed under acid conditions in an acetone solvent with a low H_2O content and then cast on the surface to be sealed. Next a short thermal treatment is applied to vitrify the resin coated surface to a tacky residue. Finally, the coated surface can be adhered to the glass surface by merely pressing the two together. Schmidt and co-workers (19) have shown that this approach is quite successful in the adherance of aluminum foil to glass containers. As with Schmidt's other sol-gel materials, each component present in the ormosil mixture brings with it certain

properties that are beneficial to solving the problem at hand. In this case, the silane precursors are chosen for their potential adhesion properties. For instance, the TEOS and the titanium tetraethoxide ($Ti(OEt)_4$) which are minor constituents in the material provide structural integrity through the formation of an inorganic network. These materials also possess a polar nature that may improve the adhesion of the glass-resin interface. The $(C_6H_5)_2Si(OH)_2$ species allows the reaction to remain processable over a long period of time by inhibiting the network development through both steric restrictions and reduced functionality. Even though the last component limits the connectivity of the matrix, still brittleness occurs during thermal aging that lowers the sealing strength significantly. Thus, the addition of $(CH_2=CH)(CH_3)Si(OEt)_2$ is incorporated to provide more flexibility to the resin by forming organic bridges within the inorganic network. IR analysis confirm the occurrence of the vinyl addition reaction upon heat treatment which results in additional crosslinking of the material. This last mechanism adds the necessary ingredient to achieve appreciable sealing strength for the applications suggested.

Even though the advances reported by Schmidt and co-workers have kept this group in the limelight of the sol-gel derived organically modified systems, Mark and co-workers also have made notable contributions to the area (12-15). Instead of developing new materials as Schmidt et al. have done, Mark's group set out to find alternate methods of improving the poor tensile strength and extensibility of the polydimethlysiloxane (PDMS) elastomers through the sol-gel approach. Their first investigation concerns itself with the effect of endcapping hydroxyl terminated PDMS with different functionality endgroups (13). Various mixtures of two low molecular weight PDMS oligomers ($Mn=660$ & $2.1x10^3$) have been studied by using tetrafunctional TEOS, trifunctional vinyltriethoxysilane ($ViSi(OEt)_3$) and phenyltriethoxysilane (PhSi(OEt)) as endcapping agents (actually the silane materials serve as chain extenders and crosslinkers). The sol-gel reactions were run under atmospheric conditions (i.e., low H_2O) employing stannous-2-ethylhexanoate as a catalyst. After a incubation period of a couple days in a sealed vessel, the PDMS samples gelled to form bimodal networks, and the mechanical properties of the nominal stress (f/A where f is the equilibrium elastic force and A is

the undeformed cross sectional area), the energy to rupture (ε_r), and the maximum extensibility were monitored.

Results show that as the shorter chain content is increased the f and f/A increases sharply at the higher elongations. This is expected due to the limited extensibility of the shorter chains, and accordingly these systems also have a lower ultimate elongation. Furthermore as the endcap functionality is decreased similar effects are observed. The f and f/A decrease along with the ultimate strength and the ε_r for most of the bimodal compositions studied. However, one interesting phenomena is noted relating the ε_r with the concentration of short chains. Specifically, the ε_r displays a maximum in the composition range of 90-100 mole % short chains. This observation has been suggested to result from contributing effects of both the short and long chains (13). The presence of the small amount of long chains is believed to reduce the brittleness of the network while the higher concentration of the short chains provide structural reinforcement. Thus at the maximum ε_r, an optimum balance is reached between the two opposing effects. However, one shortcoming of this work is revealed in other studies of a similar system by Wilkes and co-workers (20-21). This group has shown that the reaction conditions influence the dispersion of the PDMS oligomers and the silane species in the network which can ultimately have a strong effect on the materials mechanical properties. It seems Mark and co-workers have neglected this consideration totally in their short report (13).

In other work by Mark and co-workers (14), the authors have conducted a similar approach in preparing silica and titanium filled PDMS networks using the sol-gel technique. However in this experiment, the PDMS oligomer which is vinyl terminated is endcapped with triethoxysilane ($(EtO)_3SiH$) through a hydrosilylation reaction with a chloroplatinic acid catalyst before being used as a starting material. The most significant result of this investigation is that they have confirmed what Schmidt et al. have reported on the presence of titanium species (17-18). This starting material if reacted correctly has been found to serve as a reinforcing agent and a network promoter. Mark's observations indicate this same behavior by

reporting that the $Ti(OR)_4$ systems showed remarkably better mechanical properties which have been attributed to the greater degree of network formation.

One novel approach that Mark and co-workers (12,15) have undertaken to reinforce the PDMS network systems is by an in-situ precipitation of silica by a sol-gel reaction. This method is of considerable importance since it alleviates many of the processing complications (high viscosities and energy intensive) that arise in the traditional silica filled PDMS elastomers. The experimental procedure proposed is quite straightforward and easy to implement. All that is required is a simple swelling of an existing PDMS network with the TEOS monomer species. After the material has reached equilibrium swelling, the system is reluxed in the presense of glacial acetic acid and a phase transfer catalyst (tetrabutyl phosphonium bromide ($(n\text{-}Bu)_4PBr$)) to precipitate the silica within the PDMS matrix (see equation 2.14) (12).

$$Si(OEt)_4 + 2H_3CCOOH \xrightarrow{(n-Bu)_4PBr} SiO_2 + 2EtOH + 2H_3CCOOC_2H_5 \qquad [2.14]$$

If the swelling and refluxing process is repeated several times, a noticeable increase in SiO_2 content is achieved. Furthermore, the presence of the SiO_2 is reflected in the improvement of the mechanical properties of the PDMS elastomer. Both the f and f/A show distinct upturns at higher elongations which are not present in the unfilled systems. Thus, one can postulate that the silica precipitation serves to reinforce the PDMS network as a matrix filler.

Wilkes and co-workers have also studied the PDMS/TEOS sol-gel systems (20-21), but from a different perspective. Their investigations have shown that a notable stucture-property relationship exists between the content of the TEOS and the PDMS and the sol-gel reactions conditions used. In most of the sol-gel systems, the initial TEOS content is greater than 50% (weight %), and surprisingly the final materials display a flexible nature with a high degree of transparency under the reaction conditions employed. Even in the high 90/10% TEOS/PDMS, the rubber modified glass still shows flexibility, but due to large sample shrinkages only small pieces could be obtained. By monitoring the tanδ (the ratio the loss

modulus E″ to the storage modulus E′) and the storage modulus in a dynamic mechanical experiment, Wilkes and co-workers reveal that the PDMS exhibits a behavior reflecting a phase separated system (20-21). Since these materials are transparent, one must assume that the sizes of the phase domains are much smaller than what the wavelength of ordinary light can detect. In the tanδ spectrum, a peak occurring in the -100°C to -90°C region is present along with another peak centered at -10°C that has considerable breadth. Huang has attributed the low temperature peak to TEOS encapsulation of PDMS rich phases while the -10°C tanδ reflects a more dispersed or phase mixed PDMS oligomer in the network (see Figure 8) (20). The higher temperature tanδ results from the reduced mobility of the PDMS chains because the ends are more tied down within the TEOS matrix. One other interesting occurrence is noted for the E′. In all the TEOS/PDMS materials, the E′ shows an upward rise beginning at temperatures greater than 200°C. With speculation, Wilkes and co-workers have associated this unusual glass behavior with a rubbery elasticity effect (20).

By varying the sol-gel reaction conditions, Wilkes et al. have shown that there is a systematic effect on the mechanical behavior revealed in the dynamic mechanical experiments (20-21). For instance as the hydrolysis water is increased from R=2 to R=4, the tanδ spectrum changes accordingly. Since an increase in water content results in a more complete hydrolysis and a greater degree of network formation, the intensity of the tanδ in both the low and high temperature regions is suppressed. This result is believed to be due to two events occurring in the network: (1) a lower concentration of dangling free PDMS chain ends and (2) a higher degree of network formation which promotes further attatchment of the PDMS chains. Similar effects have also been observed with changing of the acid content (21). The tanδ in these experiments show that the low temperature peak at ca -100°C decreases with increasing acid content while the -10°C tanδ grows at the expense of the low temperature one (see Figure 8). Huang has attributed this effect again to the better dispersion of the PDMS oligomer in the glass matrix and to a lower degree of PDMS chain extension. From a hydrolysis perspective, the results coincide with what is expected since at higher acid contents (lower pH's) the hydrolysis reaction of the TEOS proceeds more rapidly. Thus, the PDMS chains have less of

a chance to self condense, and a better phase mixing results. Mechanical experiments reveal that the better phase mixed TEOS/PDMS materials (higher acid content) display a lower initial modulus and greater maximum extensibility.

A similar structure-property study has also been conducted by Huang, Glaser, and Wilkes (22) using a TEOS/polytetramethylene oxide (PTMO) hybrid material. In this work, the effects of the silicon alkoxide endcapped PTMO oligomer molecular weight, the TEOS content, and the addition of the titaniumisopropoxide on the physical properties of the elastomer modified glass were monitored. On the whole, the PTMO material's behavior parallels that of the PDMS systems as the reaction parameters are varied, but generally the TEOS/PTMO glasses have better mechanical properties than their counterparts. For example the 50/50% (initial wt%) TEOS/PDMS(2000 Mw) displays an ultimate strength and a maximum extensibility of ca 1.6 MPa and ca 105% ,respectively, while the 50/50% TEOS/PDMS(1700 Mw) has only a 1.1 MPa and a 8.0% ultimate strength and extensibility for roughly the same molecular weight oligomer.

Furthermore, the TEOS/PTMO hybrid glasses exhibit a similar microphase separation behavoir in the dynamic mechanical results like that occurring in the TEOS/PDMS materials. As discussed earlier, the phase regions are believed to result from the presence of two different molecular environments which place translational restrictions on the oligomer chains. These environments can be summarized as follows: (1) a well phase-mixed region where the oligomer endgroups are tied strongly to the inorganic network (Type 1), and (2) an oligomer phase-rich region that maybe is highly self-condensed and/or possibly encapsulated by a highly condensed TEOS network (Type 2) (22). The occurrence of the Type 1 & 2 behavior in the TEOS/PTMO glasses has been observed in differential scanning calorimetry (DSC) and small angle X-ray (SAXS) experiments, and also has been shown to be affected by the PTMO oligomer molecularweight and the TEOS content. For instance, as the molecular weight is increased from 650, 1000, 2000 for the PTMO (note that oligomer Mw is based on the unendcapped PTMO) , the glass transition temperature (T_g) shifts to lower temperatures, and the characteristic length of the interdomain spacing increases. Huang has attributed this ef-

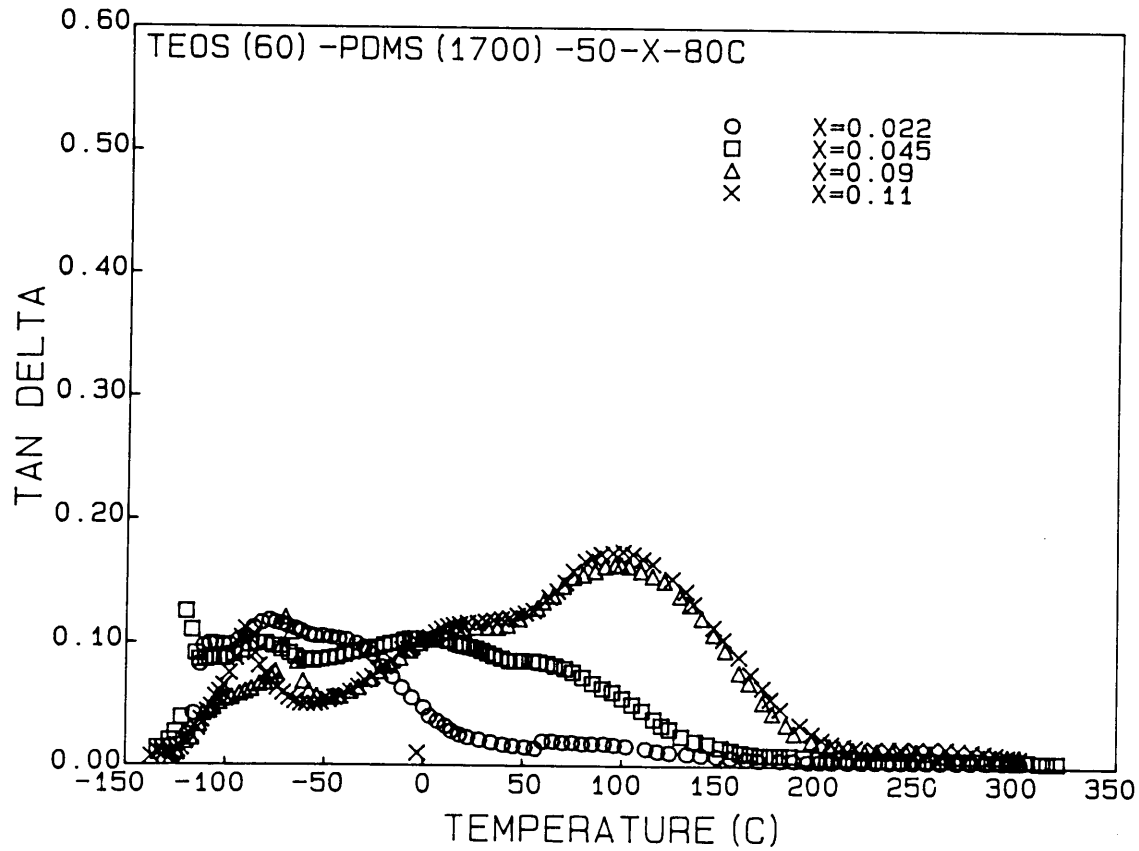

Figure 8. **Effect of acid content on the tanδ for a sol-gel prepared 48/52% TEOS/PDMS(Mw=1700) glass (21):** (◇) 0.022, (X) 0.045, (+) 0.09, and (△) 0.111 HCl/TEOS molar ratio.

fect to the poorer phase mixing of the higher molecular weight oligomers and their greater chain lengths which results in an overall decrease in both the Type 1 & 2 behaviors (22).

In the experiments where the initial TEOS weight percent is increased from 50 to 70, the authors report some interesting behavior in the mechanical properties (22). As one might imagine, the flexibility of the TEOS/PTMO materials for a set PTMO molecular weight decreases as the glass content is increased. However, the mechanical experiments show that there is a significant difference between the 50 & 60% and the 70% TEOS samples. The initial modulus of the 50 & 60% glass content species is almost twenty times lower than the 70/30% TEOS/PTMO sample. Such a large difference in modulus indicates that a significant change in the glass network structure has occurred. Wilkes et al. have suggested that a better dispersion of the TEOS and the PTMO regions has occurred in which a more 'co-continuous' structure may have developed (22). This type of behavior is believed to be a promoter of a Type 2 environment. Wilkes and co-workers in further studies using theoretical models and dynamic mechanical and SAXS experiments have supported this postulation, but due to the complexity of the subject it will not be covered presently (22).

The addition of titanium isopropoxide has also been found to affect the structure-property relationship of the PTMO/TEOS materials. Since in earlier work by Schmidt et al. (16-18) and Mark et al. (14), the presence of the titanium has been shown to be a network promoter or condensation catalyst for the inorganic sol-gel reaction, the results conveyed by Glaser (22) nicely follow with those reported in the literature. The mechanical data indicates that the titanium containing compounds increase the initial modulus (Young's modulus) and decrease the extensibility of the TEOS/PTMO based materials. This consequence is expected due to the titanium's ability to spur the formation of the inorganic network which produces a more brittle material. Further studies have been conducted using the SAXS and the dynamic mechanical techniques and their results also support the role of the titanium species as a condensation catalyst (22).

Besides the ormosil work presented here, the authors of Parkhurst et al. (39) and Riffle et al. (40) plus many others have begun to publish beneficial information on the different as-

pects of preparing and characterizing the organically modified silicates. In the future, if the current interest is sustained at the present level, the fruits from this science will grow accordingly and will hopefully reach the point to where this technique becomes a useful industrial process for specialized applications.

3.0 Experimental

3.1 Plan of Investigation

In the past, the preparation of organically modified sol-gel glasses have been primarily synthesized with elastomeric components of hydroxyl terminated PDMS and silane endcapped PTMO by Wilkes et al. (20-22). At the present time, only Schmidt and Phillip have attempted to incorporate a glassy component (below the T_g) in a sol-gel inorganic network (16-19). Their experimental method combines a sol-gel mechanism with an independent free radical reaction sequentially that requires a tedious and complex reaction procedure which this author feels can be a avoided. It is the intention of this author to simplify the method considerably by developing a suitable synthesis route that only necessitates the use of the sol-gel mechanism to incorporate the glassy oligomeric species. Thus, both the inorganic and organic multicomponent mixture can be reacted simultaneously to promote an efficiently intermixed inorganic-organic network in one simple step.

Wilkes and co-workers and Mark and co-workers have used this approach in the preparation of their rubber modified systems (20-21 & 12-15). In order to a make an ormosil glass by this manner, the organic or oligomeric species to be incorporated in the network must be functionally reactive with the silicon alkoxide precursor during the course of the sol-gel reaction. Two ways have been investigated in the literature (14,22) with both involving some form of an endcapping procedure to place silicon alkoxide functional groups on the ends of the

oligomer chains. The first method deals with the addition of trialkoxysilane to vinyl terminal groups located on at least two ends of the oligomer through a hydrosilylation reaction using a platinum based catalyst. Typically, the hydrosilylation reaction's yields are lower than 75%, and this may ultimately have a deleterious effect on the physical properties of the sol-gel derived ormosil glass (41). The other endcapping scheme relies on the principles of traditional polyurethane chemistry, specifically, the reaction of an isocyanate functional group with an amine or hydyroxyl terminated species to form either urea or urethane linkages. This reaction normally proceeds very rapidily at room temperature to extents greater than 95% with primary amines in the absence of a catalyst (42). Since an isocyanate functionalized trialkoxy silane is commercially available, this latter endcapping procedure offers a distinct advantage over the hydrosilylation reaction as long as the organic or oligomeric species can be amine or hydroxyl terminated. However, this linkage does have notable disadvantages which include a poor thermal stability and a susceptibility to urea or urethane hydrolysis during the sol-gel reaction.

Even though the urea and urethane endcapping procedure has inherent weaknesses, it still provides a very systematic approach to developing the sol-gel reactive organic precursors. All that is required is to find a sol-gel compatible amine or hydroxyl terminated oligomer of a manageable molecular weight. After a thorough inspection of several classes of glassy polymers, the amine terminated bisphenol-A-polyarylene-ether-ether-ketone (PEK) was selected. This polymer which was first synthesized at Virginia Tech. meets all the criteria specified for the endcapping and sol-gel reactions (43). In general, PEK is an amorphous engineering thermoplastic material with good solvent resistance, good thermal stability (i.e., $< 550^{\circ}C$), and a relatively high T_g of ca $130^{\circ}C$. This material is somewhat similar to the polyarylene-ether-ether-ketone (PEEK) family of polymers which are marketed by ICI Ltd. of the United Kingdom. The only real difference is that the PEK has a bisphenol-A linkage in the repeat unit which disrupts the crystallization of the polymer. Furthermore, the primary amine terminal groups of the PEK can undergo the isocyanate addition easily to form urea linkages

which consequently are more thermally stable than the urethane linkages due to the amine's greater hydrogen bonding capabilities.

In the remaining portion of this section, a brief overview is provided of the general methods of experimentation utilized in preparing and characterizing the PEK modified TEOS glasses. The first step required was the endcapping of the amine terminal PEK with isocyanatopropyltriethoxysilane to attach sol-gel reactive trialkoxy functional groups on the oligomer chain ends. After the endcapping of the PEK, then the organic precursor was mixed with a variety of TEOS contents (i.e., 0, 25, 50, 75 wt%), and sol-gel reacted to produce the **po**lymer **mo**dified **si**licate glasses termed '**pomosil**'. However before the sol-gel reaction procedure was initiated, a qualitative analysis utilizing an Infrared spectrometer (IR) was performed to verify the endcapped PEK product. Upon gelation of the final **PE**K/**TE**OS (**PETE**), the samples were vacuum dried to remove the residual solvents and then subjected to three different temperature thermal treatments (25, 100, & 200°C) for a specified time period. When the samples were returned to ambient temperature, a systematic method of experimentation was developed employing various characterization techniques to determine the effects of the thermal treatments and the TEOS content on the urea linkage and the overall pomosil stability, the degree of network formation, the glass transition temperature (T_g), and the mechanical properties of the PETE glasses. In addition to these investigations focusing on the structure-mechanical properties, a few experiments were conducted to clarify the temperature effects on the sol-gel derived pomosil materials by studying the curing kinetics.

The first experimental approach undertaken involved the soxhlet extraction of the thermally and non-thermally (25°C) cured samples to measure the sol fraction present. These results gave an indication of the completeness of the network formation. Furthermore by qualitatively identifying the extraction or sol residue by the IR technique, the effectiveness of the endcapping procedure and/or the damaging effects of the hydrolysis on the urea bond was monitored. However, the IR method can not generally distinguish between whether the endcapping reaction was unsuccessful or the urea degradation occurred. Nevertheless, the

IR technique provides a simple and efficient way of identifying what component remained unreacted after the completion of the sol-gel procedure.

In the second series of experiments, the physical and mechanical properties of the PETE materials were analyzed with differential scanning calorimetry (DSC), dynamic mechanical, and mechanical techniques. The DSC experiments provided an informative look at the pomosil's T_g and the endothermic/exothermic behavior during the temperature scan as a function of both the glass contents and prior thermal history. In the dynamic mechanical tests, similar information was derived from the storage (E') modulus and the tanδ behavior. Finally, the mechanical properties were investigated for a limited selection of samples (i.e., low glass content) to reveal the effects of the thermal treatment on the Young's modulus and the maximum extensibility. In addition to this set of experiments, small angle X-ray scattering (SAXS) tests were carried out in an effort to obtain an indication of the dispersion of the TEOS and the endcapped PEK in the pomosil matrix at the various glass compositions. Since the PETE materials displayed a behavior similar to those of the TEOS/PDMS (21) and TEOS/PTMO (22) systems, microphase separation was detected and associated with a characteristic length of the interdomain spacing as a function of the glass content. One other experimental method also was performed to show qualitatively the effect of the PETE composition and the temperature of the thermal treatment on the degree of network formation with IR spectroscopy. In this technique, the ratio of the relative intensity of the network $\equiv$Si-O-Si$\equiv$ asymmetric stretching band to the reference carbonyl stretching mode was recorded and compared for the PETE materials of differing glass contents and/or annealing treatments.

The final set of experiments was designed to shed light on the kinetics of the continuing curing reaction (sol-gel reaction) of the bulk PETE glasses revealed in the structure-mechanical survey relative to the temperature. Two different DSC methods were developed along with TGA experiments to provide information on this subject. The first DSC experiment's purpose was to show the progressive increase of a PETE sample's T_g after being exposed to higher and higher maximum scan temperatures. This DSC technique, hereafter referred to as 'stepwise DSC', was intended to indicate at what temperature the curing re-

action's effect on the on T_g becomes appreciable. The second DSC method termed 'stagewise DSC' was used to check the validity of the results found in the stepwise DSC experiments. Furthermore, TGA analyses were also used to confirm the temperature at which the onset of the curing reaction began along with giving an indication of the PETE material's thermal stability.

3.2 *Synthesis Methods*

3.2.1 Preparation of PEK Oligomer

The synthesis of the amine terminal PEK ($Mn \cong 5000$) was accomplished by varying the ratio of bisphenol-A to p-amino bisphenol-A and holding the amount of the 4,4'-difluorobenzenophenone constant (see Figure 9) (43). The starting reaction recipe consisted of 0.0922 moles of bisphenol-A, 0.016 moles of p-amino bisphenol-A, and 0.1 moles of 4,4'-difluorobenzophenone in 175 ml of NMP (n-methyl pyrrolidene). These materials were placed in a specially designed reaction apparatus (43) with 20.0 grams of anhydrous K_2CO_3 and 75 ml of tolulene (a transferring agent) with a constant nitrogen purge.

To start the reaction procedure, the precursor mixture was heated to the reflux temperature of 160°C, and water (a by product of the reaction) was removed via azeotropic distillation with toluene. After complete removal of the water was achieved, the toluene was separated and the remaining reaction mixture was heated to 170°C and held for a period of 8 to 10 hrs. Then the final reaction solution was cooled and diluted with 300 ml of THF. This solution was filtered through a fritted funnel to remove all the residual salts. The filtrate was pH = 7 balanced with glacial acetic acid and was added to a 75/25% methanol/H_2O mixture to precipitate the polymer. The collected polymer was vacuum dried at 80°C for 10 hours, and then repurified to insure the removal of all the residual salts and NMP (43).

SCHEME I

SYNTHESIS OF AMINE TERMINAL PEK

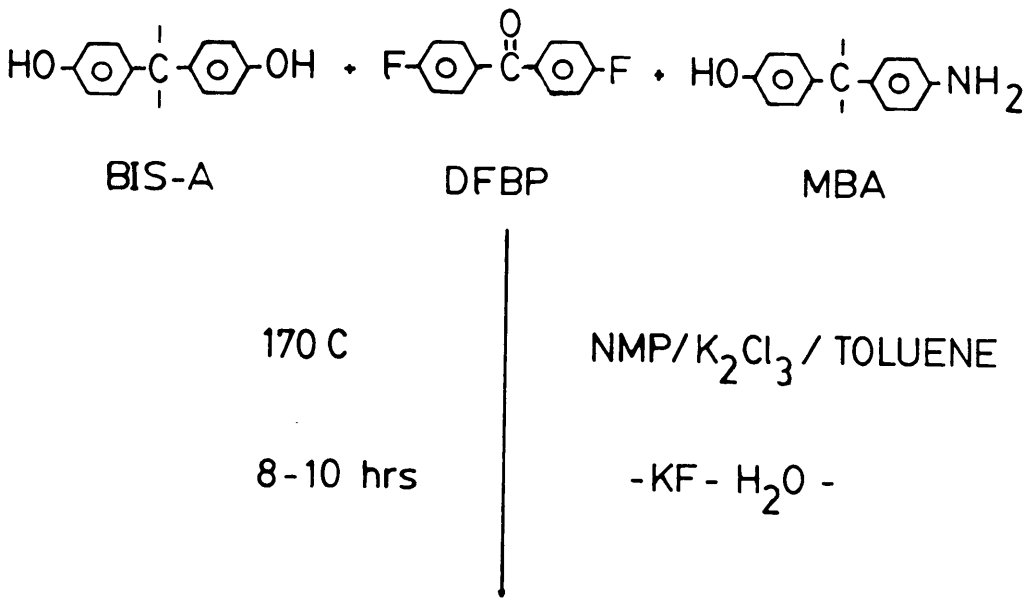

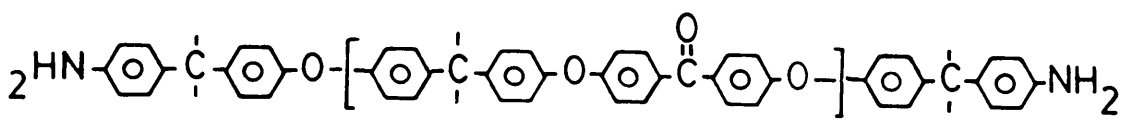

PEK

Figure 9. Reaction scheme for the synthesis of amine terminal PEK (43).

3.2.2 *Preparation of the endcapped PEK*

The synthesized amine terminated PEK (Mn≅3876) was endcapped with isocyanatopropyltriethoxysilane that was purchased from Petrach, Inc. and used without further purification (see Figure 10). The amine endgroups of the PEK were reacted with the isocyanate functional grouping of the endcapping material to form urea linkages. This reaction was carried out in dry tetrahydrofuran (THF) under a nitrogen atmosphere without the presence of a catalyst for a period of three hours. The isocyanatopropylytriethoxysilane and PEK amine groups were present in the reaction solution at a stochiometrical ratio of 1.25:1.0 (i.e., 25% excess endcapping agent). The final product mixture contained a 10 wt.% content of PEK in a THF based solution which was used as the organic starting material in the PEK/TEOS sol-gel derived glasses. However before the sol-gel reaction was performed, infrared spectroscopy was utilized to qualitatively analyze the extent of reaction.

3.2.3 *Preparation of the PEK/TEOS Glasses*

After the preparation of the endcapped material, the sol-gel technique was used to produce thin film samples with several different compositions. Samples were synthesized with the endcapped PEK and TEOS starting materials to form the glass compositions of 100/0% **PE**K/**TE**OS (**PETE**), 75/25% PETE, 50/50% PETE, and 25/75% PETE by weight (see equation 3.1). (Note that these pomosil compositions were based on the initial weight percent of the starting materials and are not truly representative of the actual composition of the final glasses). In all cases with the exception of the 100/0 PETE samples where an excess of water was employed, the hydrolysis conditions were as follows: 6 moles of water per mole of PEK plus two moles of water per mole of TEOS; 10 ml of THF per gram of PEK; a pH of approximately 2.0 adjusted dropwise with 10 N HCl. The reaction solution was refluxed for one half hour at 80°C and cast within Teflon molds. After gelation and vacuum drying to remove the

SCHEME II

ENDCAPPING OF AMINE TERMINAL PEK

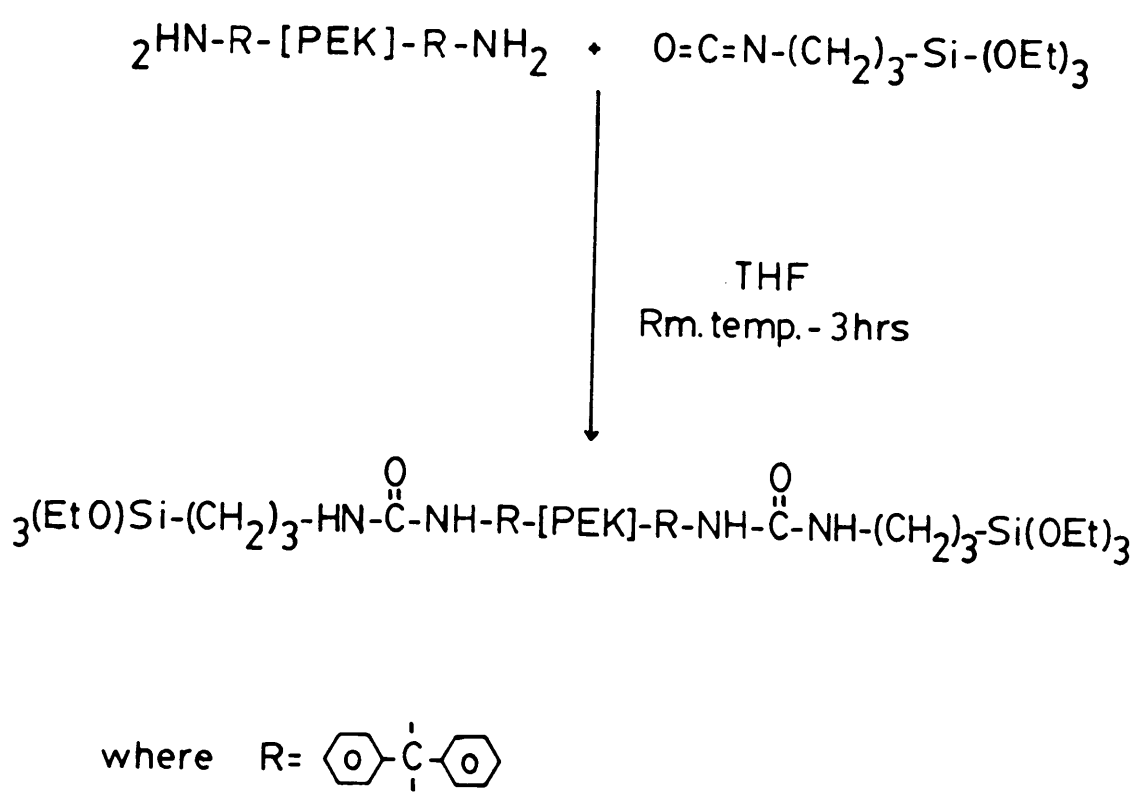

Figure 10. The endcapping reaction of amine terminated PEK with isocyanatopropyltriethoxysilane

residual solvent, the portions of the finished bulk product were then subjected to selected thermal treatments (25°C (control), 100°C, & 200°C) for a time period of six hours followed by a series of characterization studies.

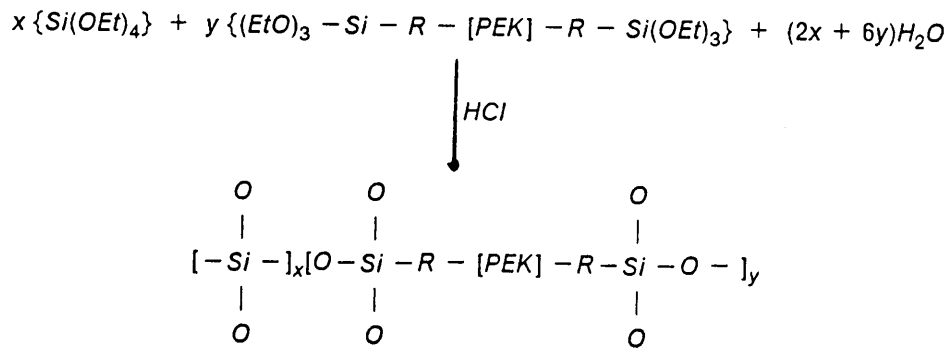

Scheme III

The PEK/TEOS Hydrolysis Condensation Reaction

3.3 *Characterization Methods*

3.3.1 Dynamic Mechanical Studies

The dynamic mechanical properties of the PEK/TEOS glasses were analyzed by a Toyo Baldwin DD-II-C Rheovibron Dynamic Viscoelastomer automated with a Hewlett Packard 9000 Series Model 216 computer and data station. The samples were temperature scanned with a 2-3°C/min rate and probed with 1/11/110 Hz to monitor the storage (E′) modulus and the tanδ behavior. Typically, the temperature range investigated was between 0-200°C, but for a

few runs the range was expanded to -130-200°C to check for sub-ambient transitions. Since no significant behavior was observed at the subzero temperatures, the majority of the data was collected over the 0-200°C region. Furthermore, the primary discussion of the results of the dynamic mechanical will focus on the data obtained with the 11 Hz frequency response.

3.3.2 Differential Scanning Calorimetry Methods

The T_g and the endothermic/exothermic behavior of the PETE pomosil glasses were monitored using a Perkin-Elmer DSC-4 Thermal Analyzer with a Model 3600 Data Station. Three sets of experimental conditions were employed to study the effects of the temperature history and glass content on the curing phenomena of the PETE materials. The first set involved the running of two consecutive DSC scans on a single sample from 25-300°C with instrument heating and cooling rates of 20°C/min and 320°C/min respectively. For the second set, stepwise DSC measurements were begun initially with a 25-100°C range, and the maximum scan temperature (Tmax) was incremented at 30°C intervals with each successive sample scan until a Tmax of 300° was reached. Again, the heating and cooling rates were 20°C/min and 320°C/min, but the sample investigation was limited to only the 25°C treated PETE materials. In the final set of experiments, individual samples of the 25°C cured category were subjected to variably timed isothermal preheating schemes at the temperatures of 100, 130, 160, and 190°C for hold times of 5, 10, 15, 20, and 30 minutes. After the sample received its specified thermal pretreatment, the material was then scanned from 25-300°C with the earlier prescribed heating and cooling rates to gather information on the effect of the prior thermal history on the PETE's T_g.

3.3.3 *Infrared Analysis*

IR analysis was performed using a Nicolet 5DXB FTIR Spectrometer with a 1 mW HeNe laser. The purpose of these experiments was to monitor the evolution of the network formation with increasing temperature thermal treatments of the PETE glasses. Also, this method was useful in identifying the extraction residue produced in the soxhlet extraction tests which gave an indication of whether degradation of the network was occurring during either the sol-gel reaction or the thermal treatments. Sample preparation of the PETE glasses were carried out using the KBr pellet technique, while the sol residue samples and other starting materials were analyzed as thin films cast on a KBr window.

3.3.4 *Mechanical Experiments*

The mechanical experiments were conducted with an Instron Model 1122 Mechanical Tester to determine the Young's modulus and maximum extensibility of the PETE glasses as a function of the curing temperature. (However due to the brittle nature of the higher glass content materials, only the 100/0% composition was able to be tested). Microdumbells 10 mm in length were the designated sample size, and a 20%/min initial extension rate was utilized.

3.3.5 *Small Angle X-ray Scattering Studies*

The SAXS investigation was carried out to detect the presence of microphase separation in the PETE pomosils and to establish a characteristic length of the interdomain spacing if a multiphase structure developed. A standard Kratky small angle X-ray camera was utilized with a Siemmens Ag Cu 40/2 X-ray source operated at 40 kV and 20 mA by a GE XRD-6 gen-

erator. The scattered intensity was monitored with a M. Braun position detetector marketed by the Innovative Technology, Inc.

3.3.6 Soxhlet Extraction Experiments

The soxhlet extraction experiments were performed to provide a qualitative indication of the degree of network information achieved through the sol-gel reaction and the post thermal treatments. Sample preparation of the PETE materials consisted of first a removal of all the dissolved solvents under vacuum, and then a finely chopping of the samples to increase the extractable surface area. All of the analyses were run in a standard soxhlet extraction apparatus using THF or methylene chloride as solvents for a minimum of 24 hours. The final weights of the PETE materials were measured to determine the amount the of sol fraction removed, and the extraction solvent was distilled off to recover the sol residue for identification purposes.

3.3.7 Thermal Treatments

The PETE glasses were exposed to 25, 100, 200°C thermal treatments for a period of six hours to additionally cure or to further the extent of the network formation. A Fisher Model 497 Isotemp Programmable Ashing Furnace was used to thermally treat the selected samples under atmospheric conditions. In all of the thermal profiles, a slow heating and cooling procedure was devised for each hold temperature to alleviate any problems that may be encountered from dissolved solvent evaporation and/or thermal expansion.

3.3.8 Thermogravimetric Analyses

The TGA measurements were made with a Perkin-Elmer TGS-2 Thermogravimetric Analyzer over the temperature range of 50-750°C with a 10°C/min scan rate in air. The purpose of these experiments was to provide a secondary confirmation of the continued thermal curing phenomena at the elevated thermal treatments. This was done by monitoring the weight loss occurring at certain temperatures which can be associated with the by-products of the sol-gel reaction. Furthermore, these tests also indicated at what temperatures the curing mechanism became significant and where the pomosil began to degrade.

4.0 Discussion of Results

4.1 Physical Aspects

In the early stages of the investigation before the heating treatments and the structural characterization studies were performed, it was necessary to substantiate as to whether the two step synthesis procedure utilized was successful in developing the desired pomosil glasses, specifically, a network glass that contains an inorganic-organic intermeshed matrix with covalent bonds serving as the junction interface between the inorganic and organic components. The first question that needs to be addressed is whether the amine terminal PEK was completely endcapped with the isocyanatopropyltriethoxysilane. IR analysis of the reactant PEK and the endcapped product indicate qualitatively that indeed the urea linkage had been formed which is representative of the endcapped PEK oligomer (see Figure 11). This can be determined by inspecting the 3450 cm^{-1} region of the IR spectrum of the both the reactant and product materials. The reactant PEK has a primary amine terminal group which produces two sharp but weak N-H stretching bands in the 3450 cm^{-1} region while in the endcapped PEK, the newly formed urea linkage results in the development of two secondary -NH- functionalities. The secondary -NH- groups, located adjacent to the potentially strong electron withdrawing carbonyl, give rise to only one broad and weak intensity N-H stretching band in the same region. Cursory survey of the IR spectrum of the reactant and product PEK's support the occurrence of the endcapping reaction, but reveal very little information on the

extent. Since both the primary and secondary amines absorb in the 3450 cm^{-1} region and may superimpose on one another, it is hard to accurately calculate the extent of reaction using this technique. Nevertheless, the absence of the two primary amine bands and the strong presence of the secondary -NH- stretch clearly suggest that the endcapping reaction's extent is relatively high ($>95\%$) which is expected from the literature (42).

The second question that must be addressed pertaining to the synthesis of the PEK/TEOS (PETE) glasses is whether the sol-gel reaction has any deleterious effects on the urea linkages. For example, if the urea linkage is hydrolyzed during the sol-gel reaction, the endcapped PEK reverts back to the amine terminal form and becomes only a filler in the inorganic-organic network. The last situation is also evident if at least one of the amine terminal bonds is not properly functionalized with the addition of the trialkoxysilane through the endcapping reaction. Thus, after the preparation of the 100/0%, 75/25%, 50/50%, and 25/75% PETE glasses, samples of the materials were subjected to soxhlet extraction to remove any free PEK, if any, which underwent subsequent IR analysis to check for the presence of primary amine functional groups. The occurrence of the two primary N-H stretches in the 3450 cm^{-1} region should provide a good indication of urea degradation and/or the incompleteness the endcapping reaction.

The initial soxhlet extraction experiments of the different composition PETE samples reveal that a poor degree of network formation is being achieved by the sol-gel reaction procedure. This is shown by the relatively high percentage of sol-fraction observed in the uncured (25°C cured) PEK/TEOS materials (see Table 1.0). However, IR analysis of the soxhlet extraction residue (sol-fraction) produce some interesting data. The IR spectrum of both the extraction residue and the endcapped PEK starting material are identical which suggests that the incomplete network formation is the result of a poor extent of the sol-gel reaction and is not likely a degradation and/ or endcapping problem (see Figure 12). This last finding is further confirmed by the soxhlet extraction results. Inspection of the percentage sol-fraction as the glass content is increased for the 25°C cured samples display a notable trend (see Table 1.0). That is, as the glass content of the PETE system is increased, the sol-fraction percentage

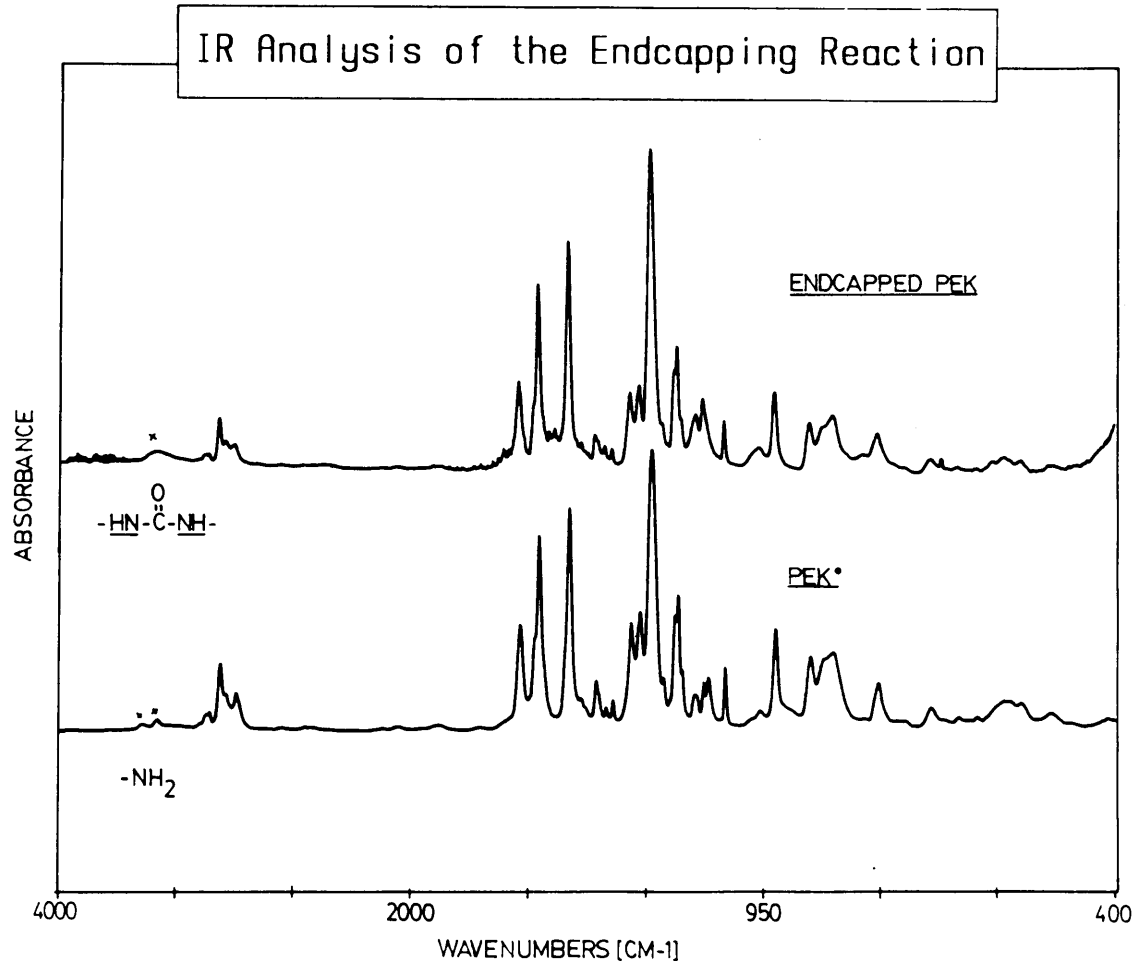

Figure 11. IR analysis of the isocyanate endcapping reaction.

drops accordingly. For instance, 100/0% PETE has a 25.8% sol-fraction while the 25/75% PETE has only 2.44%. This phenomena is attributed to a greater degree of network formation occurring in the higher glass content mixtures. This is to be expected since the addition of the TEOS precursor adds four more potential network sites per monomer which in turn enhances the probability of the trialkoxysilane terminated PEK being incorporated into the network.

In the lower glass content materials, especially the 100/0% PETE species, it is believed that the lower degree of network formation results from vitrification. As the sol-gel reaction continues, the T_g of the entire system increases due to an overall molecular weight buildup and finally approachs the temperature of cure where vitrification occurs. As a result, the glassy PEK oligomer drops below its relative T_g and the mobility of the chain is severly restricted. This restricted mobility which apparently develops somewhat above gelation reduces the probability of the trialkoxysilane endgroups finding a functional reactive partner to form the inorganic bridges necessary to produce the pomosil network. Thus, a poor extent of reaction results which is reflected experimentally in the high sol-fraction percentages. Furthermore, as the glass content is increased the vitrification problem causes less of an obstacle to the network formation because the higher concentration of the four functional TEOS provides a greater chance for the endcapped PEK oligomer to undergo at least one condensation reaction.

To alleviate the vitrification problem, thermal treatments were employed to overcome the diffusional and/or kinetic limitations developed during the gelation process. By heating the PETE samples at the prescribed temperatures of 100 and 200°C for 6 hrs, a remarkable difference in the sol-fraction is noted (see Table 1.0). The sol fraction of the 100°C cured samples dropped dramatically to lower than 5.0% for all the PETE compositions while the 200°C cured PETE materials slightly gained weight during the extraction experiments which is still currently an unsolved mystery. After some preliminary investigations into the problem, certain experiments have shown that the weight uptake is not due to absorbed water and/or the changing of the PETE chemistry. The only plausible explanation at this time is that the 200°C cured system's network structure is so dense that it has trapped a some residual of solvent in the

Table 1. Soxhlet Extraction Results.

SOXHLET EXTRACTION RESULTS FOR PETE GLASSES

SAMPLE	Mw PEK	WT.IN(g)	WT.FIN(g)	%EXTR.
100% PEK				
NO CURE	4000	1.0576	0.7840	25.80
100 C CURE	4000	0.2126	0.2038	4.40
200 C CURE	4000	0.2657	0.3003	-13.02
75/25% PETE				
25 C Cure	4000	-------	-------	-------
100 C CURE	4000	0.2411	0.2397	0.58
200 C CURE	4000	0.4199	0.4835	-15.15
50/50% PETE				
25 C Cure	4000	0.9340	0.7696	17.60
100 C CURE	4000	0.2669	0.2599	2.62
200 C CURE	4000	0.3032	0.3315	-9.33
25/75% PETE				
25 C Cure	4000	0.4432	0.4324	2.44
100 C CURE	4000	1.0065	0.9941	1.23
200 C CURE	4000	0.2819	0.2807	0.43

SAMPLES WERE CURED FOR 6 HRS IN AIR

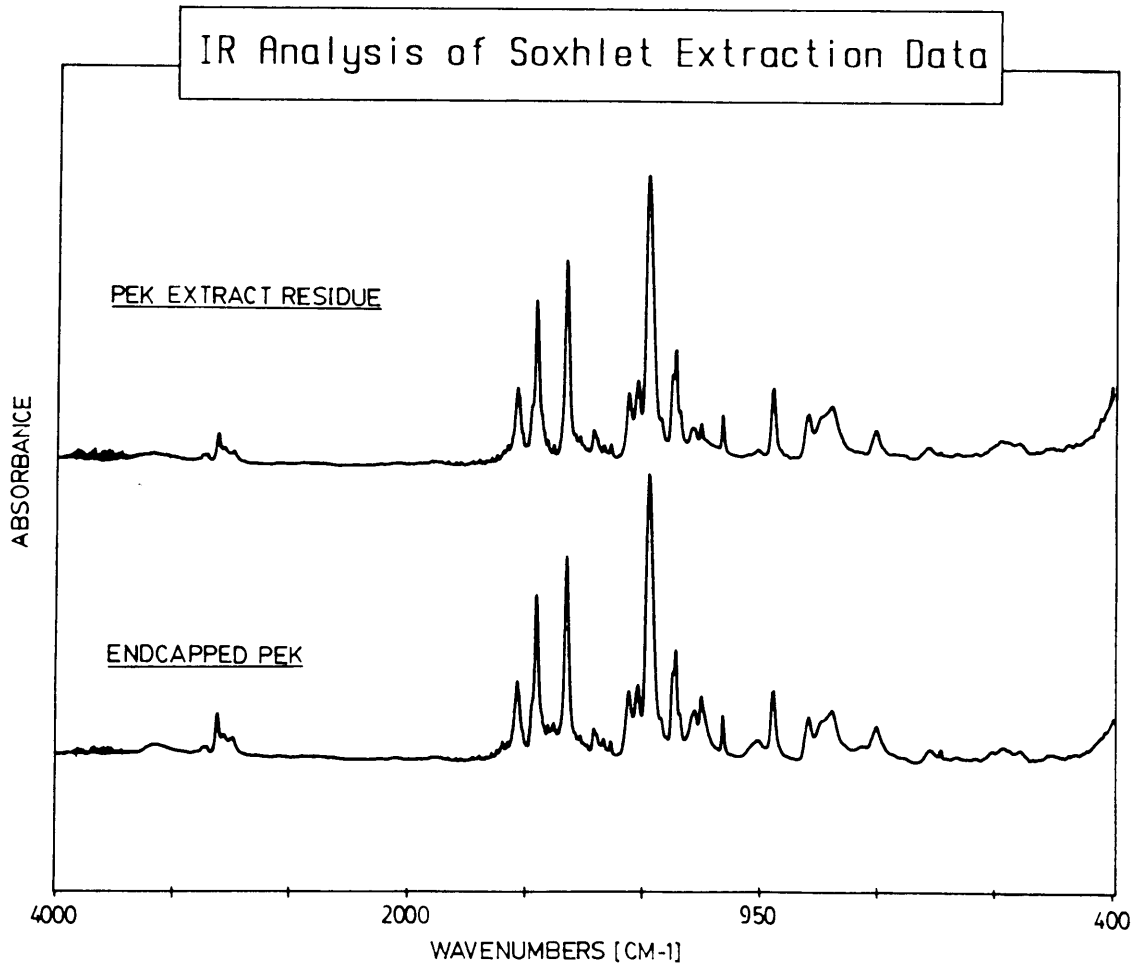

Figure 12. IR analysis of endcapped PEK and soxhlet extraction residue (sol-fraction).

matrix during the extraction process. Even after dehydration experiments at 200°C for extended periods, still no appreciable weight loss is observed. This last result reflects the baffling nature of this phenomena, and since it does not appear to have occurred through some form of degradation, the author has let this question remain unanswered for now.

Even though the 200°C cured materials appeared to have gained weight after extraction, the general scope of the results show a systematic decrease in the sol-fraction as the temperature of the thermal treatment is increased. This occurrence is associated with the continued sol-gel curing of the PETE materials during the heat treatments, and a more thorough account of this effect is discussed in the following sections. In short, the thermal treatments allow the endcapped PEK oligomer to overcome the kinetic and/or diffusional limitations present at ambient temperatures, so the organic constituent of the pomosil may participate in the sol-gel reaction more effectively and become apart of the matrix structure.

In addition to the reduction of the sol-fraction with the 100°C and 200°C thermal treatments, the speculative physical appearance and physical properties reveal a substantial change. Lets first summarize the physical nature of the sol-gel derived glasses that have not been thermally cured. For instance, all of the PETE glasses (100/0%, 75/25%, 50/50%, & 25/75%) prepared by the sol-gel process are crack free and monolithic in form and can be shown to form a hard and scratch resistant coating when cast on a wood, metal, or glass substrate which is one potential application for this material. They possess a yellow-gold hue similar to that of the pure PEK oligomer and are transparent with the exception of the 50/50% PETE system. In the latter system, misicibility problems of the PEK and TEOS result in a phase separated system. Generally, as the amount of the TEOS content is increased in the PETE material, the sample brittleness increases along with the sample shrinkage during gelation. The 100/0% PETE glass have no notable sample shrinkage, a fairly flexible nature, and a smooth texture somewhat similar to that of a mylar film while the 25/75% PETE glasses experience large sample shrinkage, brittleness, and as might be expected a more inorganic glass-like behavior.

After the thermal treatment of the PETE systems at 100 and 200°C, the appearance of the pomosil glasses is altered significantly in comparison with the 25°C cured control group. In all cases, the curing process results in a darkening of the glasses. For example, the 100°C cured glasses develop a slightly darker shade of yellow-gold whereas the 200°C materials exhibit a vivid auburn color. Also with increasing temperature thermal treatments, the samples experience greater sample shrinkages which is associated to the densification of the materials from the continuing sol-gel reaction. In the 100/0% PETE, the volume is reduced by ca 6.8% and ca 10.2% for the 100°C and 200°C treatments while the 25/75% volume is reduced significantly more. However, the volume shrinkage of this particular composition was hard to determine because the material warped and cracked into smaller pieces at the higher thermal treatments. Beside these observations, a distinct difference in the mechanical properties is noted. The 100°C treated samples are tougher than the 25°C cured control group, but the 200°C are more brittle than the 100°C which is especially evident in the higher TEOS content systems (i.e., 50/50% & 25/75% PETE). This last artifact is attributed to the enhanced level of crosslinking or connectivity occurring in the pomosil glasses. In the 25°C cured material, the poor degree of network formation has produced a brittle material through the lack of structural integrity, while the 100°C cured intermediate group has attained a level of crosslinking where the mechanical properties are appreciable. Finally, under the 200°C thermal treatments, the degree of crosslinking has proceeded to the point where the mechanical properties begin to reflect an increased brittleness. Thus offhandedly, one can suggest that the PETE glasses follow the theoretical nature of a crosslinked system in which at low and high degrees of crosslinking poor mechanical properties are observed.

One other point that deserves mentioning is the significant weight loss occurring through the removal of the ethoxy functional groups during the poly(hydrolysis-condensation) reaction. Up to this point, the sol-gel glasses have been referred to as having the compositions of 100/0%, 75/25%, 50/50%, and 25/75% PETE which are based on the initial weight percent of the added PEK and TEOS in the starting reaction mixture. Truly, these compositions do not accurately represent the final glass compositions formed through the sol-gel reaction. For

example, hypothetically if the poly(hydrolysis-condensation) mechanism is carried out to an extent of 100%, the PEK undergoes a ca 3.4% weight loss while the TEOS loses ca 71% of its initial weight which changes the beginning PETE glass compositions from 100/0%, 75/25%, 50/50%, and 25/75% to the final ones of 100/0%, 91/9%, 77/23%, 53/47% PEK/TEOS, respectively. Thus in the real situation, the final PETE material's composition lies somewhere between these two respective extremes depending on the extent of the sol-gel reaction. Since the extent of the sol-gel reaction has not theoretically or experimentally been determined for these systems, the initial weight percent compositions will be used as the principal nomenclature even though these values do not reflect the true composition of the posmosil glass.

4.2 Structural/Mechanical Effects of Thermal Curing

After subjecting the PETE glasses to thermal treatments of 100°C and 200°C, already notable changes have been found in the physical and mechanical appearance of the glasses through the soxhlet extraction tests and the experimental observations. These results tentatively suggest that the underlying sol-gel reaction is continuing during the thermal treatments to produce a greater crosslinked species. In light of this, it is informative to show through other experimental techniques (i.e., DSC, dynamic mechanical, mechanical, etc) how the structural and mechanical nature of the systems are also affected by the thermal treatments.

In a general sense, the curing phenomena can be discussed in view of the Time Temperature Transformation (TTT) diagram proposed by Gilham (44) for the epoxy network systems to envision the effects of the thermal treatment on the PETE's T_g and degree of network formation. Typically, the higher temperature thermal treatment produces a network system with a higher T_g as long as degradation does not occur (see Figure 13). Simplistically, the PETE materials should also fit this pattern even though there are inherent differences between the PETE systems and the epoxy materials for which the TTT diagram was developed for. For

instance, the TTT diagram applies to a continuous thermal curing of a monomeric species at a set experimental curing temperature that evolves a network with a T_g consistent with this experimental temperature. In the PETE systems, the thermal curing process is not continuous, and the PEK has already a set bulk T_g before thermal curing begins. As a result, the T_g of the PETE material is not consistent with the experimental curing temperature.

Nevertheless, by subjecting the PETE glasses to subsequent thermal treatments of 100°C and 200°C, the network T_g should obey the guidelines established by the TTT diagram. For example, when the PETE reaction solution is allowed to gel at room temperature, this step can be represented by a horizontal line on the TTT diagram at the lower end of the temperature scale. Since the material at this reaction temperature encounters vitrification problems, the curing line stops just beyond the gel-liquid interface (gel-point) which is somewhat representative of the PETE's T_g and of the degree of network formation achieved (point 1 on Figure 13). At this point, then two of the samples are given step temperature jumps shown as vertical lines on the TTT diagram (note that the vertical lines are not the actual paths of curing process, but only a schematic representation) placing the final state of these samples deep into the gelled glass region (points 2 & 3 on Figure 13). In the PETE's case, the 200°C cured glass lies deeper and higher on temperature scale than either the 100°C or 25°C cured samples signifying a higher T_g and a greater degree of network formation.

The DSC measurements of the PETE's T_g nicely follow with the behavior predicted by the TTT diagram of Gilham (44). In the survey of the DSC 1st scans of the 100/0% , 75/25% , 50/50% , and 25/75% PETE glasses as a function of cure temperature, it is clearly evident that the pomosil T_g increases distinctly for the 100°C and 200°C thermal treatments with the exception of the 25/75% PETE (see Figure 14-17). This material's glass content is so high that the PEK oligomers transition is hard to distinguish between the endothermic/exothermic behavior occurring during the scan. The remaining compositions of the PETE glasses follow the general trend of the increasing T_g with the higher temperature thermal treatment. Also, one can note a change in the endothermic/exothermic (evaporation of solvent or H_2O/heat of reaction) behavior associated with the continuing sol-gel reaction during the DSC scan. This

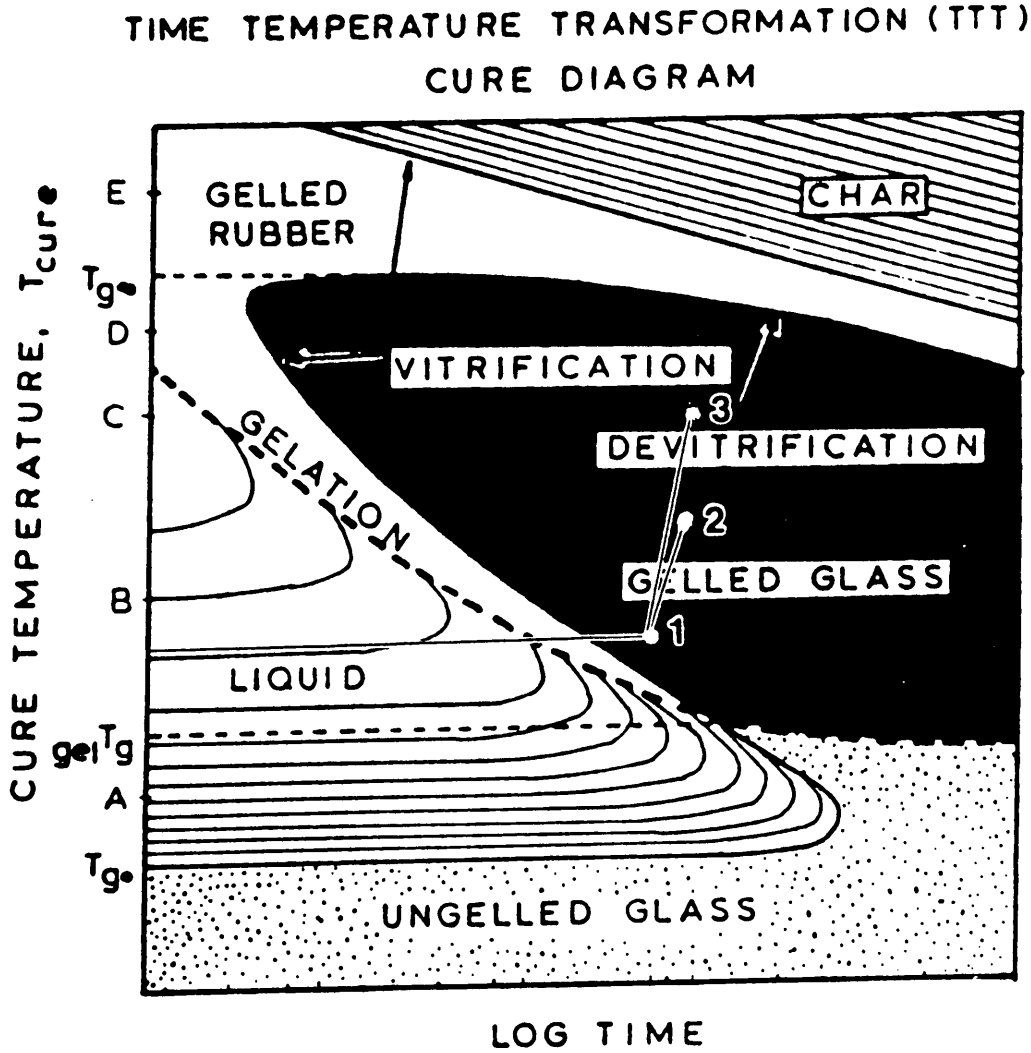

Figure 13. Time Temperature Transformation diagram from Gilham (44).

effect normally begins to appear just after the onset of the PETE's T_g and carries on up to temperatures of ca 200°C. In the 100°C thermally treated samples, the temperature range of the complex endothermic/exothermic behavior is decreased significantly while in the 200°C cured PETE materials this effect is hardly noticeable (see Figures 14-17). One interesting situation occurring in the 25°C control group glasses is that the PETE glasses display a substantially lower T_g (ca 70°C) than what is found for the pure PEK oligomer ($T_g \cong 130°C$). This phenomena has been attributed to a plasticization effect of the PEK sol-fraction present in the uncured PETE materials.

By inspecting the DSC 1st scans as a function of glass content for a set cure temperature, the complex endothermic/exothermic effect can be shown to be a direct result of the continuing sol-gel process (see Figures 18-20). For example, as the glass content is increased for the 25°C cured PETE glasses, the transition appearing at approximately 70°C grows substantially with increasing glass content. This evidence suggests that the endothermic/exothermic nature observed is associated with the sol-gel curing of the TEOS species during the DSC scan. Once again if the 100°C and 200°C treated material's DSC scans are surveyed, the endothermic/exothermic behavior decreases systematically with the higher temperature thermal treatments. This last result indicates that in the 100°C and 200° curing treatments, the PETE samples have already completed much of the the sol-gel reaction that is evident during the 25°C control group DSC scans.

Furthermore, if the same PETE samples are scanned again under the exact conditions as before, there is a curious effect of the DSC 1st scan's thermal history on all of the PETE glasses T_g's. For instance, the 100/0% , 75/25% , and 50/50% pomosils all display relatively the same T_g (i.e., $\sim$175°C) for the three different thermal treatments (see Figures 21-24). In short, the previous DSC sample scan up to 300°C at 20°C/min removed the effects of the prior sample history and implemented a new one. This new thermal history, which is the same for every DSC scan, is reflected throughout the PETE compositions by developing a network structure with a fairly consistent T_g . This last phenomena follows in accordance with the T_g behavior predicted by the TTT diagram.

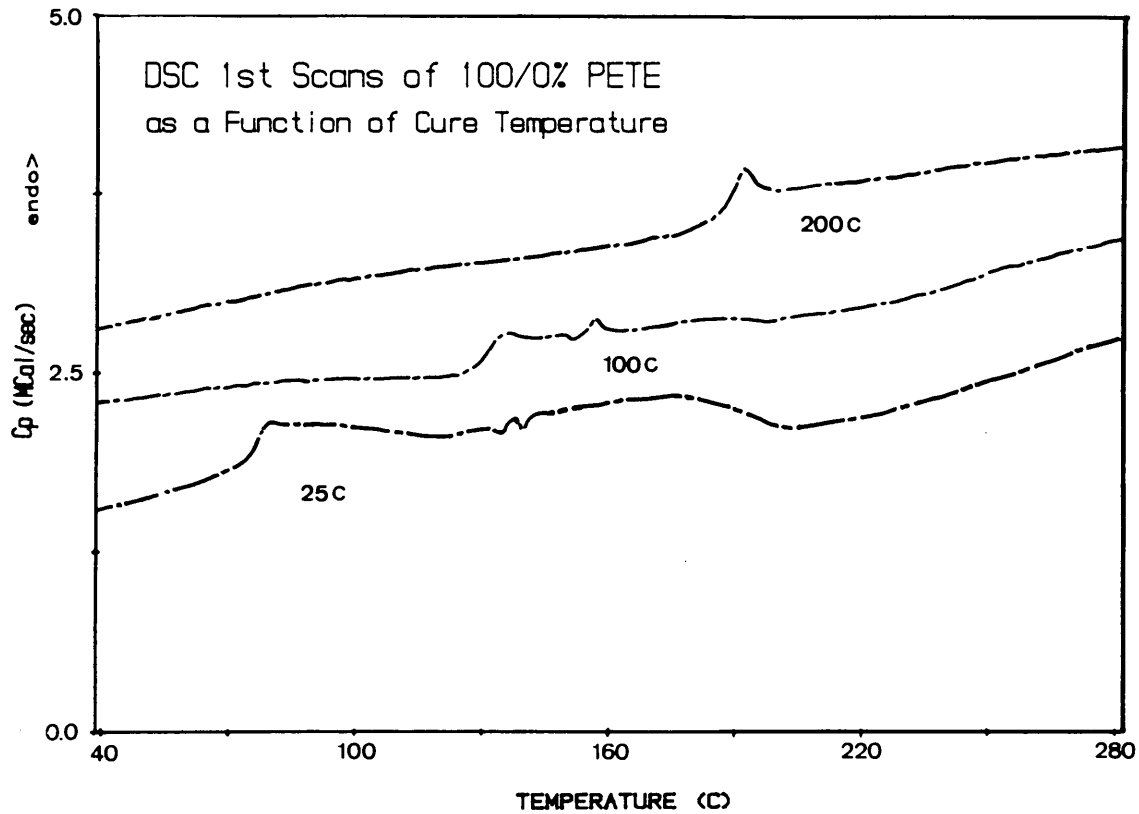

Figure 14. DSC 1st scans of 100/0% PETE as a function of cure temperature.

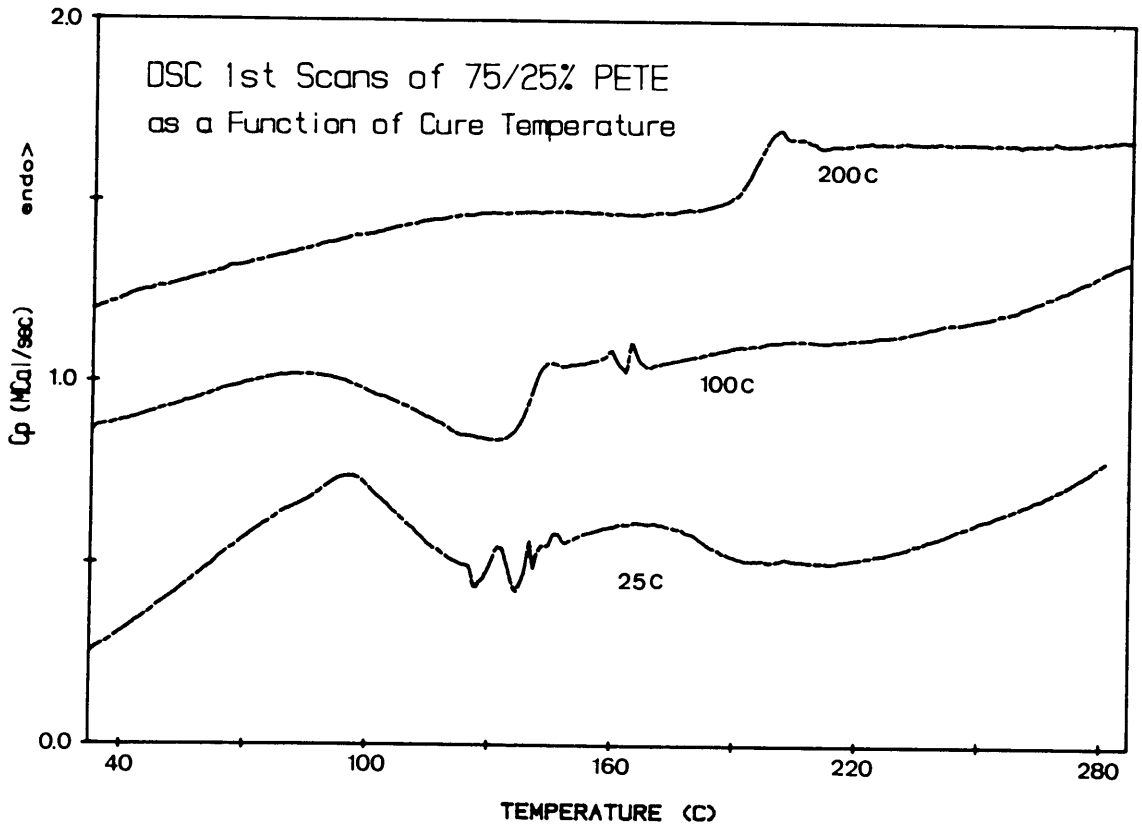

Figure 15. DSC 1st scans of 75/25% PETE as a function of cure temperature.

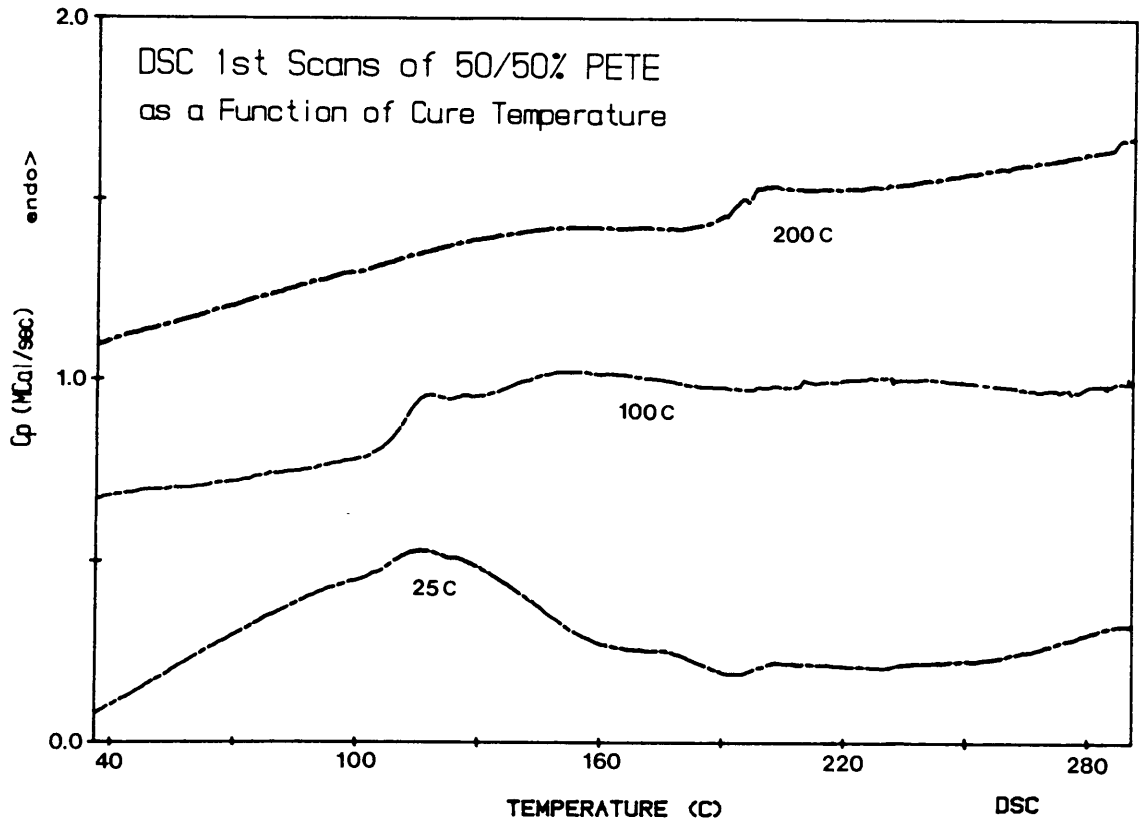

Figure 16. DSC 1st scans of 50/50% PETE as a function of cure temperature.

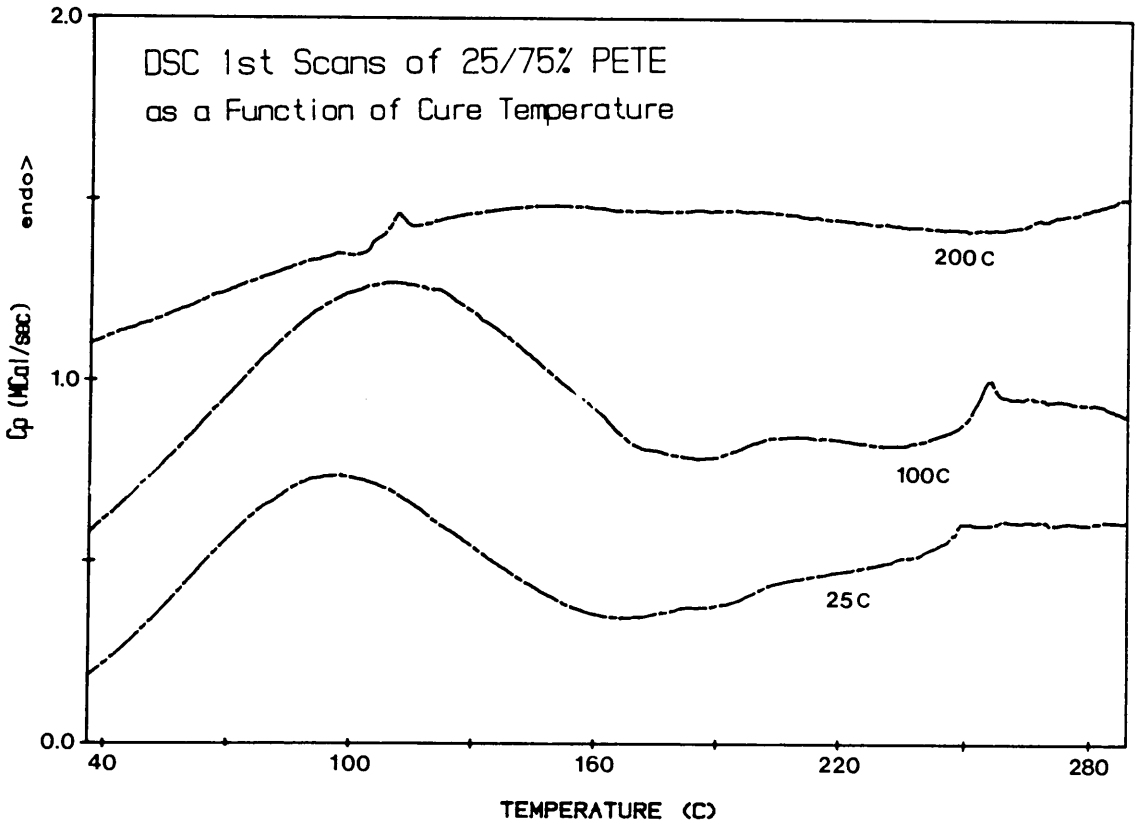

Figure 17. DSC 1st scans of 25/75% PETE as a function of cure temperature.

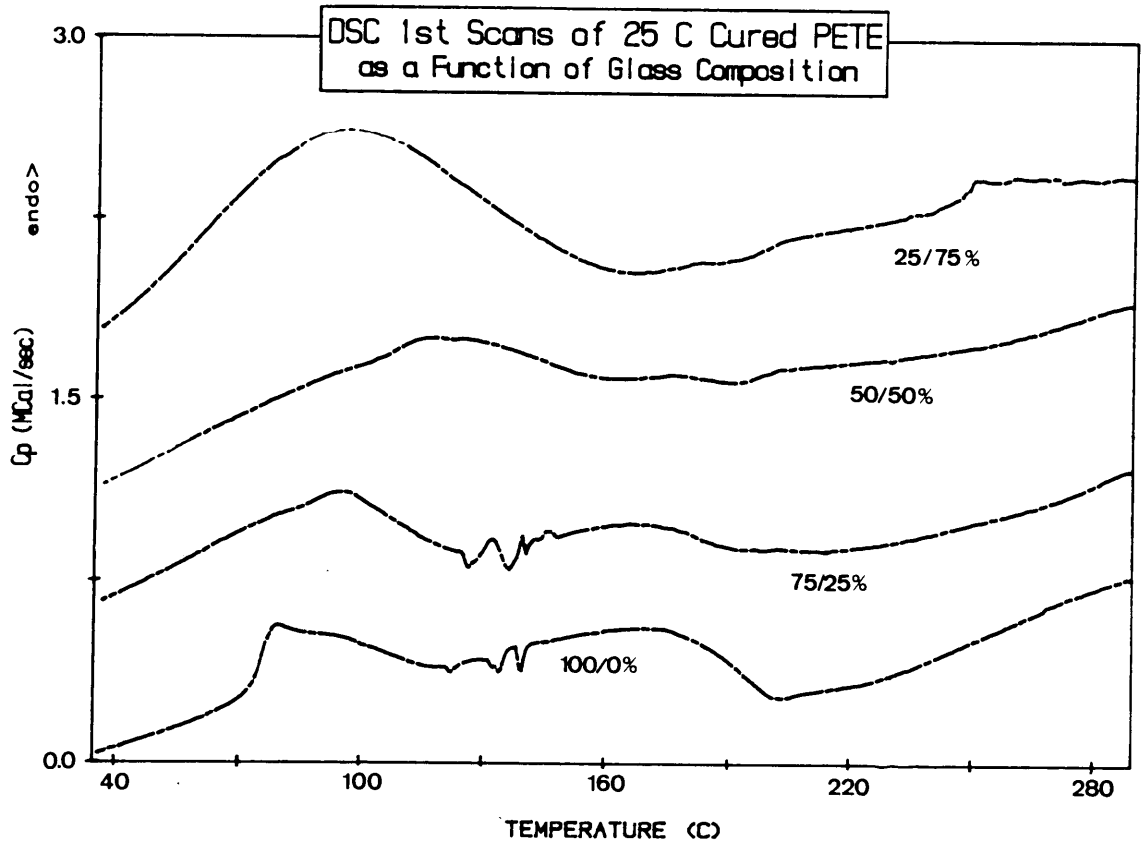

Figure 18. DSC 1st scans of 25°C cured PETE as a function of glass composition.

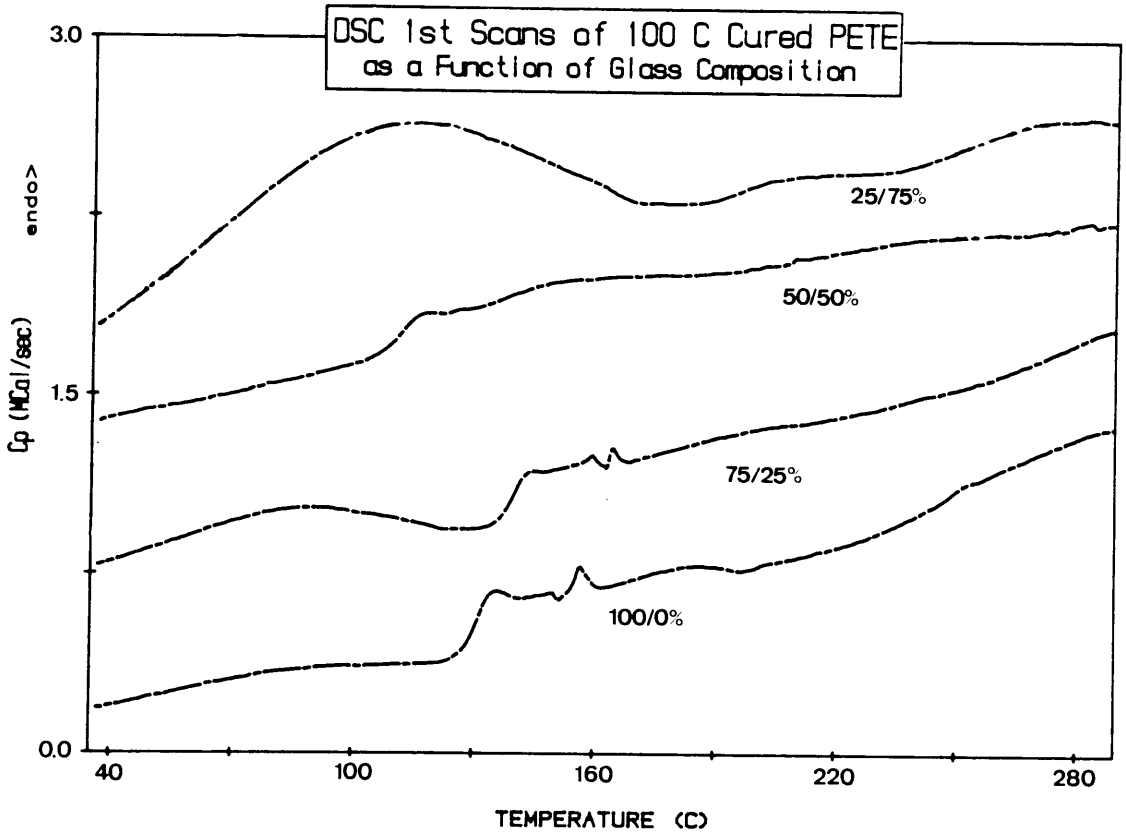

Figure 19. DSC 1st scans of 100°C cured PETE as a function of glass composition.

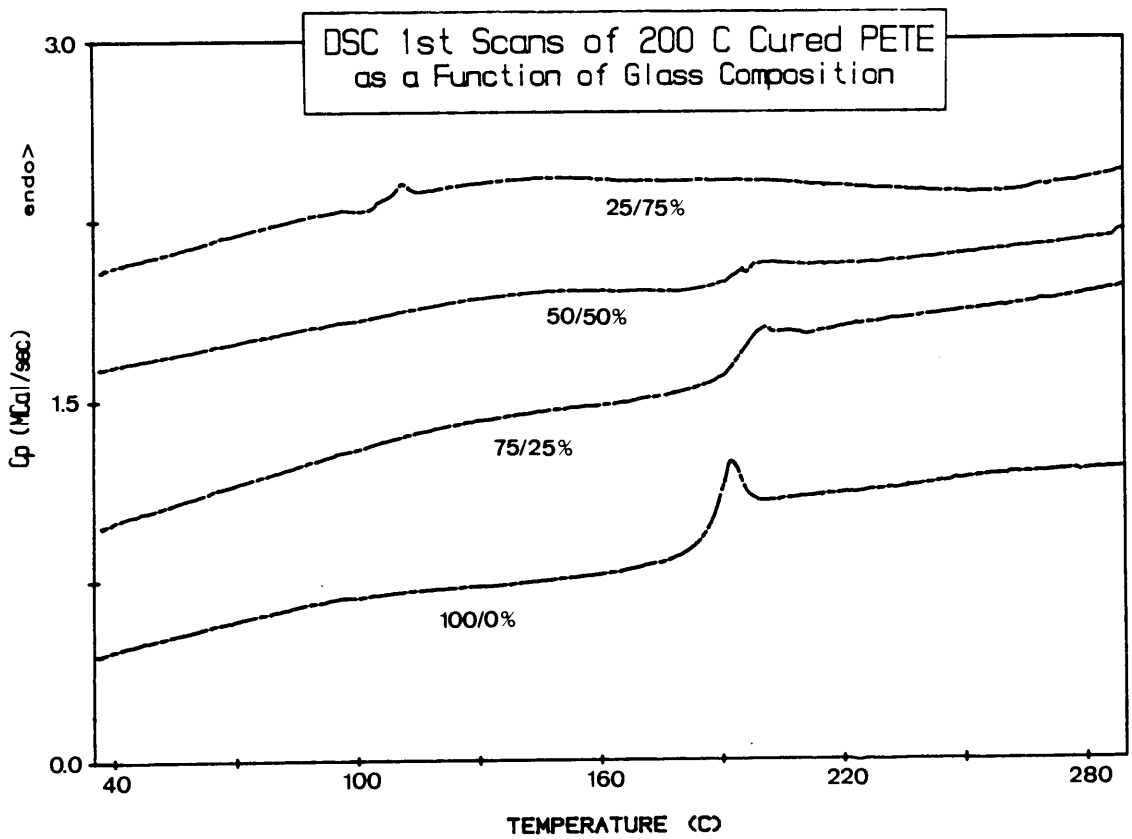

Figure 20. DSC 1st scans of 200°C cured PETE as a function of glass composition.

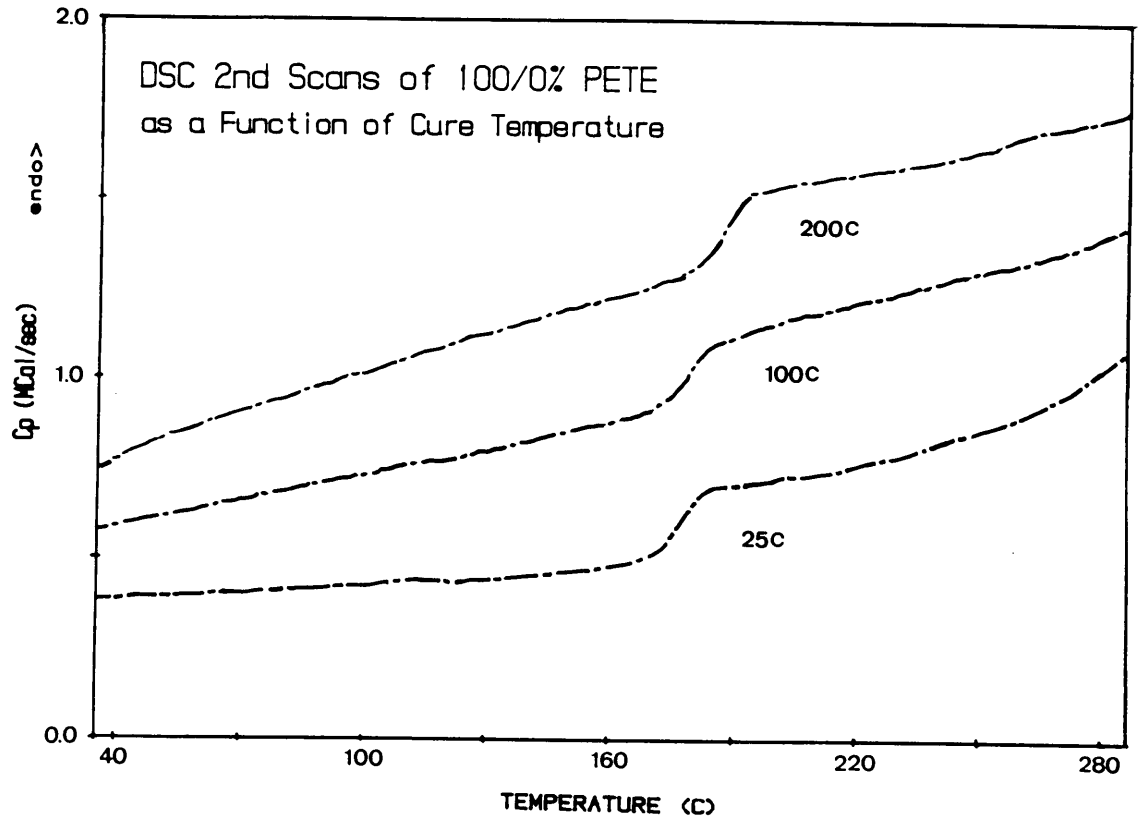

Figure 21. DSC 2nd scans of 100/0% PETE as a function of cure temperature.

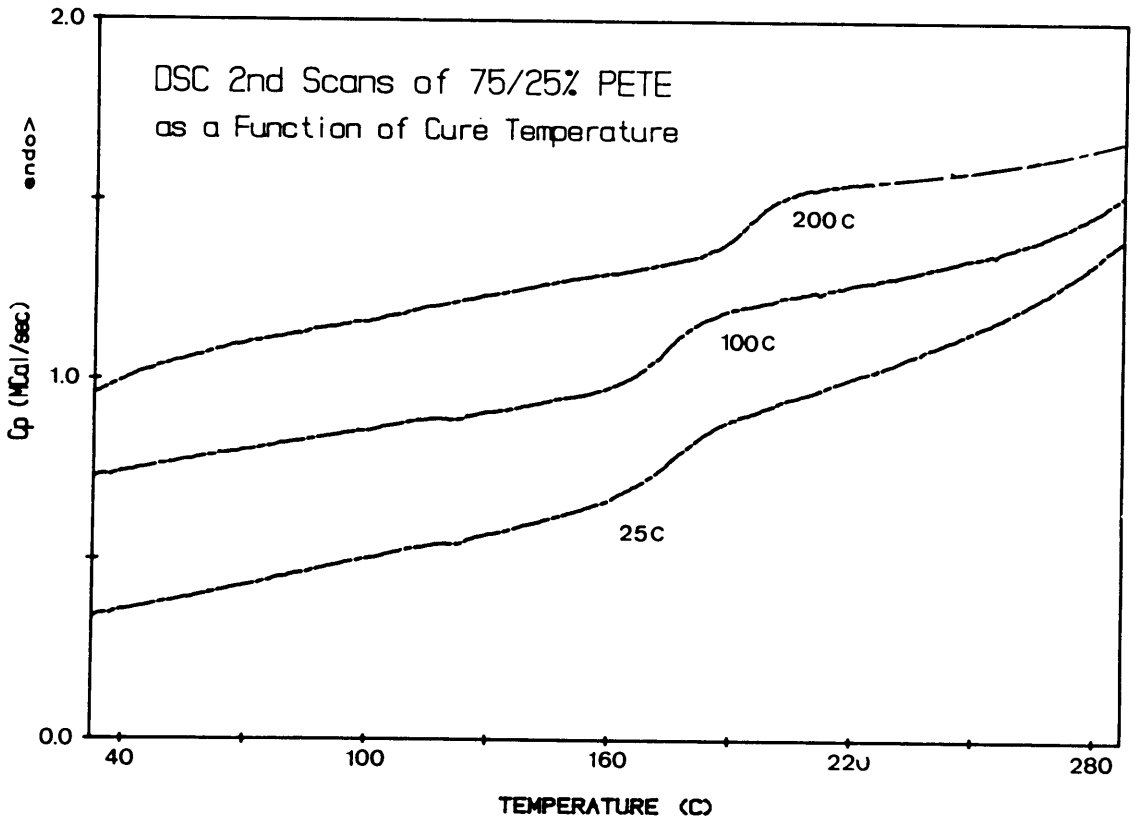

Figure 22. DSC 2nd scans of 75/25% PETE as a function of cure temperature.

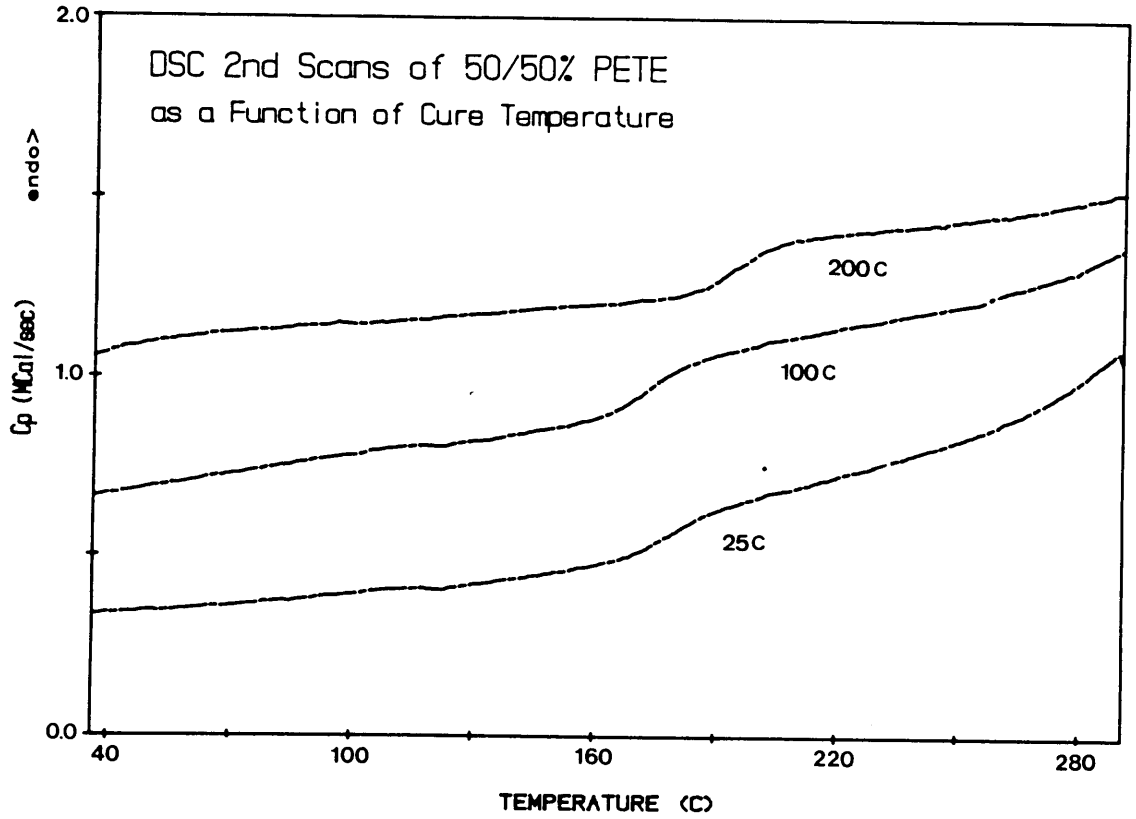

Figure 23. DSC 2nd scans of 50/50% PETE as a function of cure temperature.

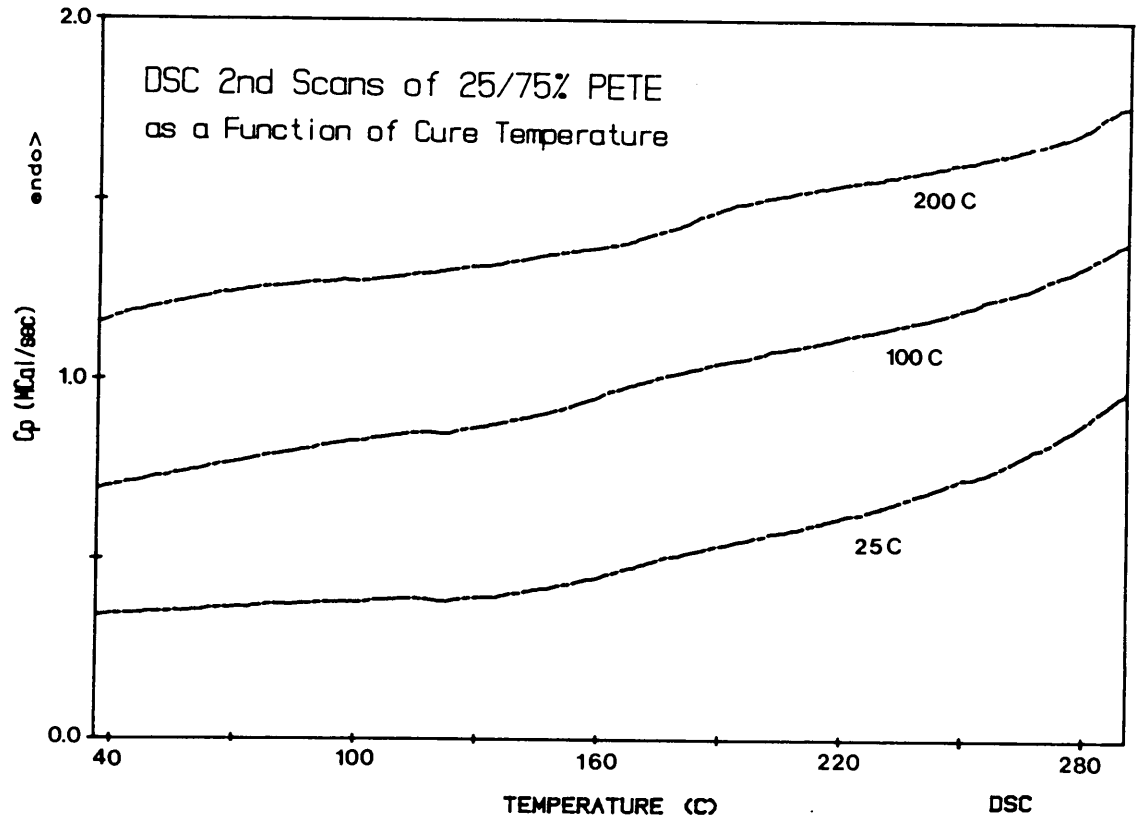

Figure 24. DSC 2nd scans of 25/75% PETE as a function of cure temperature.

In comparing the DSC 2nd scans of the various glass compositions as a function of the cure temperature, one important observation is noted for the 25°C, 100°C, and 200°C treated PETE glasses. The T_g of the pomosils begins to occur over a broader and broader temperature range as the glass content of the material is increased until it is hardly discernible (see Figures 25-27). This last effect is clearly seen in the 25/75% PETE glass in which the T_g is hard to distinguish. This phenomena may be attributed to two conditions that arise in the PETE glasses. First, as the glass content is increased, the PEK chain ends are tied down more thoroughly in the inorganic network which results in a lower chain mobility at the T_g that tends to broaden the glass transition. Secondly, the lower concentration of PEK present in the pomosils of high glass content represent a smaller portion of the sample. Thus, at the high glass contents a smaller transition is detected.

The dynamic mechanical experiments also reveal a similar pattern of behavior illustrated by the DSC experiments in regards to the thermal treatments subjected upon the PETE systems. By monitoring the tanδ and the storage modulus (E′) of the PETE glasses, the cure temperature and the glass content can be shown to have a significant influence on the mechanical properties of the pomosil (see Figure 28-35). For example, the tanδ, the ratio of the loss to the storage modulus (E″/E′), is a good indicator of the PETE T_g, while the storage modulus produces information on the elastic behavior of the material over the temperature spectrum of study. When both measurements are used in conjunction with one another, their interpretation can provide a fairly complete analysis of the mechanical properties of the PETE glasses over a broad range of temperatures.

In the analysis of the tanδ spectrum of the PETE glasses as a function of the cure temperature, the results parallel those observed in the DSC 1st scans (see Figure 28, 30, 32, & 34). That is, as the cure temperature of the thermal treatment is raised to 100°C and 200°C, the tanδ shifts to higher and higher temperatures. In the 200°C cured samples, the tanδ is shifted almost out of the region of study in the higher glass content samples. These findings once again are attributed to the greater degree of network formation occurring during the 100°C and 200°C thermal treatments which leads to PETE glasses with a higher T_g. In the 100/0% ,

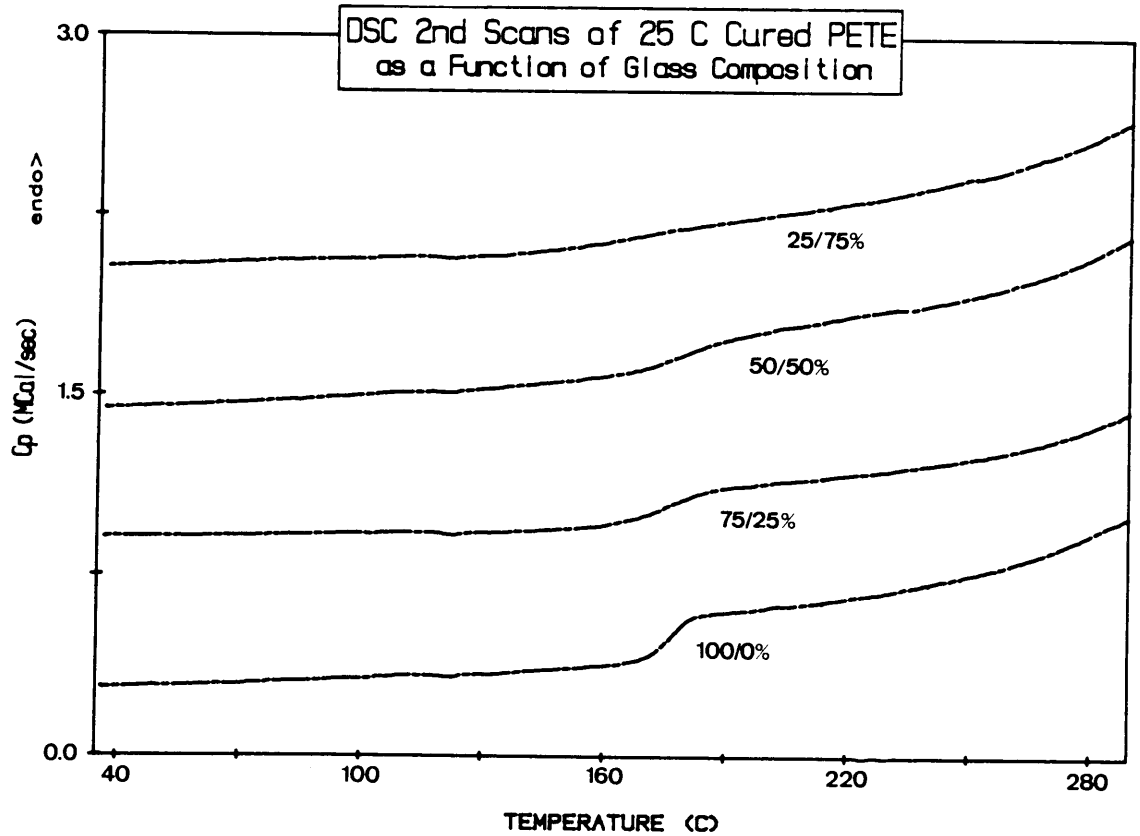

Figure 25. DSC 2nd scans of 25°C cured PETE as a function of glass composition.

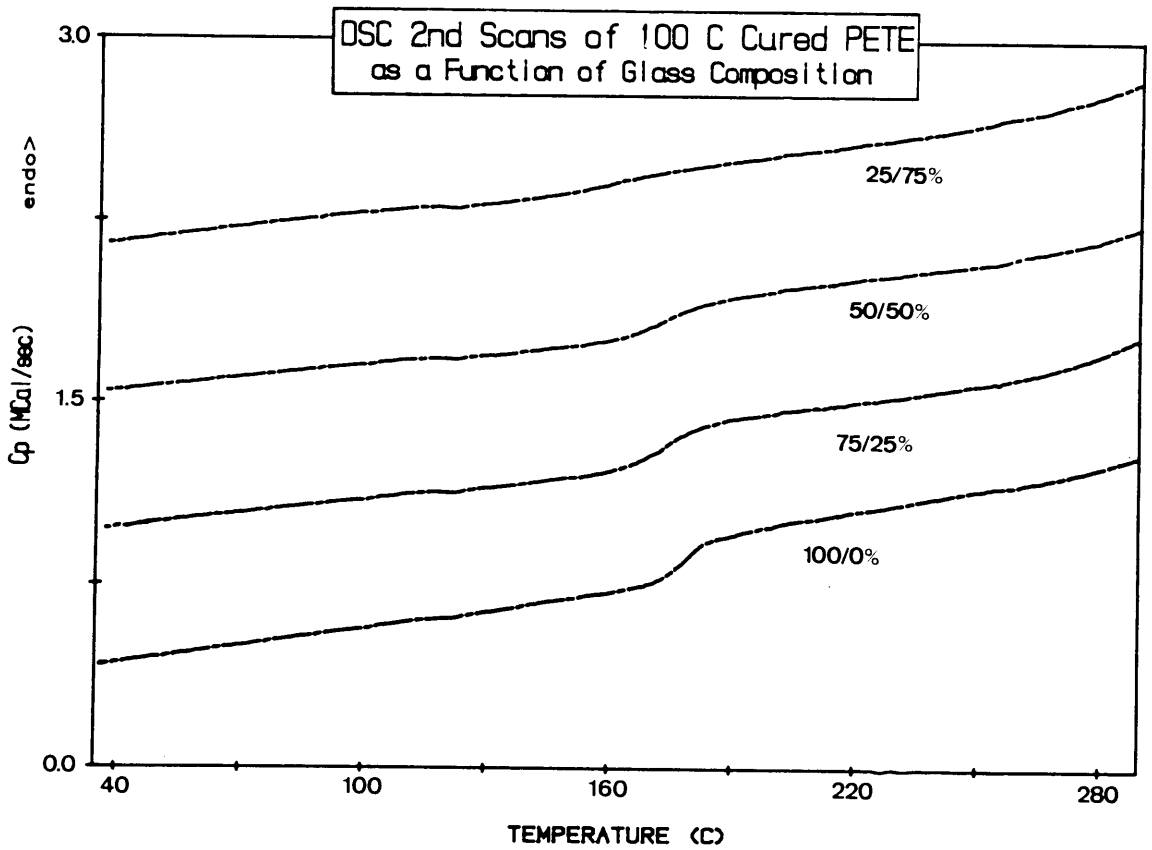

Figure 26. DSC 2nd scans of 100°C cured PETE as a function of glass composition.

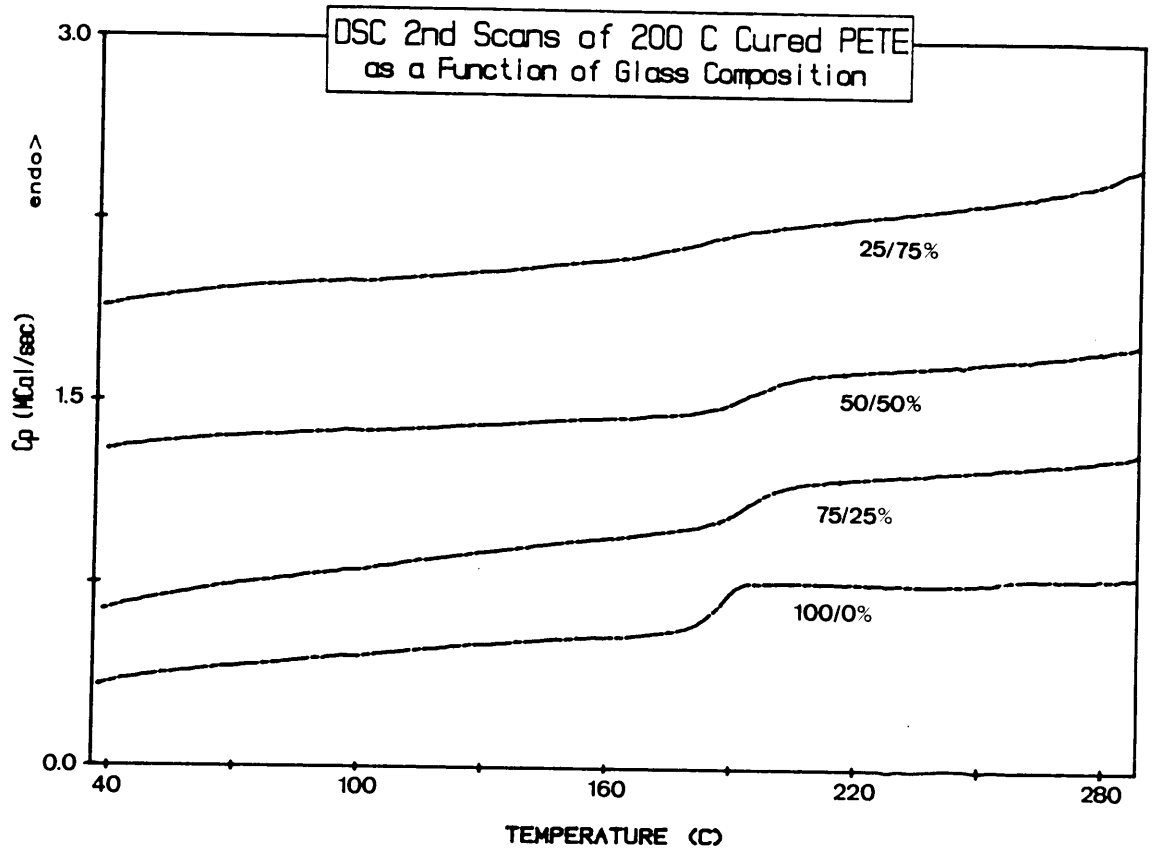

Figure 27. DSC 2nd scans of 200°C cured PETE as a function of glass composition.

75/25% , and 50/50% compositions, the 25°C cured PETE's tanδ appears in the range of ca 60-80°C and continues with increasing temperature until the run is terminated. (Unexpected termination of the dynamic mechanical runs occurs frequently because the samples often become too soft (above T_g) for the instrument to work properly). This broad tanδ signifies the continual curing of the PETE glasses during the temperature scan. In the 100°C treated samples, the tanδ rises between 160-190°C and tends to shift to higher temperatures with increasing glass content. This result is to be expected since the higher glass content pomosils have a greater probability of tieing the PEK chain ends more effectively into the inorganic network. This last development shifts the tanδ to higher temperatures due to the greater mobility restrictions placed on the oligomer chain.

Furthermore, this phenomena is clearly indicated in the tanδ spectrum of the 25/75% PETE glass. For the 25°C and 100°C treated materials, the tanδ is situated roughly in the same temperature region of 180-190°C. The 25°C cured tanδ behavior of 25/75% PETE is significantly different from those of the lower glass content species in that this material does not exhibit a broad peak beginning at 80°C and continuing upward to ca 200°C. As mentioned earlier, this high glass content material has a low percent of sol-fraction present in the uncured form. Thus, any additional curing occurring during the scan principally serves only to tie down the existing network more, whereas in the lower glass content species with a higher concentration of sol-fraction the thermal curing occurring during the scan is striving more to develop a network structure. This last result may explain the broadness of the tanδ behavior in terms of the mobility of the uncondensed oligomers in the pomosil glass. At the lower temperatures, the free oligomers have less restrictions on their movements until they participate in a sol-gel reaction. After this point, the mobility begins to decrease with additional curing and the tanδ continually shifts to higher temperatures causing a smearing effect on its response. Even though this last hypothesis is merely speculation, it does offer one plausible explanation to the phenomena observed.

One final point that needs to be addressed in reference to the tanδ response of the PETE glasses is the relative magnitude of the tanδ peak. A clear trend is revealed as the glass

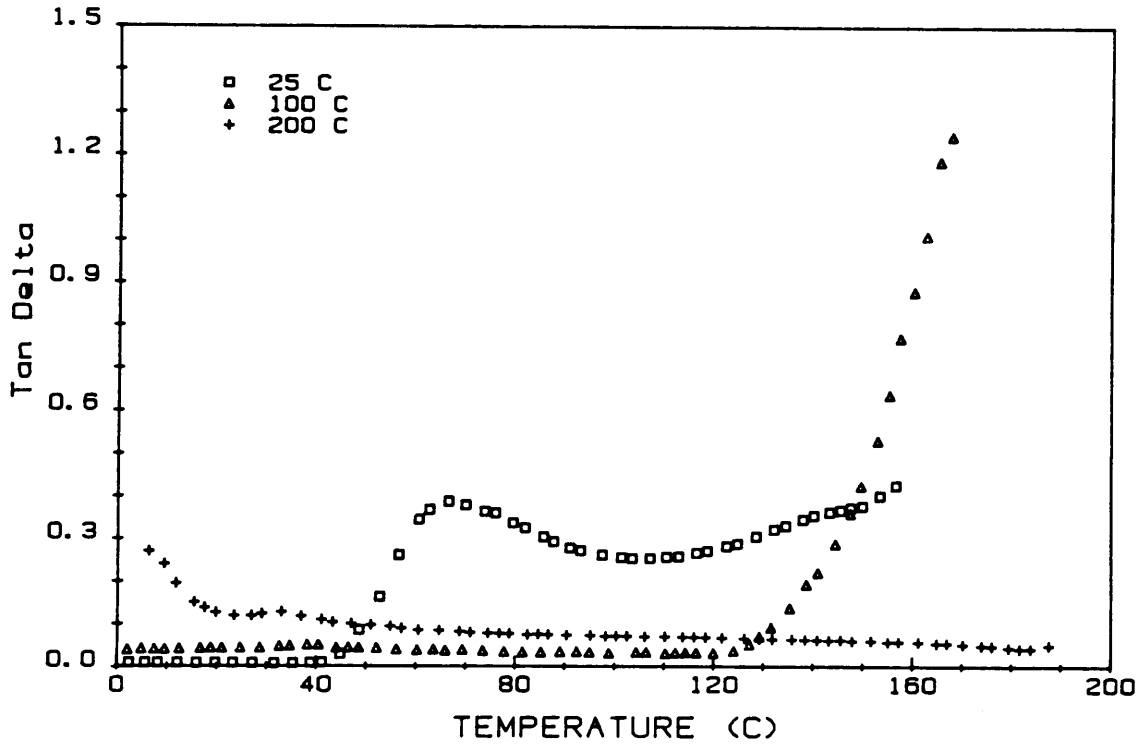

Figure 28. Tanδ spectrum of 100/0% PETE as a function of cure temperature.

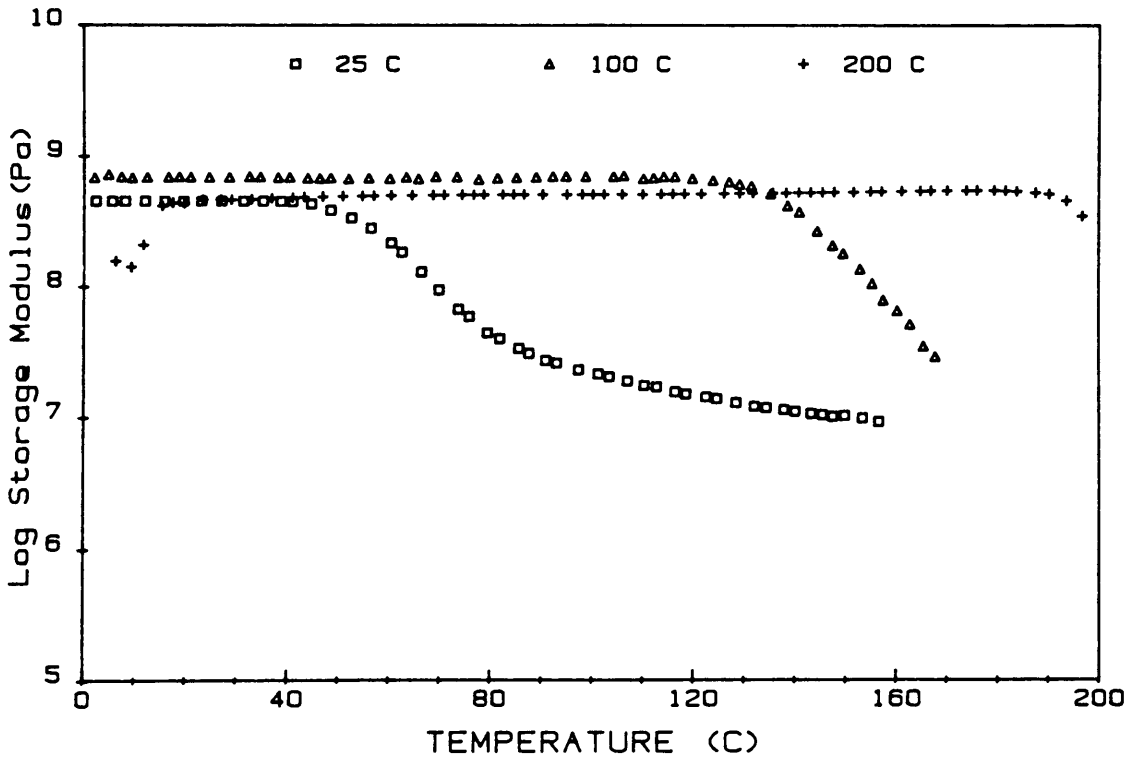

Figure 29. Storage modulus of 100/0% PETE as a function of cure temperature.

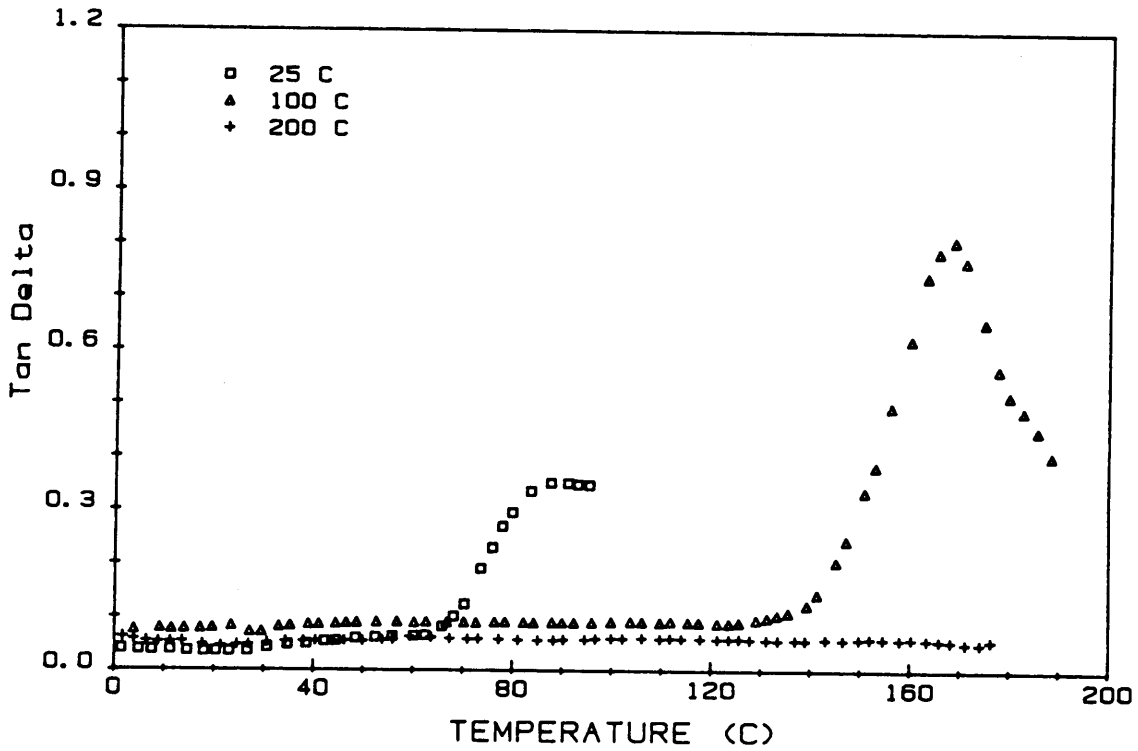

Figure 30. Tanδ spectrum of 75/25% PETE as a function of cure temperature.

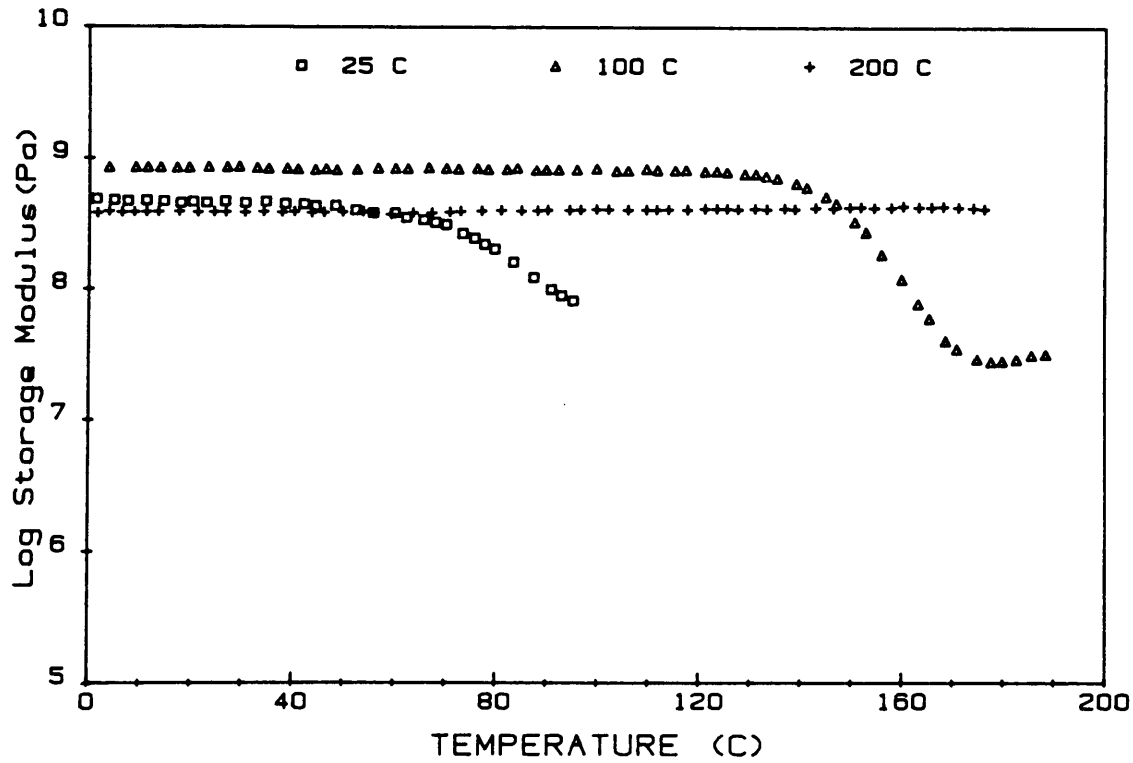

Figure 31. Storage modulus of 75/25% PETE as a function of cure temperature.

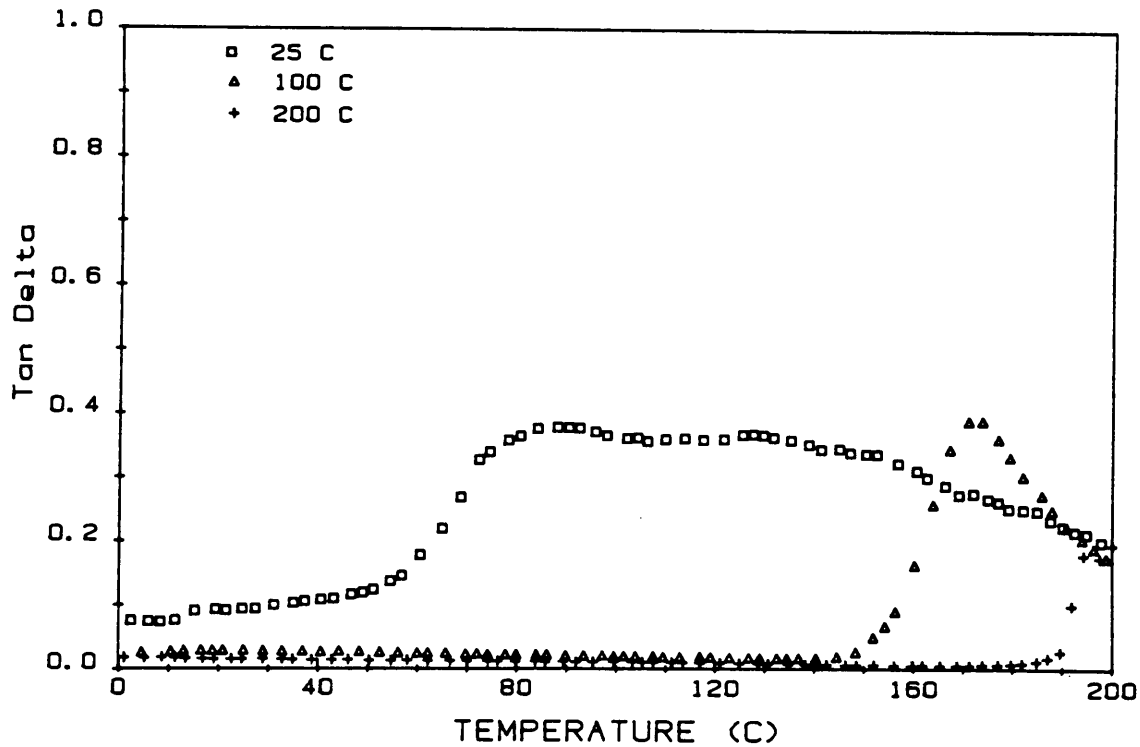

Figure 32. Tanδ spectrum of 50/50% PETE as a function of cure temperature.

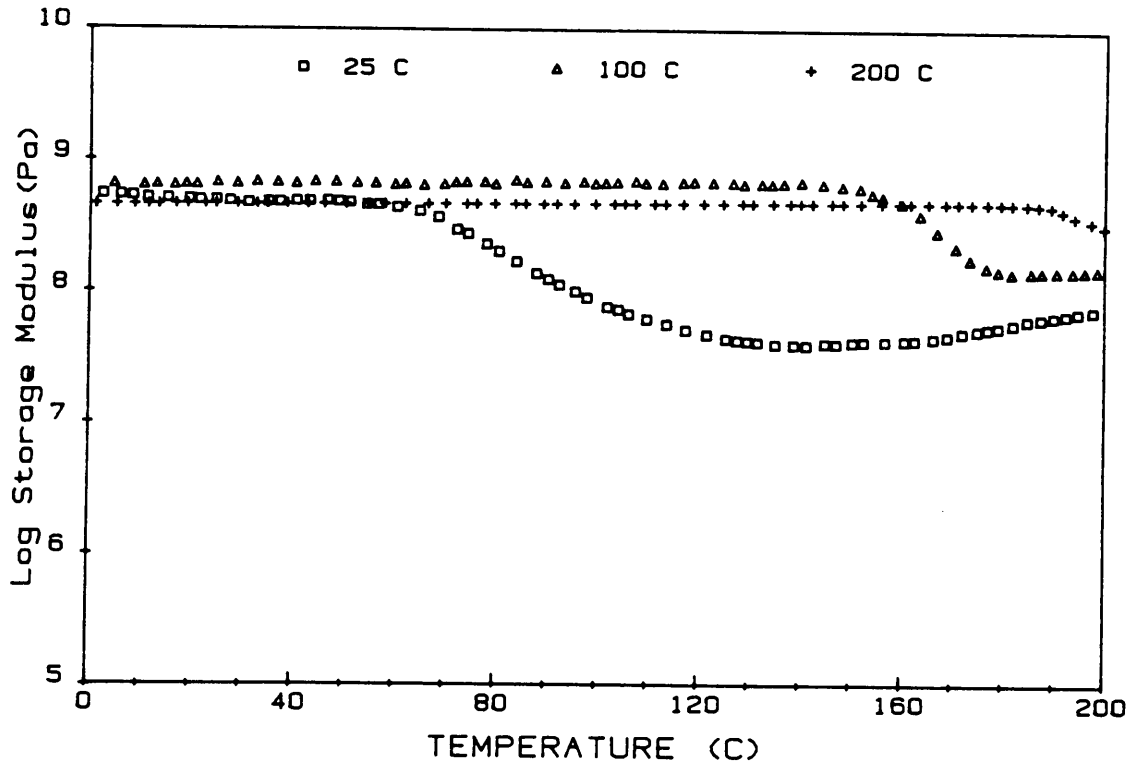

Figure 33. Storage modulus of 50/50% PETE as a function of cure temperature.

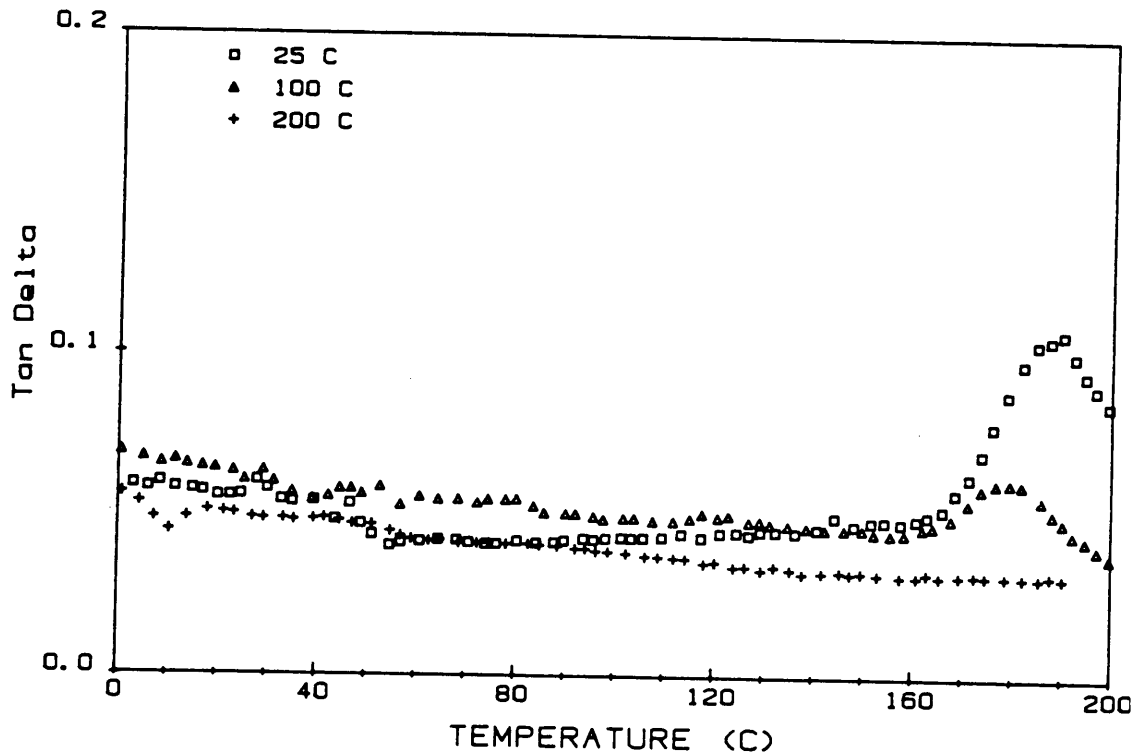

Figure 34. Tanδ spectrum of 25/75% PETE as a function of cure temperature.

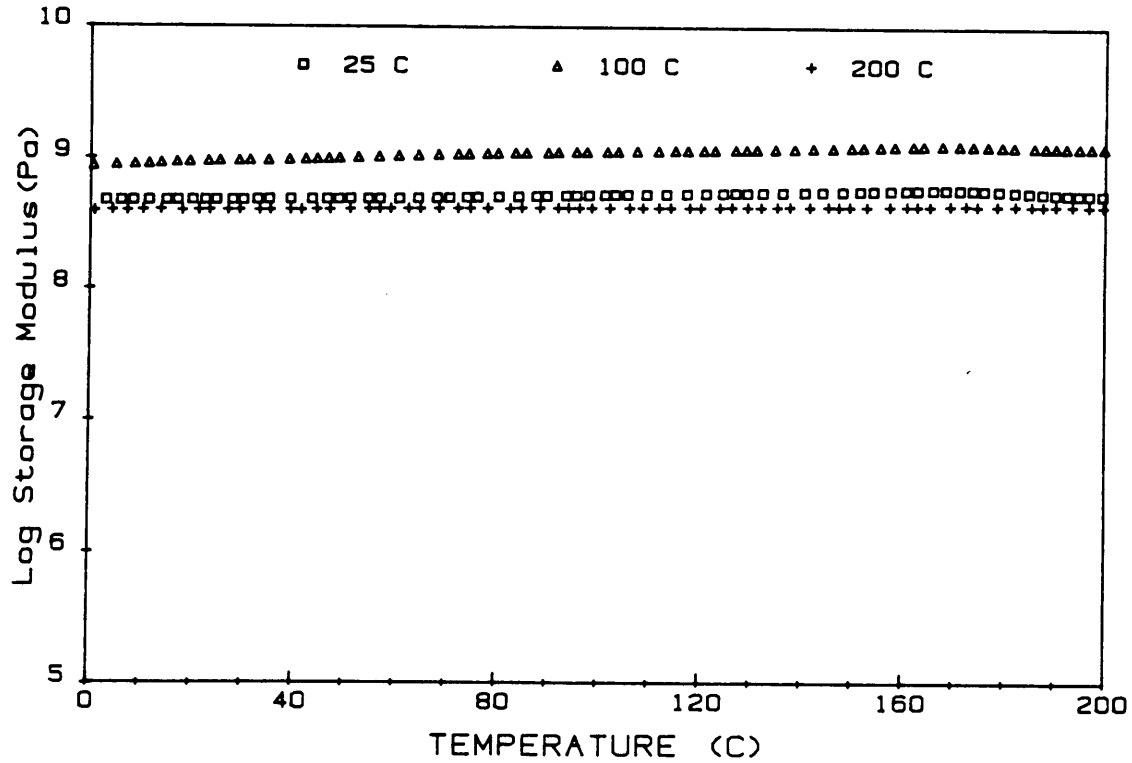

Figure 35. Storage modulus of 25/75% PETE as a function of cure temperature.

content of the PETE is increased. For example, the relative magnitude of the tanδ is suppressed systematically with increasing TEOS content for all the PETE samples. This result can be associated with one of two explanations. At the higher glass contents, an increased degree of network formation ties down the PEK chain ends more restricting the oligomers mobility and/or the PEK component comprises a lower percentage of the pomosil glass, so less response is noted for the tanδ transition. Most likely, the combined effects of these two occurrences causes a systematic suppression of the tanδ magnitude as the glass content is increased. This same trend may also be present as the cure temperature is raised for the various pomosil compositions, which would be representative of the first of the two behaviors, but incomplete data on the tanδ behavior limits this discussion further.

In monitoring the storage modulus (E′) over the same temperature region as the tanδ, once again the results parallel those displayed by both the tanδ spectrum and the DSC 1st scans as a function of cure temperature. Specifically, as the temperature of the thermal treatment is increased for a set glass content, the temperature at which the modulus begins to drop due to viscoelastic softening (onset of T_g) appears at higher and higher temperatures (see Figures 29, 31, 33, & 35). (Note that the actual glassy modulus of all the PETE materials should be approximately 10^9 Pa; the inconsistency in the data has been associated with a calibration problem of the instrument). This effect is directly linked to the degree of network formation present in the sample. However, the 25/75% PETE glass provides an exception to this softening behavior. For this pomosil, no appreciable softening is observed over the 200°C range studied which can be attributed to the high TEOS content of this particular sample resulting in a greater degree of network formation (see Figure 35). In all the other glass composition PETE's (100/0% , 75/25% , & 50/50%), the 25°C treated materials begin to soften in the 50-70°C range with the higher glass content samples softening at the higher temperatures. This same trend is more distinct in the 100°C cured pomosils, where the softening develops between 130-160°C with 100/0% PETE softening at ca 130°C and 50/50% PETE at ca 160°C. For the 200°C cured materials, the storage modulus remains constant over a considerable portion of the temperature spectrum, and finally begins to drop at ca 200°C for the 100/0% and

50/50% PETE glasses. In retrospect, the trends of the storage modulus with glass content and cure temperature are consistent with the behavior observed in the DSC and tanδ measurements. All the experiments tend to reflect that a greater degree of network formation occurs with increasing glass content and cure temperature.

Up to this point, the results of all the tests performed have indicated that as the cure temperature of PETE glasses is raised that a greater degree of network formation results. In a mechanical stress-strain experiment, this occurrence would cause an increase in the material's modulus, and indeed this is what happens in the 100/0% PETE glass. (By the way, the 100/0% PETE was the only glass pliable enough to cut the dumbbell sample shapes; thus, this is the only material on which the stress-strain properties will be reported). The stress-strain tests of the 100/0% PETE yield Young's modulus of $1.27X10^9$, $1.73X10^9$, and $1.85X10^9$ for the 25°C, 100°C, and 200°C thermal treatments, respectively. Thus, the modulus does systematically increase with the cure temperature as predicted, and ,furthermore, a remarkable change in the mechanical behavior is noted (see Figure 36). For example, the 100/0% PETE with the 100°C and 200°C thermal treatments display a yield point and have ultimate elongations 3 to 4 times that of the 25°C cured pomosil. The poor elongational properties of the 25°C cured systems are attributed to the high concentration of the sol-fraction present (~25.8%) which inhibits the structural integrity of the network. For the 100°C and 200°C treated 100/0% PETE, the sol-fraction is much lower (<5.0%), and the level of network formation is much greater. As a consequence, these materials, which are essentially the PEK self condensed polymer, exhibit more favorable stress-strain properties due to a higher degree of network formation.

From a molecular perspective, the increased temperature thermal treatments promote the further reaction of the silanol or silicon alkoxide functional groups to form ≡Si-O-Si≡ network bonds. These network bonds are readily detected by IR analysis and provide a convenient, but qualitative, method of monitoring the relative degree of network formation occurring in the PETE glasses. This is done by taking the ratio of the intensity of the strong asymmetric ≡Si-O-Si≡ stretch occurring in the 1100-1000 cm^{-1} region to the intensity of the

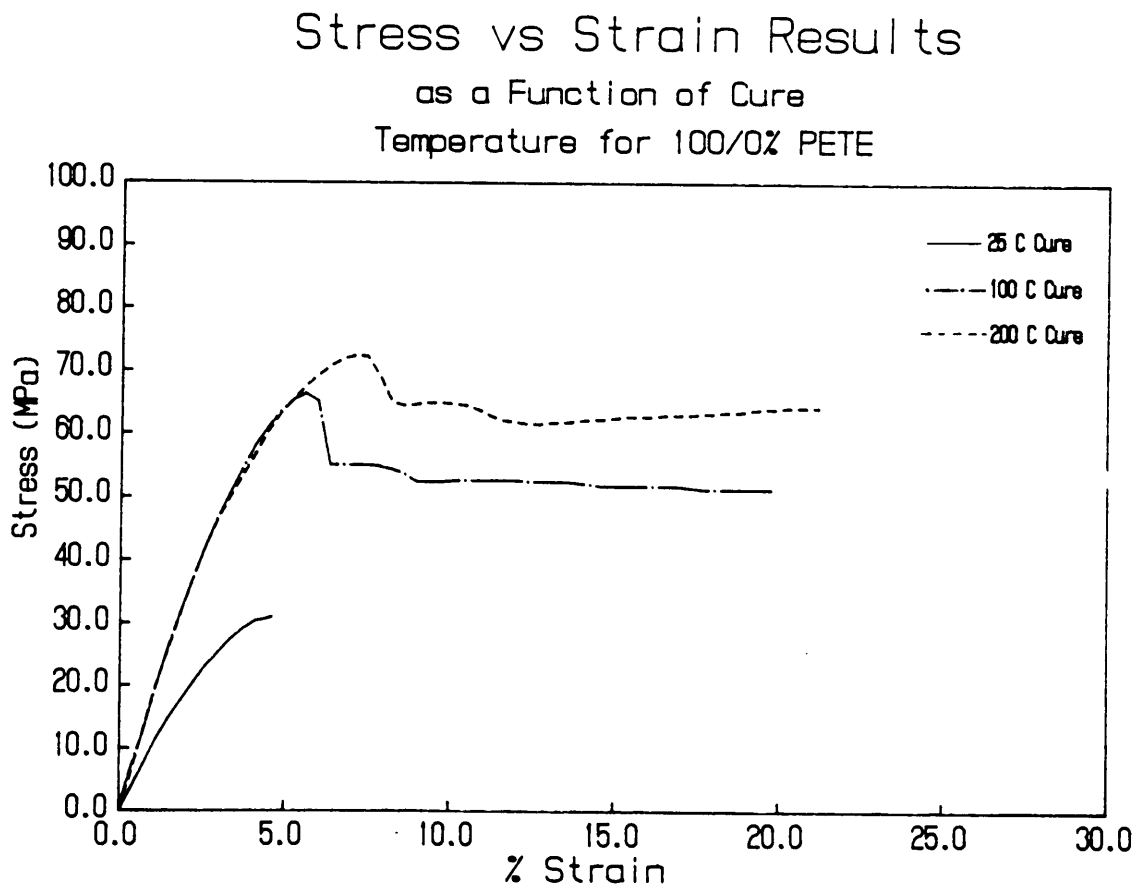

Figure 36. Stress-strain results of 100/0% PETE as a function of cure temperature.

reference carbonyl stretch of the PEK found at ca 1651 cm^{-1} (45). One other peak of interest is the broad ≡Si-OH stretching mode centered at 3400 cm^{-1}. However, since the silanol appears to be hydrogen bonded with water (i.e., an unbonded ≡Si-OH displays a sharp absorbance usually at 3690 cm^{-1} (45)) either introduced in the sample preparation or trapped in the matrix, the absorbance intensity of ≡Si-OH is not representative of the actual concentration of silanol functionalities present that would allow a better interpretation of the extent of the sol-gel reaction.

Nevertheless, the R ratio is one qualitative means of monitoring the relative degree of network formation in respect to the thermal treatments and glass contents of the PETE pomosils. For instance in the 75/25% , 50/50% , and 25/75% PETE, the R ratio increases systematically with the temperature of the thermal treatment which directly indicates an increase in the connectivity of the ≡Si-O-Si≡ matrix (Figures 37-39). This same trend is also observed with the increasing glass content for a set temperature thermal treatment. The 25°C and 200°C treated pomosils have R ratios of 2.15:3.11:8.31 and 5.01:6.06:11.63 for the 75/25% , 50/50% , and 25/75% PETE compositions (see Figures 40-41). The higher glass content samples which can form a greater number of ≡Si-O-Si≡ bonds yield the highest R ratios of the lot. This last result is consistent with ideas proposed earlier for the degree of network formation.

In addition to the molecular information obtained on the degree of crosslinking, one other experimental study was undertaken to get an idea of the morphological structure of the PETE samples. In a previous experiment not mentioned in this study, an 11000 Mn endcapped PEK was incorporated into a PETE glass with varying amounts of glass contents using the sol-gel technique. The gelled PETE pomosils with a considerable amount of TEOS added (>50%) in the starting solution macrophase separated into two distinct regions (one composed of the TEOS and the other the PEK oligomer). This evidence suggests that the solubility parameters of the TEOS and the PEK are substantially different. However when the 4000 Mn PEK is used in the current study, only the 50/50% PETE glass has any appearance of a phase separation (i.e., a translucent glass). Still, the large difference in solubility parameters noted in the higher

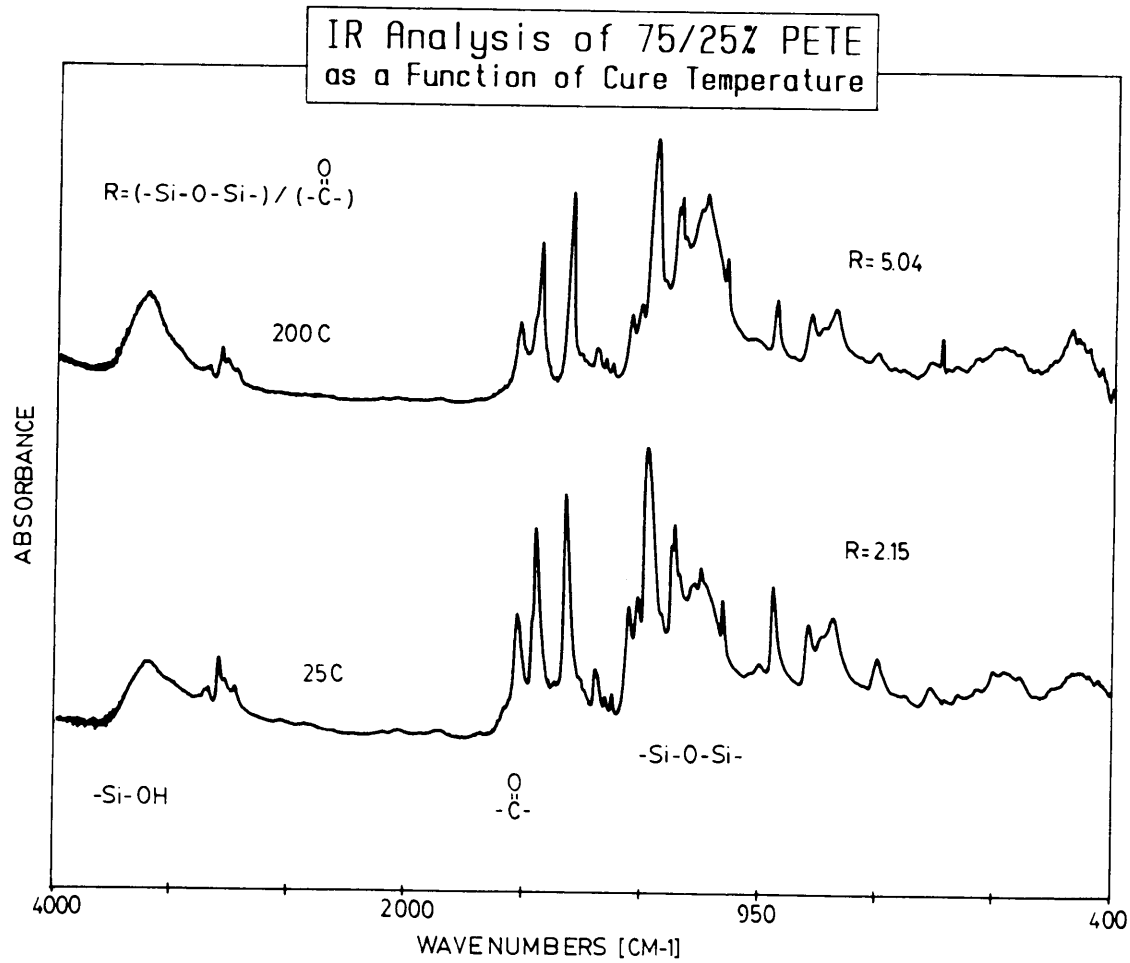

Figure 37. IR analysis of 75/25% PETE as a function of cure temperature.

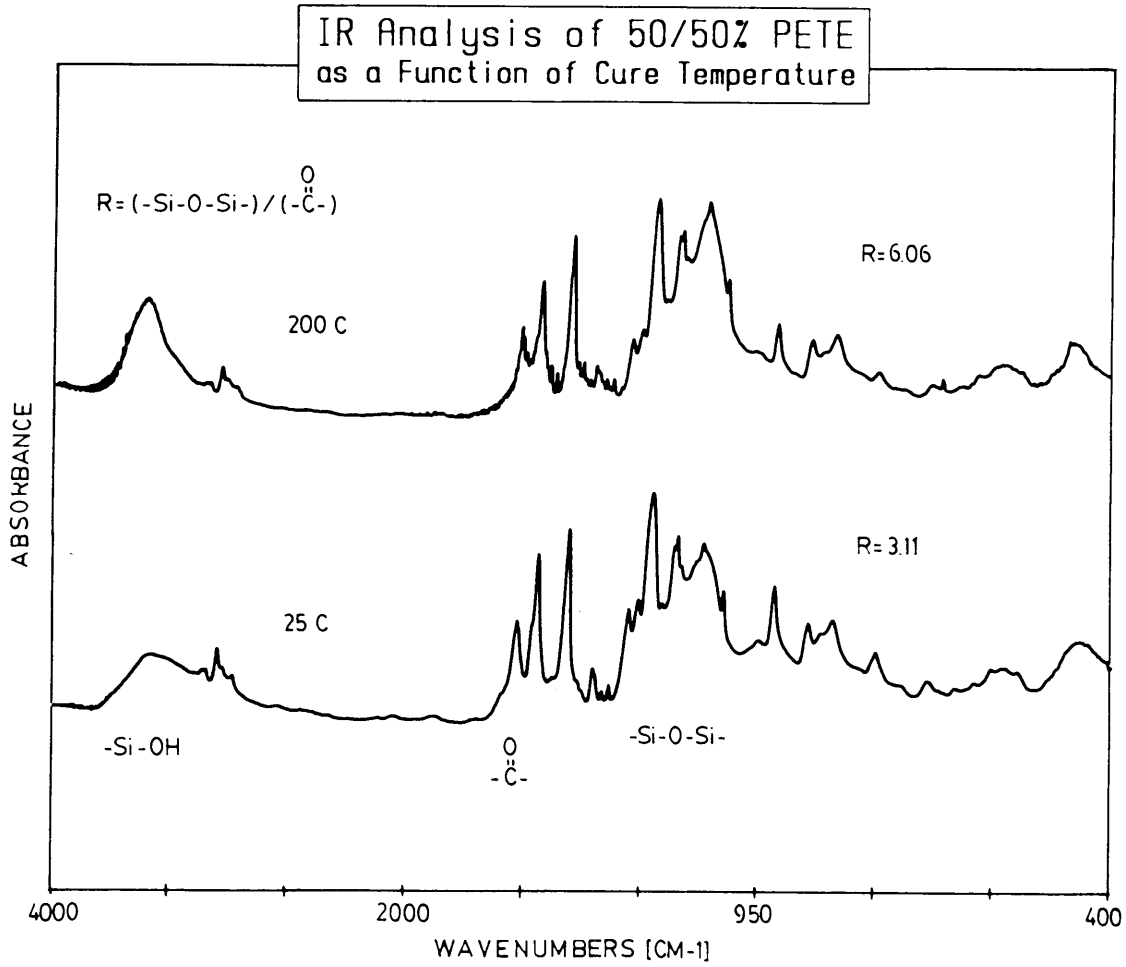

Figure 38. IR analysis of 50/50% PETE as a function of cure temperature.

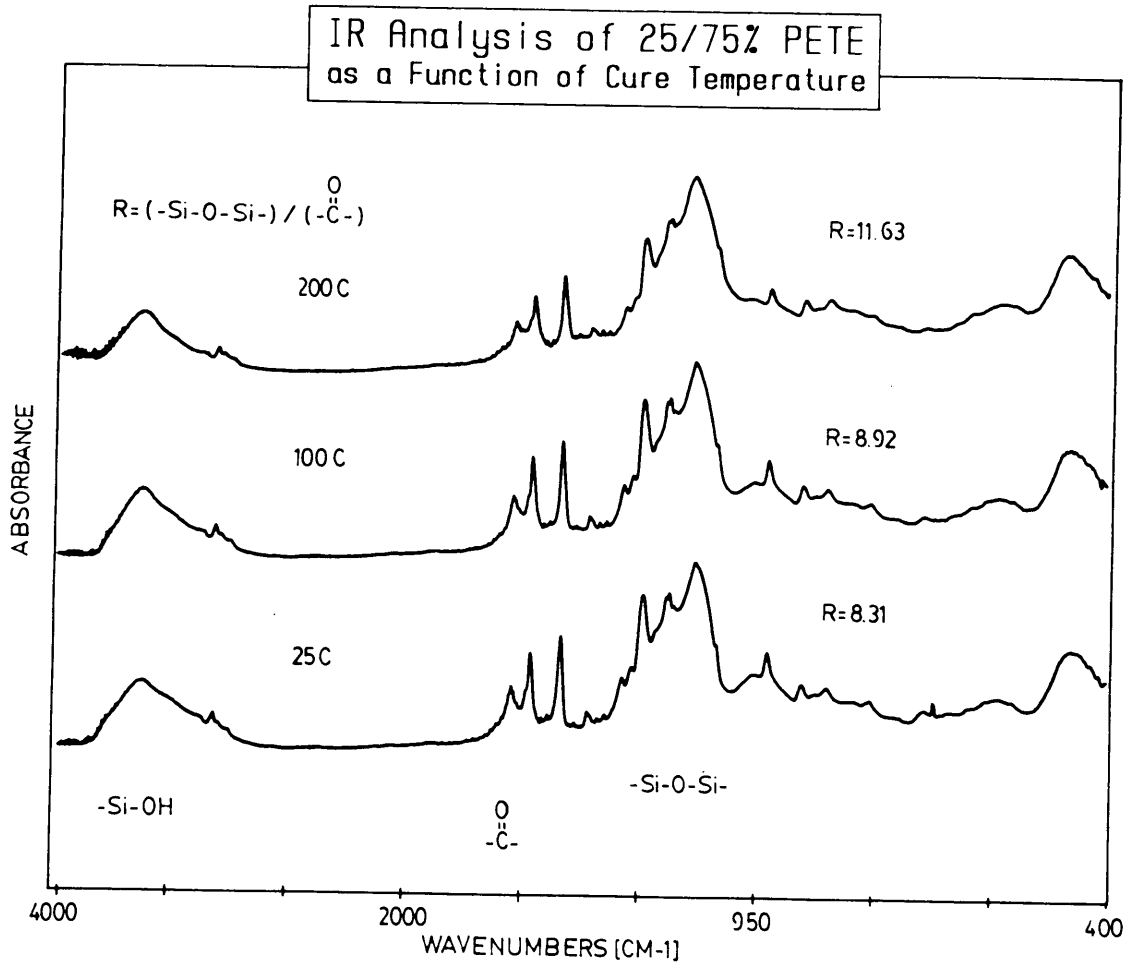

Figure 39. IR analysis of 25/75% PETE as a function of cure temperature.

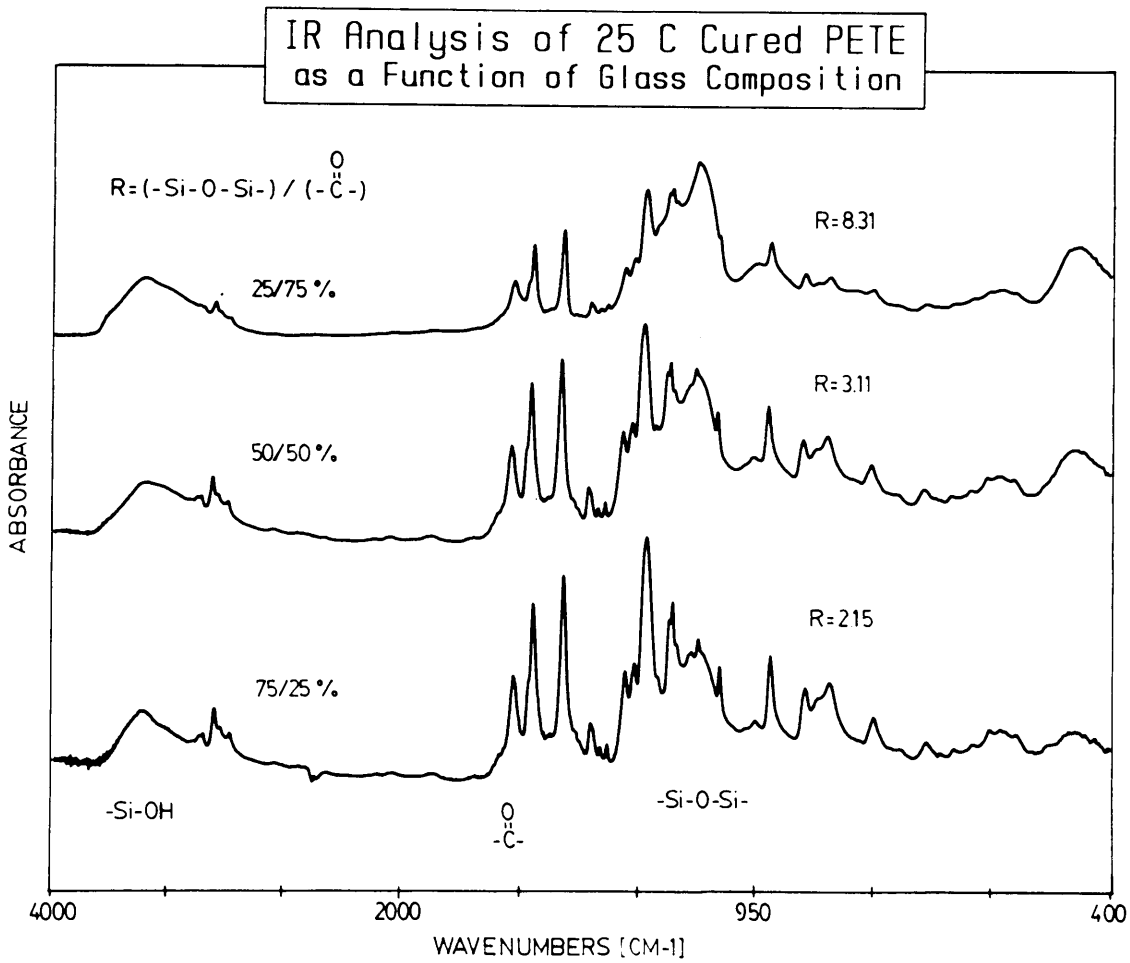

Figure 40. IR analysis of 25°C cured PETE as a function of glass composition.

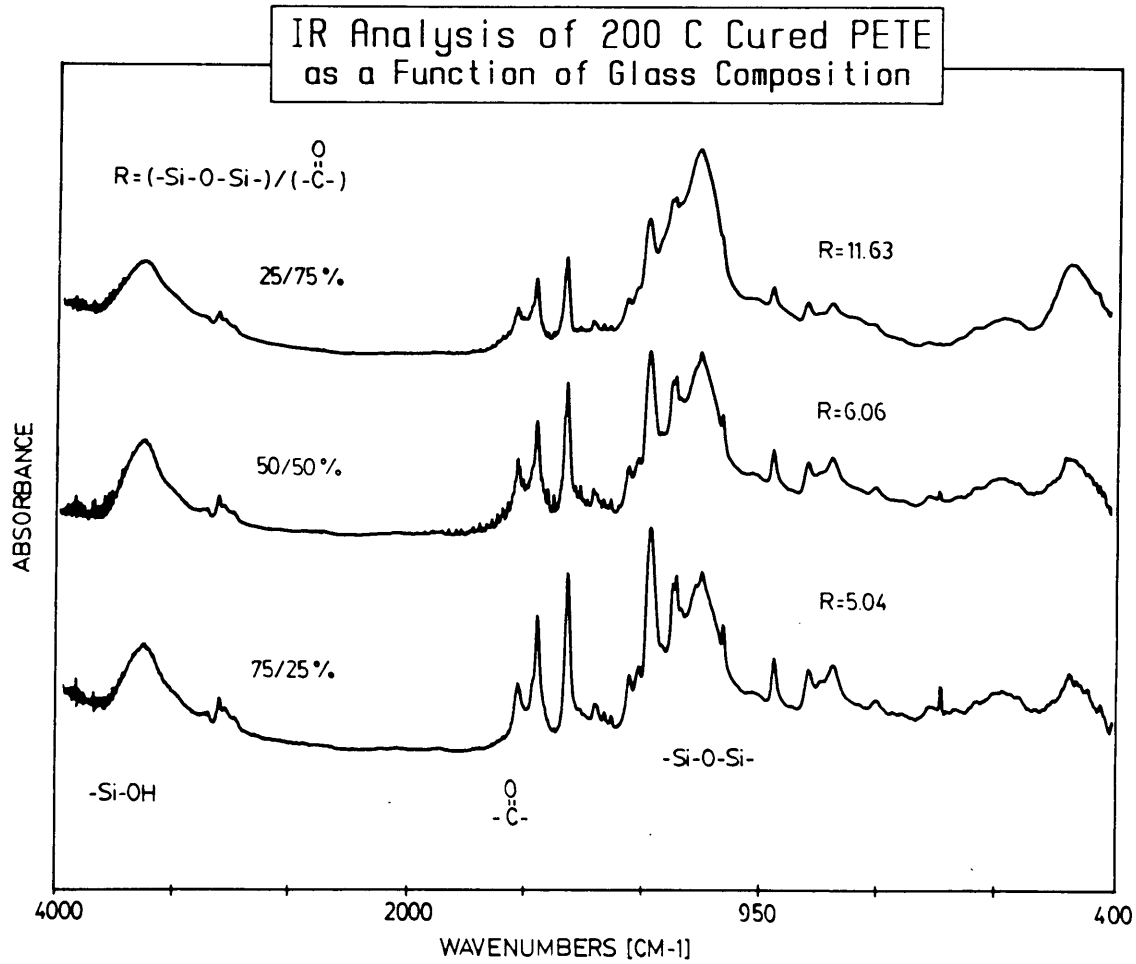

Figure 41. IR analysis of 200°C cured PETE as a function of glass composition.

molecular weight PEK leads one to believe that maybe a microphase separation is occurring on a much smaller length scale.

Scanning electron microscopy (SEM) and small angle X-ray (SAXS) techniques were employed to find whether this last assumption is valid. The SEM scans reflect no microphase separation in the micron range, and thus if present it must be on much smaller length scales than can be detected by this instrument. However in the SAXS experiment which probes still smaller length scales, the data shows that there is a microphase separation and a relative periodicity in the electron densities present in the PETE glasses. If one assumes the PETE system is a dense two phase system (i.e., PEK and TEOS phases), then the degree of phase separation can be correlated to the difference in the electron densities of the scattering regions from the rearrangement of the scattering invariant (see equation 4.1) (46).

$$\overline{\Delta\rho^2} = 4\frac{\pi}{V}\int_0^\infty s^2[\frac{I(s)}{i_e}]ds \qquad [4.1]$$

The V is the volume of the illuminated scattering domains, the I(s) is the collected scattered intensity of the X-ray beam, and i_e is the Thompson constant for the scattered intensity of a single electron. Thus, equation 4.1 simply states that an increasing I(s) corresponds to a greater difference in the electron intensities between the two regions, thereby implying less phase mixing or a greater degree of phase separation. In addition to this information, SAXS can also often reveal if there is a periodicity in the placement of the two different scattering regions of the TEOS and PEK phases. This is indicate by the occurrence of a maximum in the plot of the smeared intensity, $\tilde{I}$ (s) (the smearing results from the slit geometry of the X-ray beam window due to a smearing of the scattering angles collected) versus the scattering vector (s) which is inversely related the characteristic length between the scattering regions and is a rearrangement of Braggs law (see equation 4.2).

$$S = \frac{1}{d} = \frac{2}{\lambda} \sin \theta \qquad [4.2]$$

The d is the characteristic length, λ the wavelength of the X-ray monochromatic source, and θ the Bragg scattering angle or one half of the radial scattering angle. In the SAXS measurements of the 75/25% , 50/50% , and 25/75% PETE, the results indicate a periodicity or orderly dispersion of the TEOS and PEK scattering regions by displaying a peak in the smeared I(s) versus s plots that has been associated to the characteristic length or interdomain spacing between the PEK and TEOS phases (see Figures 42-44). This peak in the SAXS spectrum reveals that the microphase separation occurring is on the order of the nanometer (nm) length scale in these pomosil glasses.

By plotting the characteristic length between the PEK and TEOS phase regions as a function of glass content, the PETE pomosils reveal a systematic trend with increasing TEOS content (see Figure 45). That is, as the TEOS initial weight percent is increased, the characteristic length or the interdomain spacing also increases. After much interpretation, it has been postulated that the PEK and TEOS form a blocky type of network structure with the TEOS glass regions located at the PEK chain ends and with the oligomer connecting these regions (see Figure 46). This analogy is somewhat similar to a triblock polymer system. Thus as the glass content is increased, the TEOS regions grow at the oligomer chain ends resulting in a larger interdomain spacing between the PEK and TEOS phases.

To check the validity of this model, an estimate of the hypothetically extended chain end to end distance was calculated for the PEK oligomer to see if the length scales correspond to those determined in the SAXS scattering experiments (see Appendix A). The final value of this calculation, ca 19.15 nm, falls nicely within the 8-30 nm range displayed by the SAXS method. (Note that the characteristic lengths determined from the smeared intensity data are larger than the actual lengths determined from the desmeared scans). Thus, this last result is one supportive indication that the PETE glasses are reflective of the proposed blocky network structure.

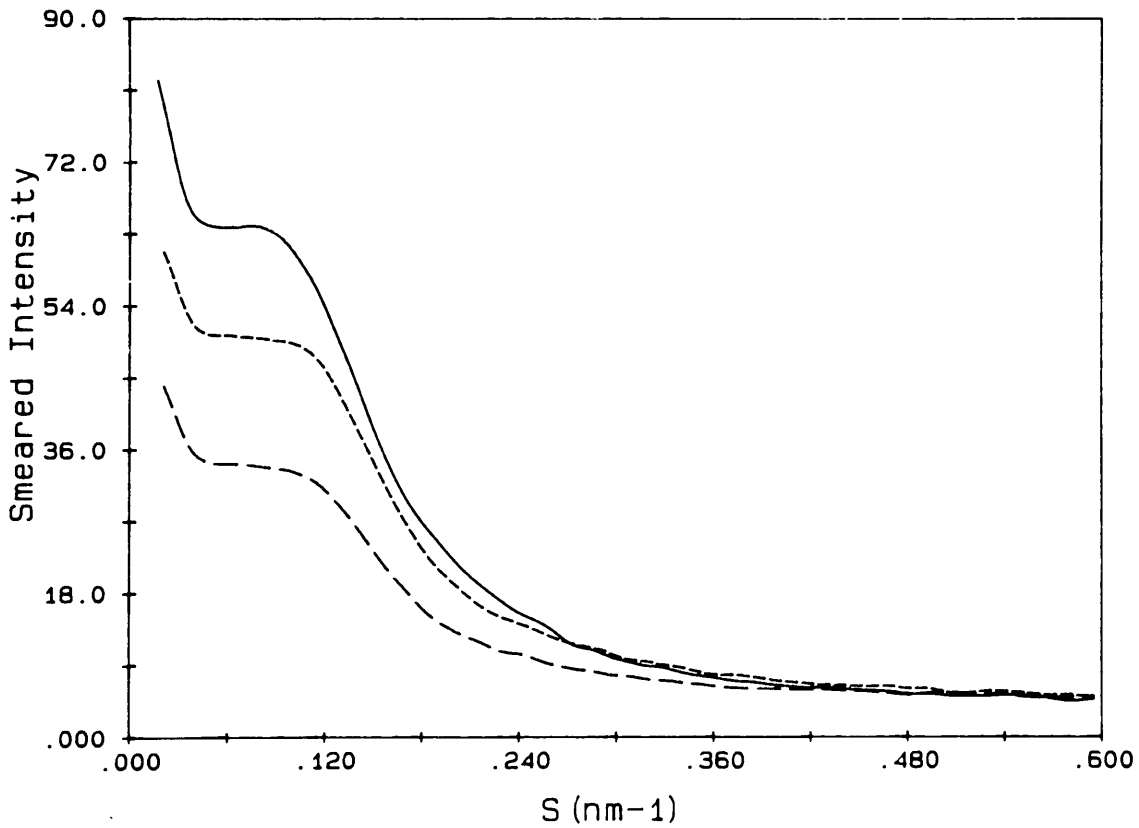

Figure 42. **SAXS scans of 75/25% PETE as a function of cure temperature:** (— — —) 25°C cured, (- - -) 100°C cured, and (——) 200°C cured.

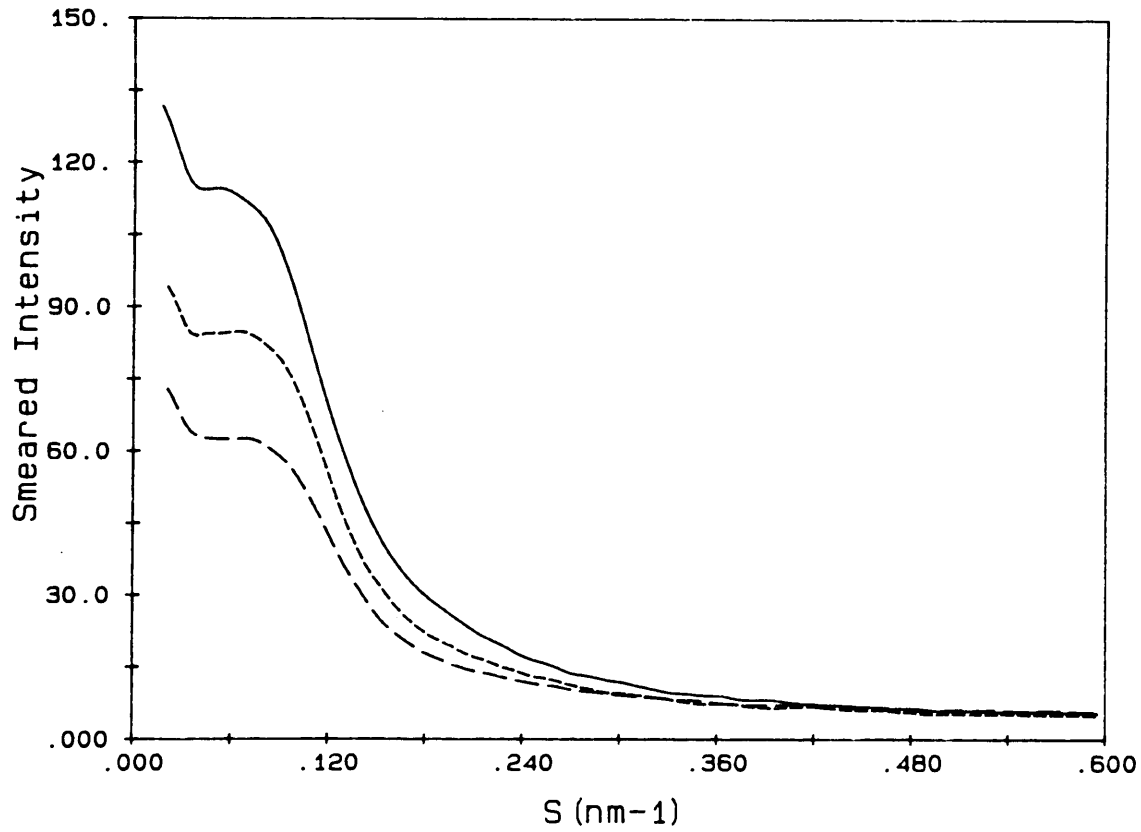

Figure 43. SAXS scans of 50/50% PETE as a function of cure temperature: (— — —) 25°C cured, (- - -) 100°C cured, and (——) 200°C cured.

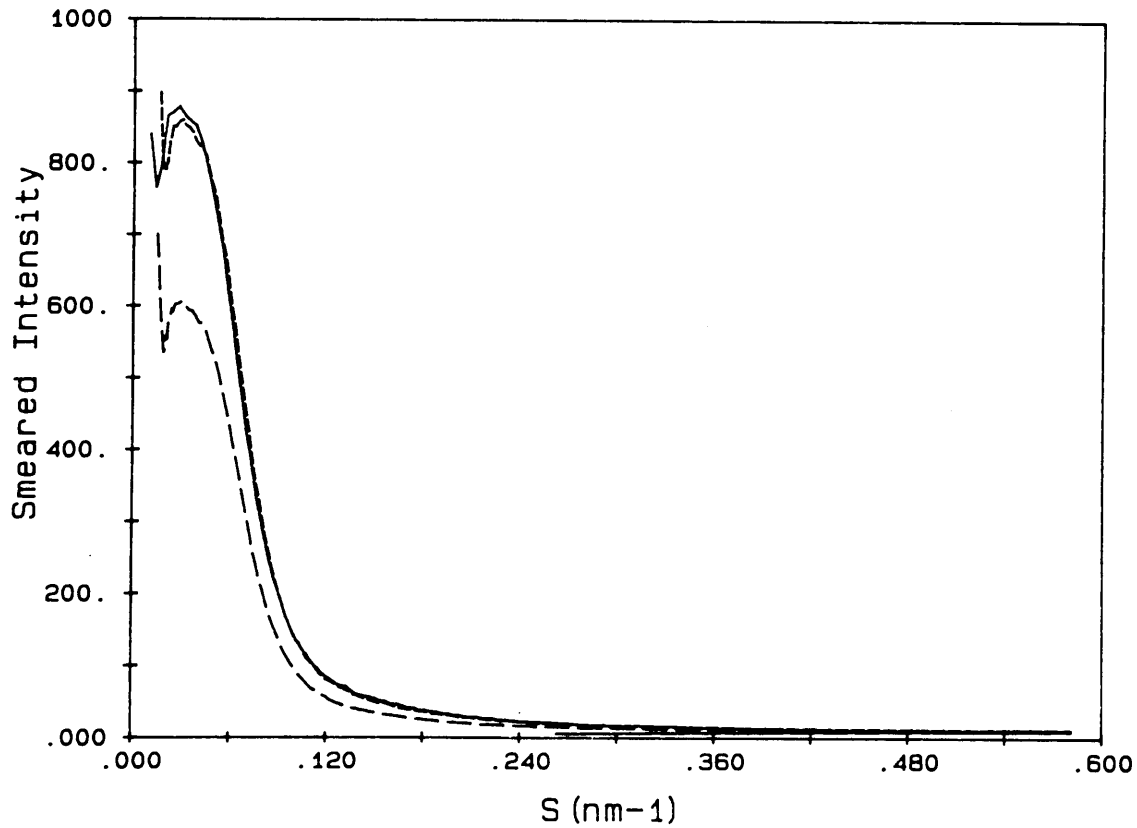

Figure 44. **SAXS scan of 25/75% PETE as a function of cure temperature:** (— — —) 25°C cured, (- - -) 100°C cured, and (——) 200°C cured.

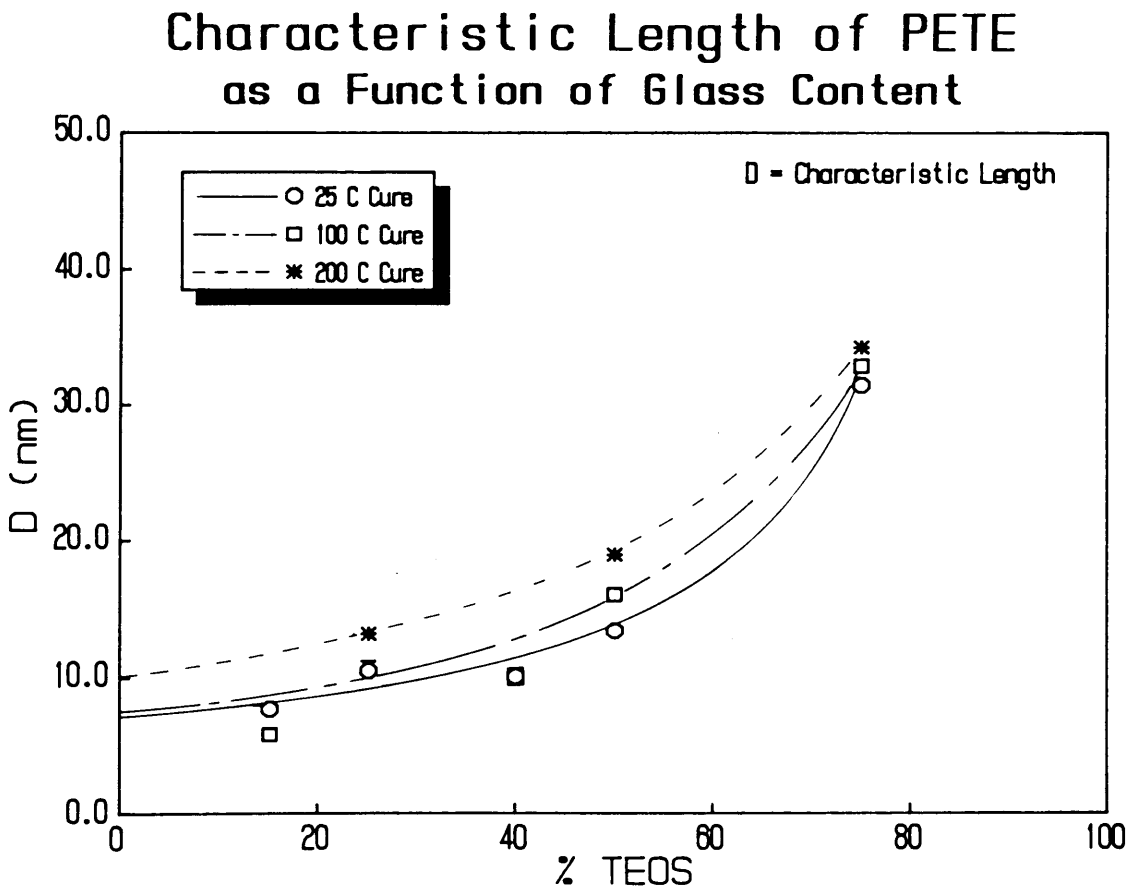

Figure 45. Characteristic length of the PETE glasses as a function of TEOS content and cure temperature.

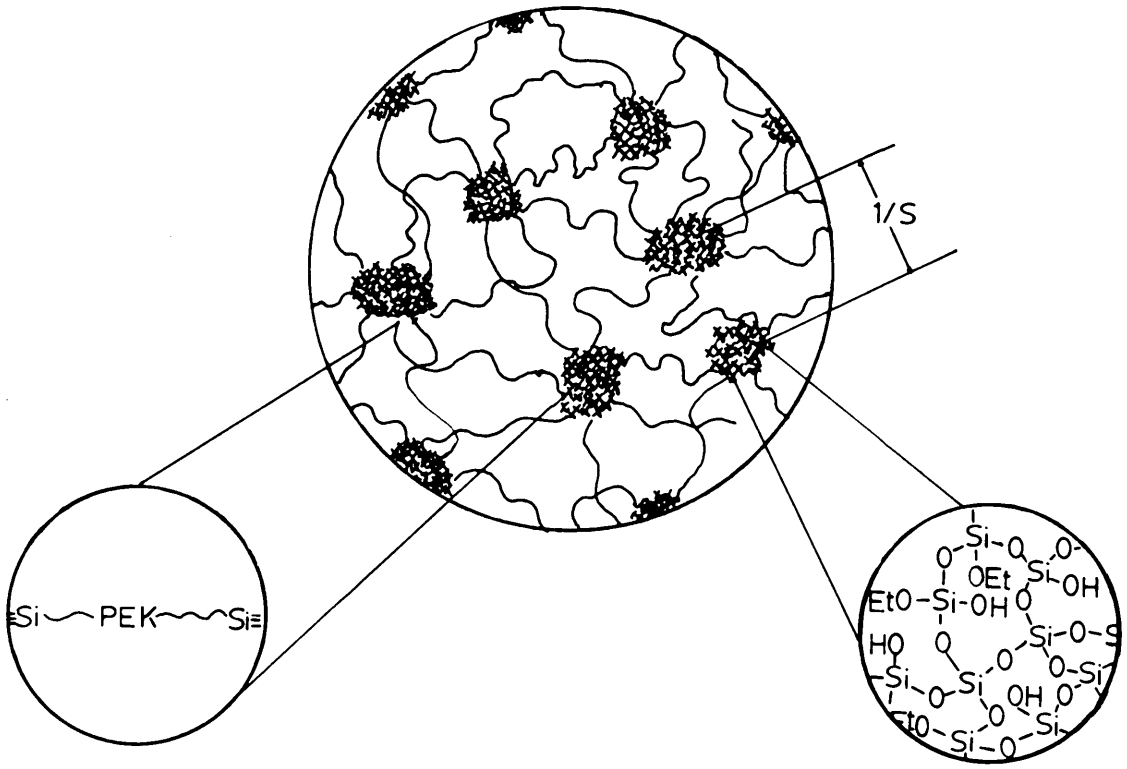

Figure 46. SAXS postulated structural model of PETE glasses.

One other interesting observation noted in the SAXS data is that there is a distinct increase in the scattering intensity with both increasing glass content and temperature of the thermal treatment. In the thermal treatment analysis, the higher scattering intensity is attributed to the densification of the TEOS regions, which creates sharper contrast between the electron densities between the PEK and TEOS phases (i.e., $>\overline{\Delta\rho^2}$). The densification of the TEOS is attributed to the continuing of the sol-gel reaction. That is, as the alkoxy groups or silanol groups hydrolyze and/or condense to form ≡Si-O-Si≡ network bonds, both the weight lost during the reaction and the further matrix substitution of the silicon atoms serve to densify the inorganic network structure. This results in greater difference between the electron densities of the TEOS and PEK domains which directly corresponds to a greater I(s) by equation 4.1. One other baffling point that is revealed with increasing temperature of thermal treatment is that the characteristic length between the two regions tends to increase. This effect is the opposite of what is occurring on the macro scale since it has been shown earlier that the PETE glasses shrink upon heating. No plausible explanation has been confirmed to explain this effect presently. One reason may be just due to the sharpening of the SAXS peak with the thermal treatments, or another may be that the shrinkage of the TEOS phase regions located at the PEK chain ends may extend the oligomer a small amount resulting in a larger interdomain spacing.

4.3 Curing Kinetics

In the previous two sections, much has been said about why and how the thermal treatments through furthering of the sol-gel reaction affect the mechanical and structural properties. These thermal treatments have been shown to promote a greater degree of network formation and a higher pomosil T_g, but nothing has been mentioned on how or what time frame these events have occurred. In short, the curing kinetics associated with the sol-gel

reaction can be directly correlated to the temperature of the cure and the amount of glass content present in the PETE material. Three experimental techniques have been employed to characterize this effect, so that in the future optimum curing times and temperatures may be implemented to attain the final designated PETE network structure.

The first experimental method utilized was the stepwise DSC technique in which a particular sample was re-scanned to higher and higher maximum temperatures (Tmax). The results of these tests indicate that as the glass content is increased in the PETE glasses, the lower the curing temperature necessary to achieve the final T_g of the material ($\sim$175°C) (see Figures 47-50). This clearly is seen in the extreme cases of the 100/0% and 25/75% PETE samples. For example, the 100/0% PETE's T_g remains essentially constant until a Tmax of 160°C is reached. After this point, the T_g begins to shift upward with the higher and higher Tmax scans until it is stabilized at ca 170°C. In the 25/75% PETE, the apparent T_g begins to shift upward with the first increment of Tmax and for the most part has reached its maximum value by a scan Tmax of 190°C. Looking back at the proposed model developed from the SAXS results, the curing behavior of the different glass content PETE materials can be simply explained. At the lowest glass contents (i.e., 100/0%), only the polymer endcapps can undergo the additional crosslinking to raise the network T_g. Also at the lower temperatures, the glassy state of the PEK oligomer ($T_g \cong 130$°C) restricts the mobility of the alkoxy chain ends, and the sol-gel curing proceeds slowly. As the Tmax is increased above the PEK T_g, which may be higher than the normal PEK T_g depending on the degree of crosslinking present already, the reactive chains ends' mobility is restored, and now they can seek out an reactive partner to undergo a crosslinking reaction. In the situation of the high glass content material (i.e., 25/75%), the diffusional or mobility limitations cause less of a hindrance to the curing reaction due to the higher concentration of potentially reactive network sites introduced by the TEOS species. Furthermore, according to the proposed structural model, the TEOS monomers congregate around the PEK chain ends, which facilitate the incorporation of the oligomer into the network. Thus, in the higher glass content systems, the thermal curing requires that enough energy be present to initiate the sol-gel mechanism and not necessarily enough to

overcome the diffusional restrictions imposed on the PEK oligomer. A quick inspection of the plot of the T_g versus Tmax for the 25°C cured PETE glasses supports this interpretation and shows that indeed the temperature sensitivity of the PETE (i.e., ability to crosslink) increases as the glass content increases (see Figure 51).

A survey of the TGA analyses for the thermally treated PETE glasses as a function of glass content strike a remarkable resemblance to the data found in the stepwise DSC experiments (see Figures 52-54). For example in the 25°C cured PETE, the weight loss over the first 200°C for the different glass contents conform exactly to the behavior shown in the T_g versus Tmax plot (see Figures 51 & 52). That is, at the lower temperatures, the higher glass content pomosils show weight loss which is an indirect indicator of the continuing sol-gel reaction while the lower glass content compositions, particularly the 100/0% PETE, do not begin to show weight loss until about ca 160°C. This identical behavior between the stepwise DSC's T_g and the TGA weight loss data lends further support to the proposed structural model. Inspection of the 100°C and the 200°C treated PETE's TGA results also display this similar behavior, but the weight loss associated with the sol-gel reaction is much less, which is to be expected since the thermally cured pomosils have already completed much of the sol-gel reaction.

Further confirmation of the last statement is seen when the TGA results are analyzed as a function of the cure temperature (see Figures 55-58). In this set of data, it is evident that the weight loss decreases as a function of the cure temperature for a particular glass composition. Also, the data reflects the earlier findings that the higher glass content pomosils are more sensitive to temperature than the lower glass content species even after thermal treatment. Realistically, this is always true because the higher glass content PETE glasses have a greater number of sol-gel reactions taking place during the temperature scan. In addition to these findings, the TGA results also reflect the thermal stability of the PETE glasses. In all of the glass compositions, the PEK oligomer seems to withstand temperatures up to ca 550°C under atmospheric conditions before degradation begins occur.

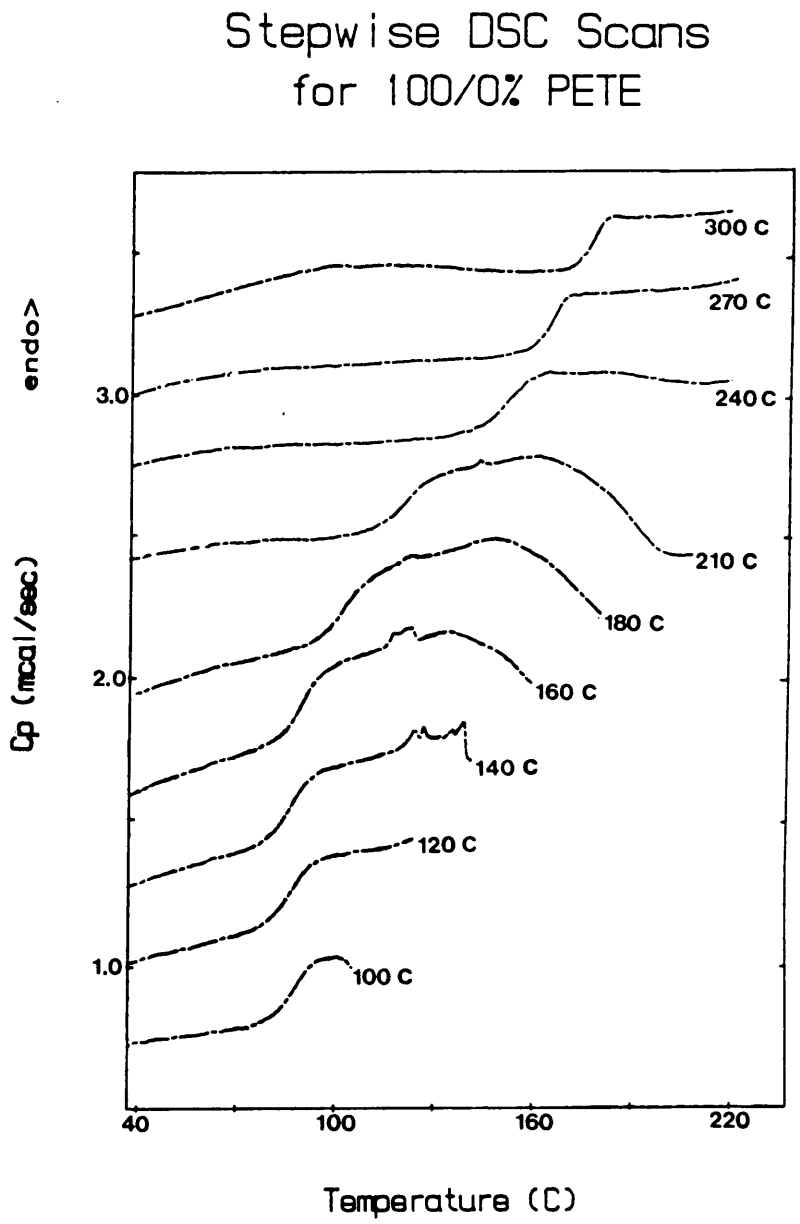

Figure 47. Stepwise DSC scans of 100/0% PETE.

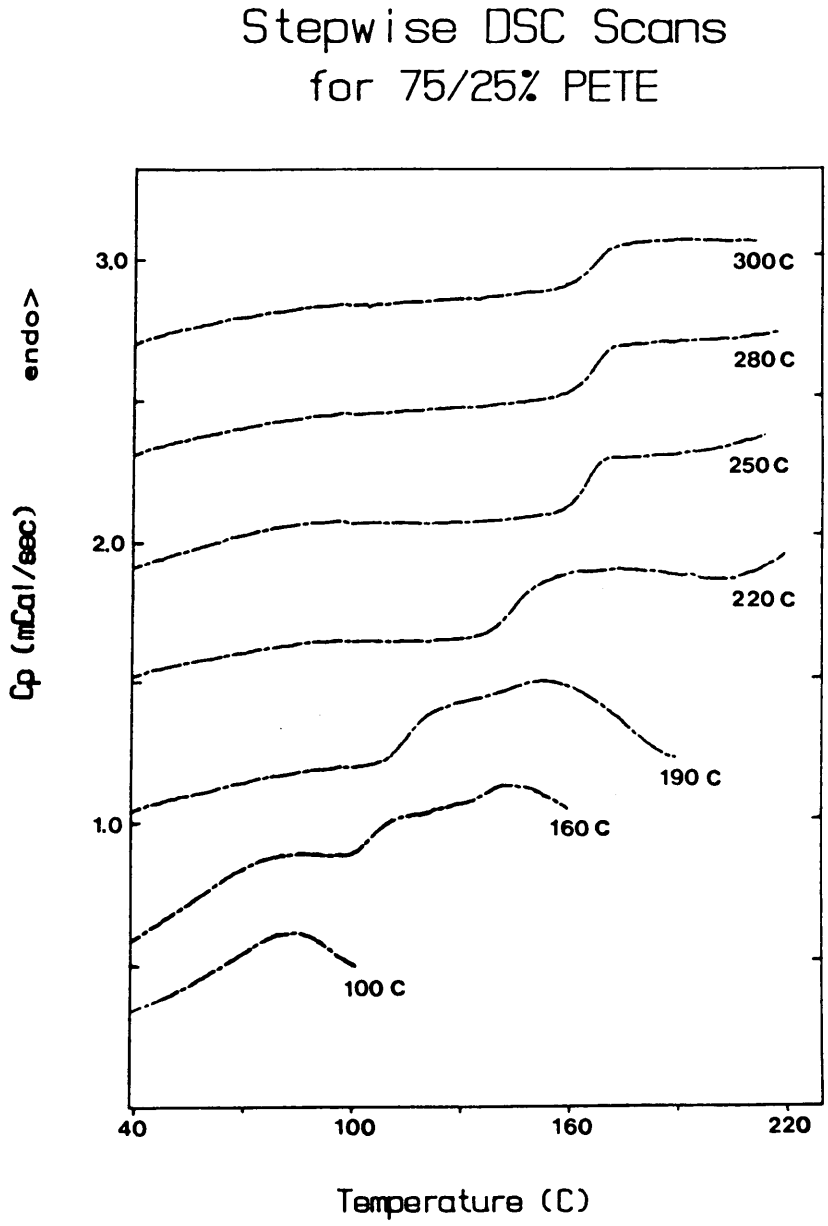

Figure 48. Stepwise DSC scans of 75/25% PETE.

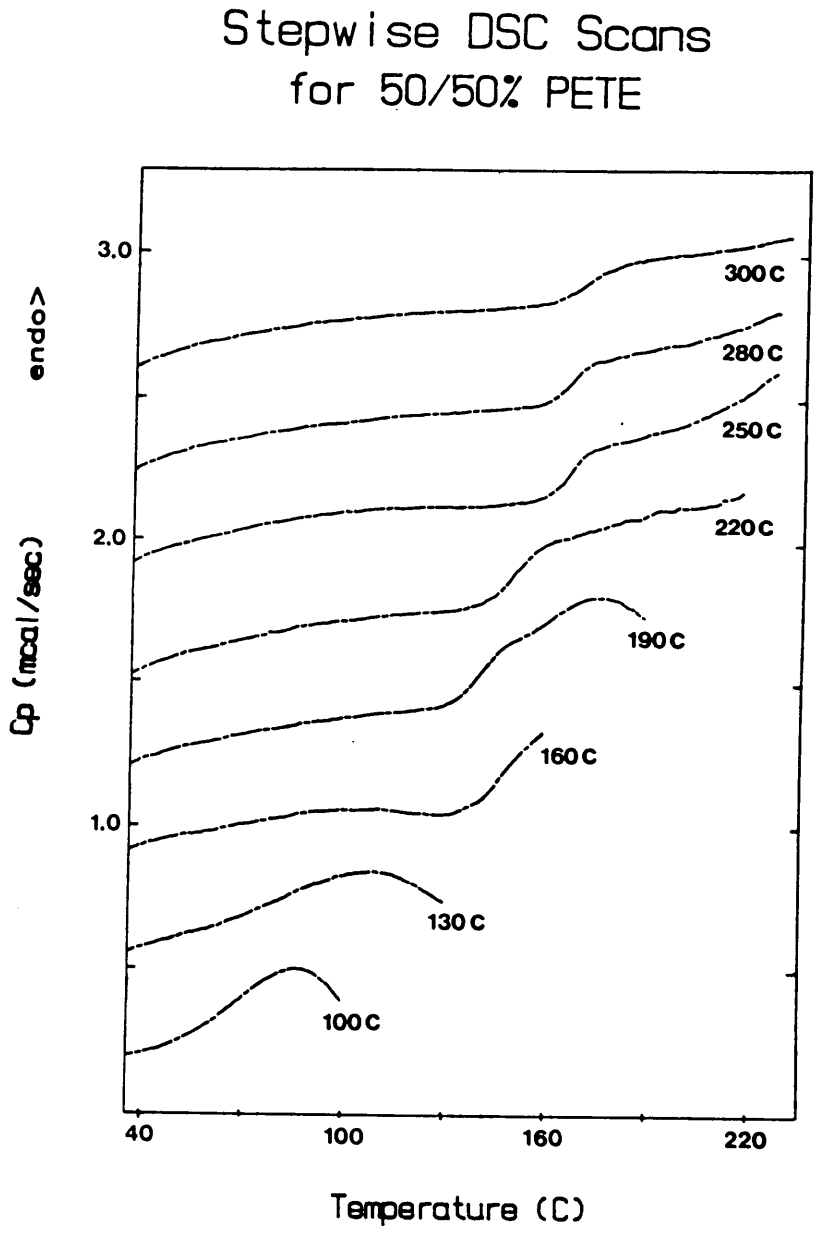

Figure 49. Stepwise DSC scans of 50/50% PETE.

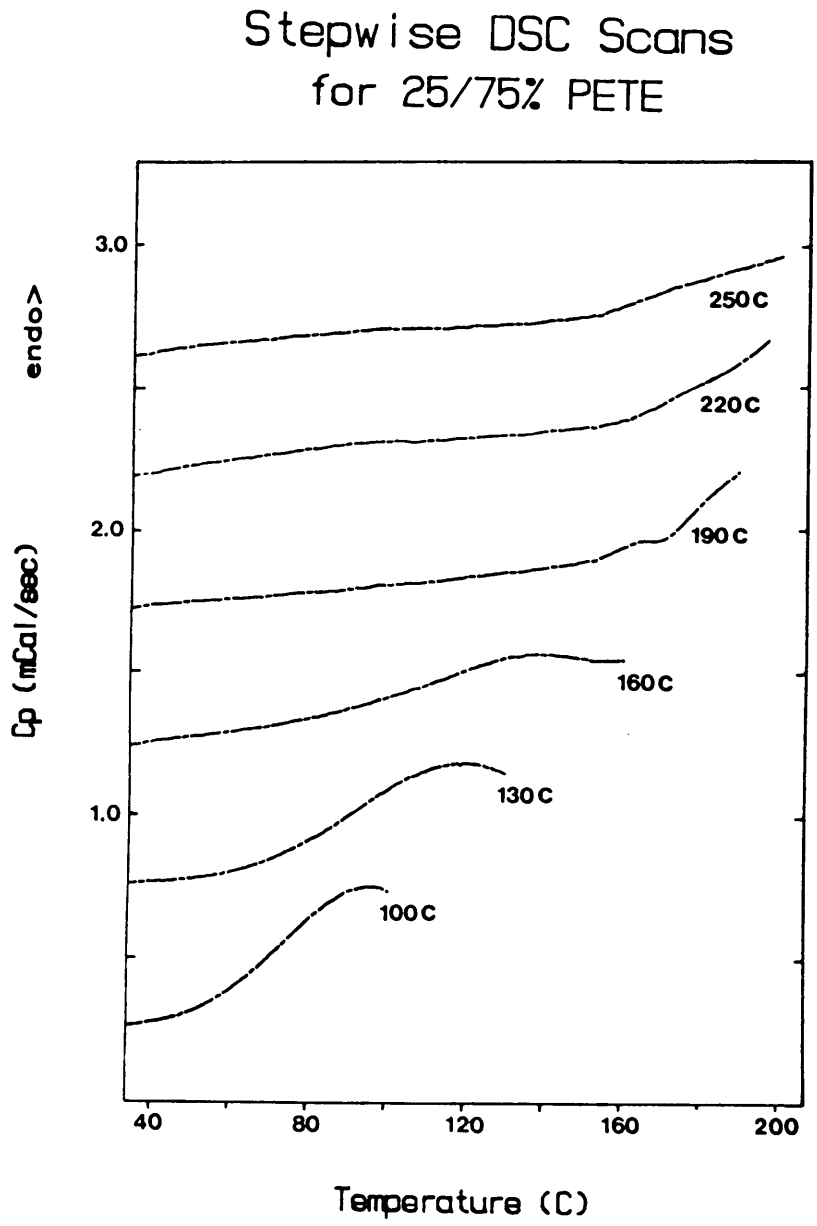

Figure 50. Stepwise DSC scans of 25/75% PETE.

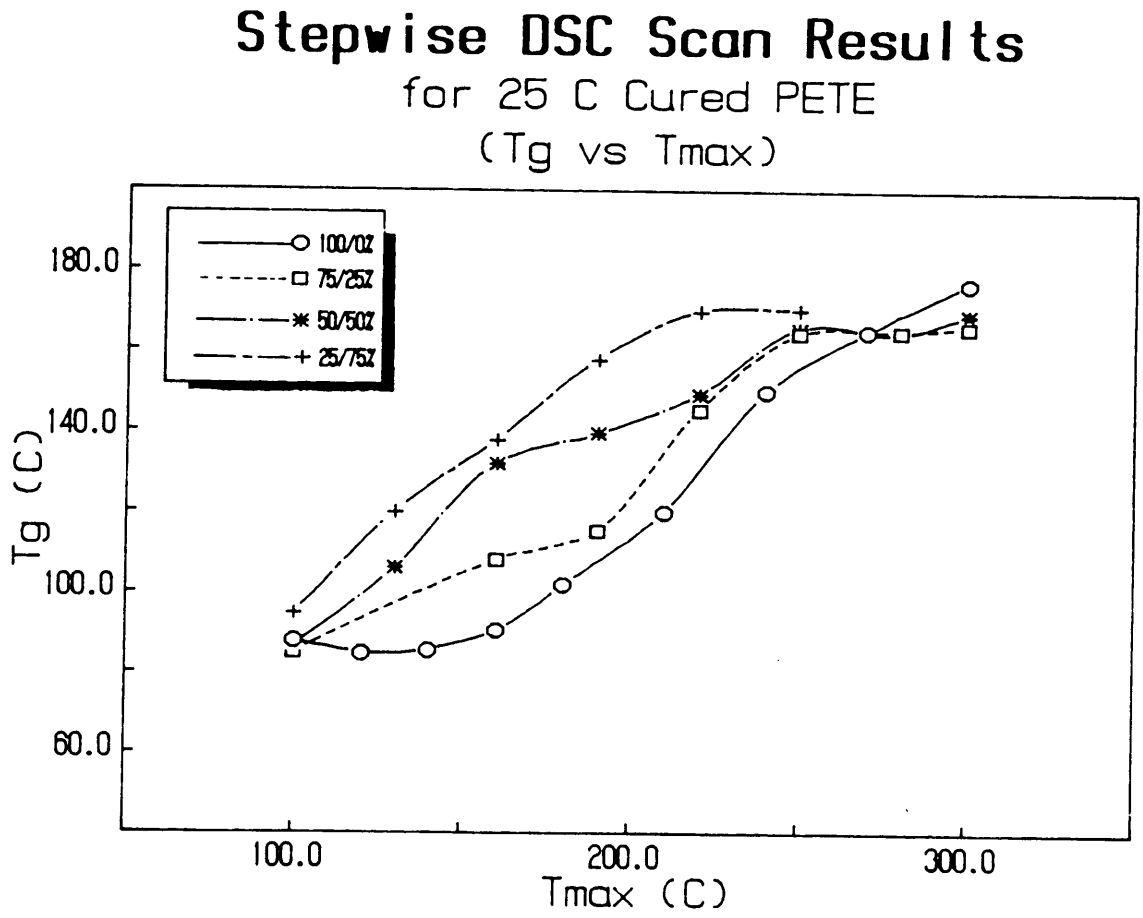

Figure 51. Stepwise DSC results for 25°C cured PETE.

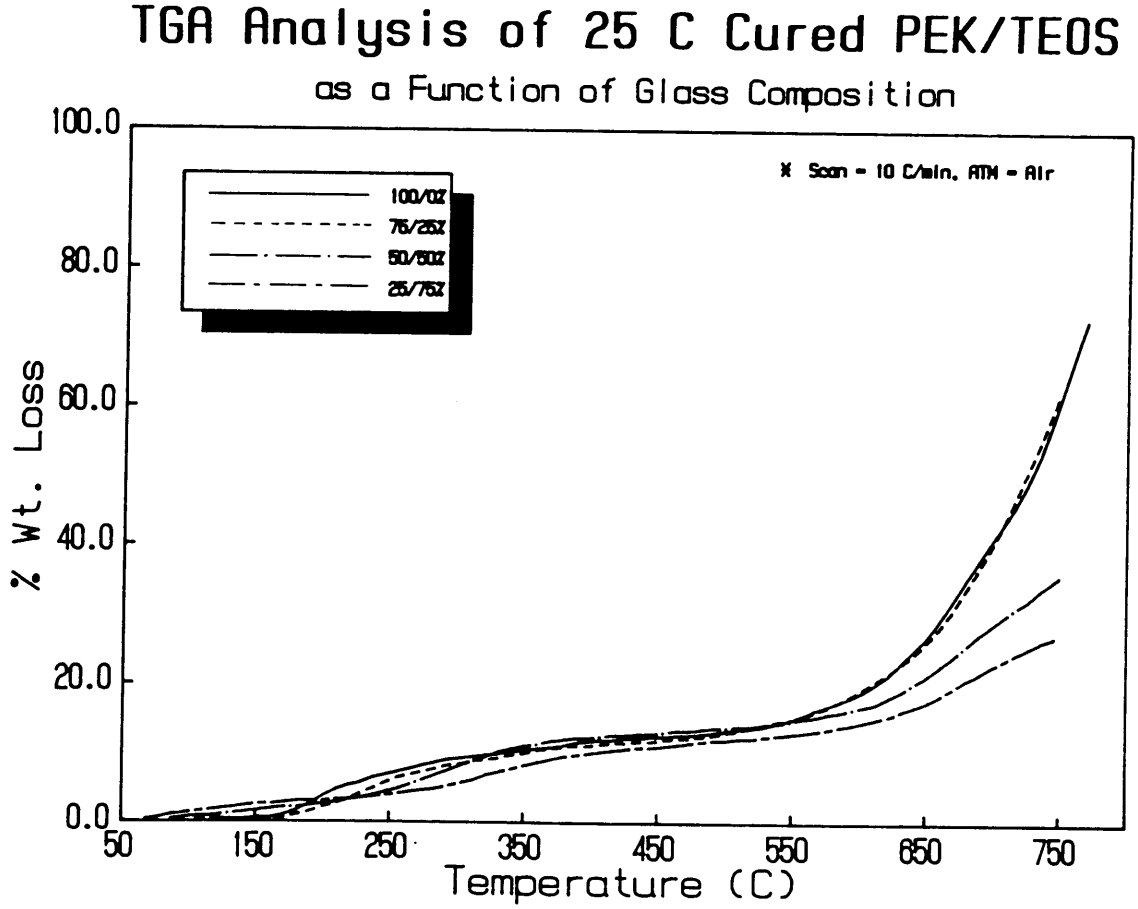

Figure 52. TGA analysis for 25°C cured PETE as a function of glass composition.

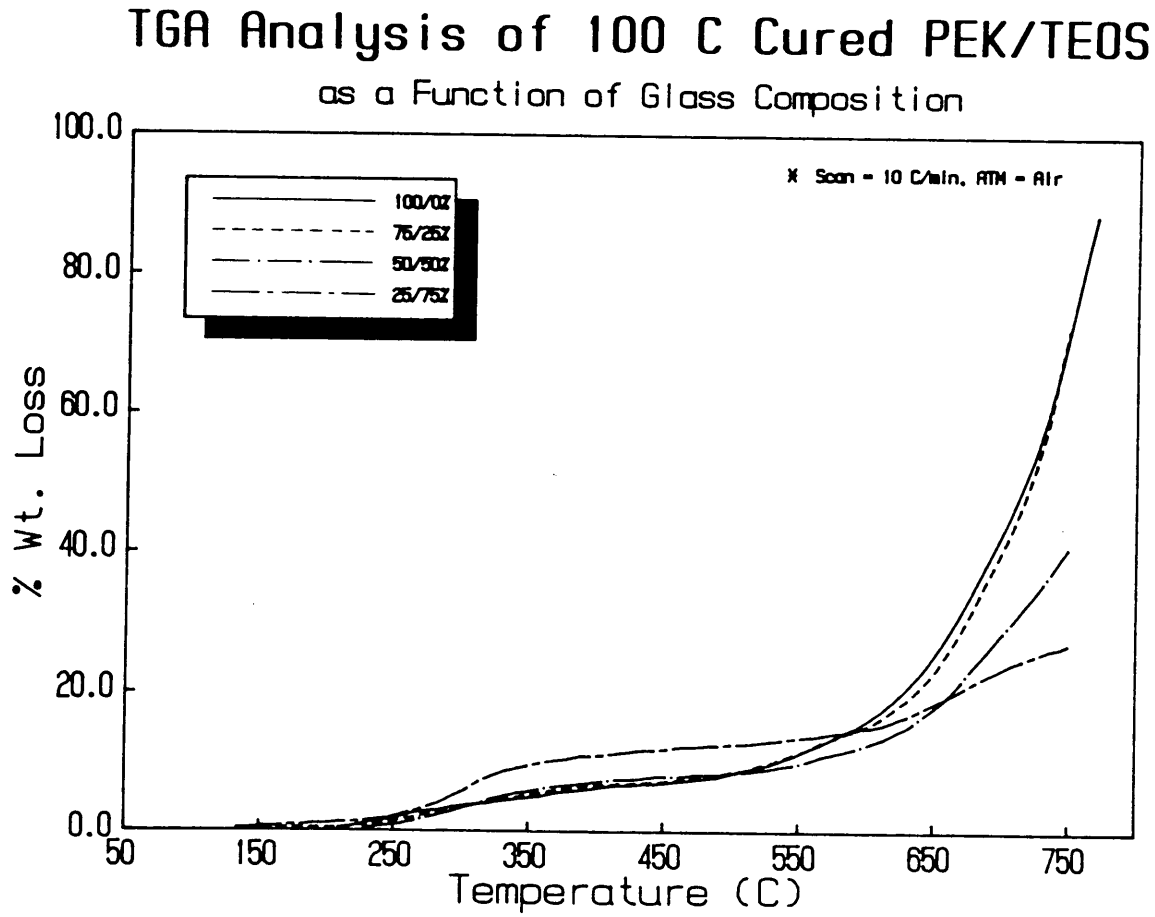

Figure 53. TGA analysis of 100°C cured PETE as a function of glass composition.

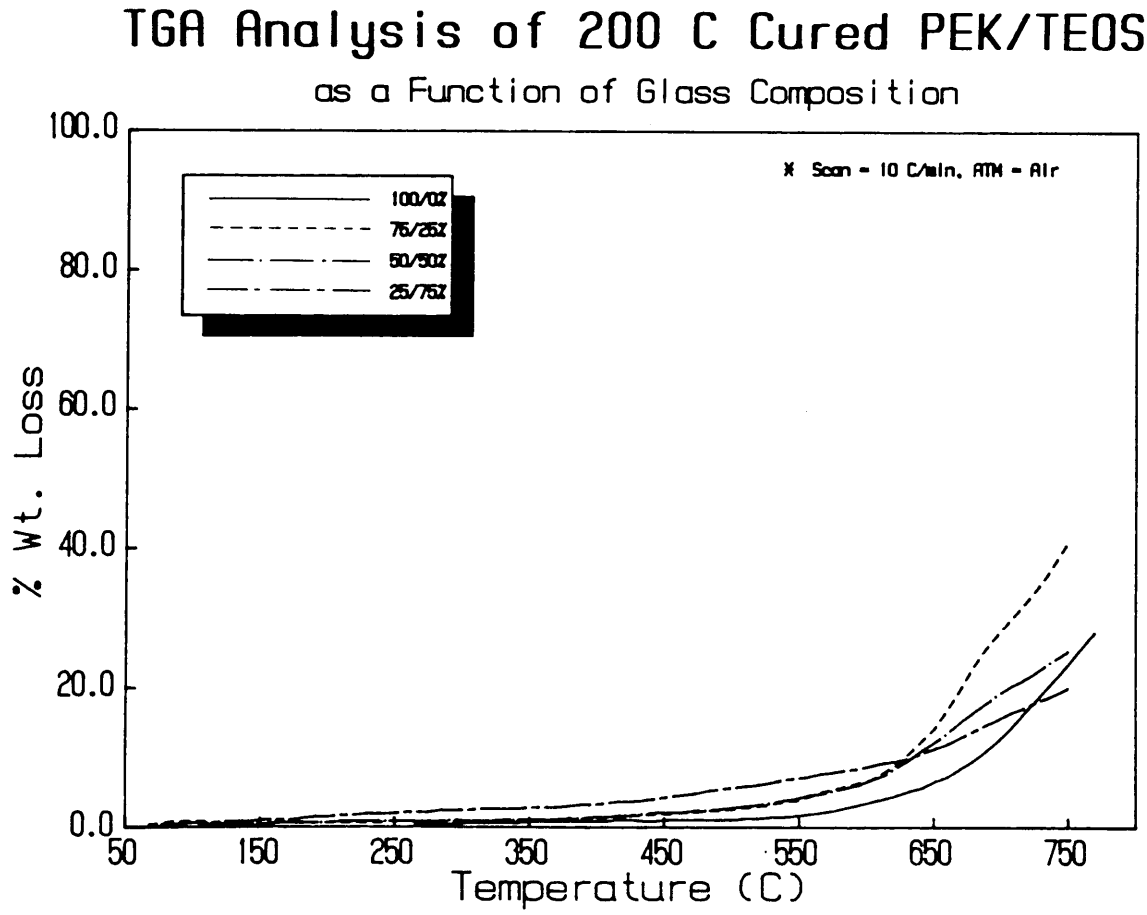

Figure 54. TGA analysis of 200°C cured PETE as a function of glass composition.

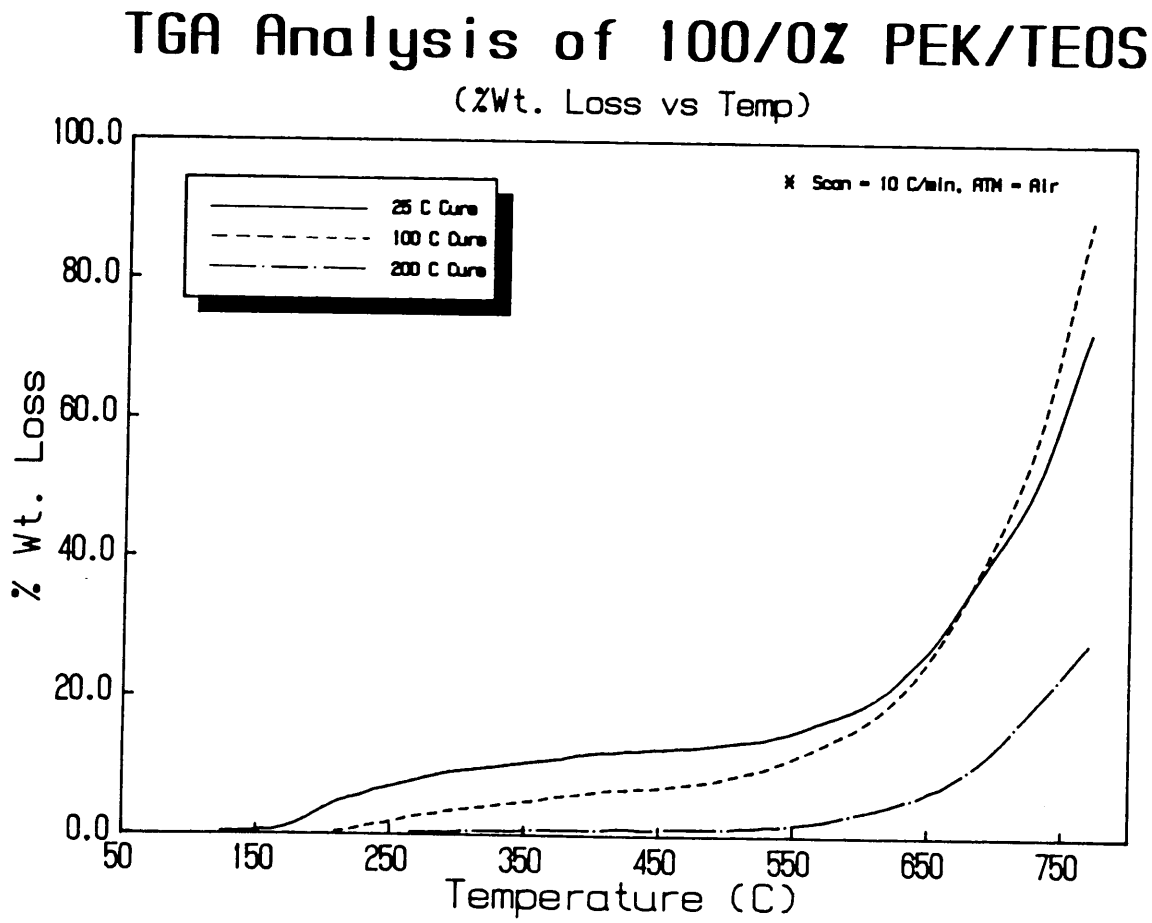

Figure 55. TGA analysis of 100/0% PETE as a function of cure temperature.

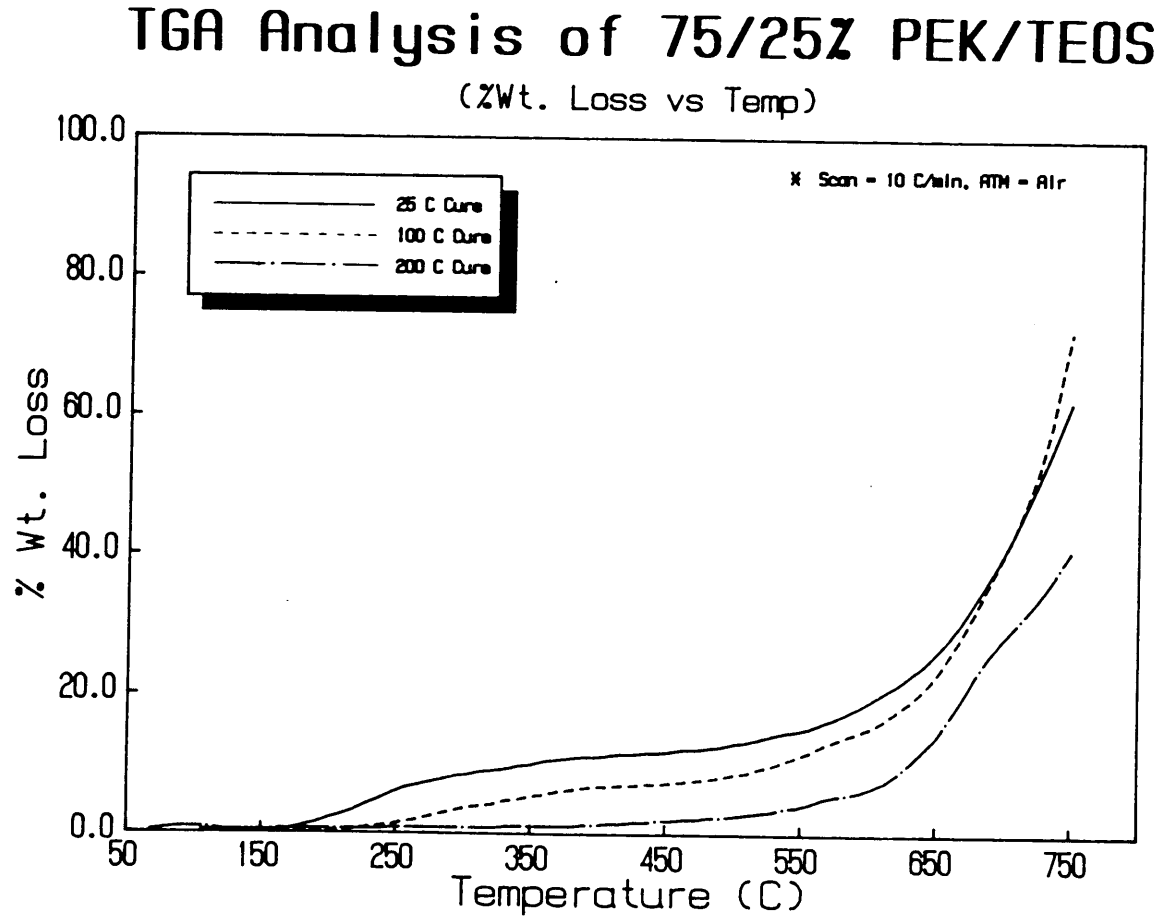

Figure 56. TGA analysis of 75/25% PETE as a function of cure temperature.

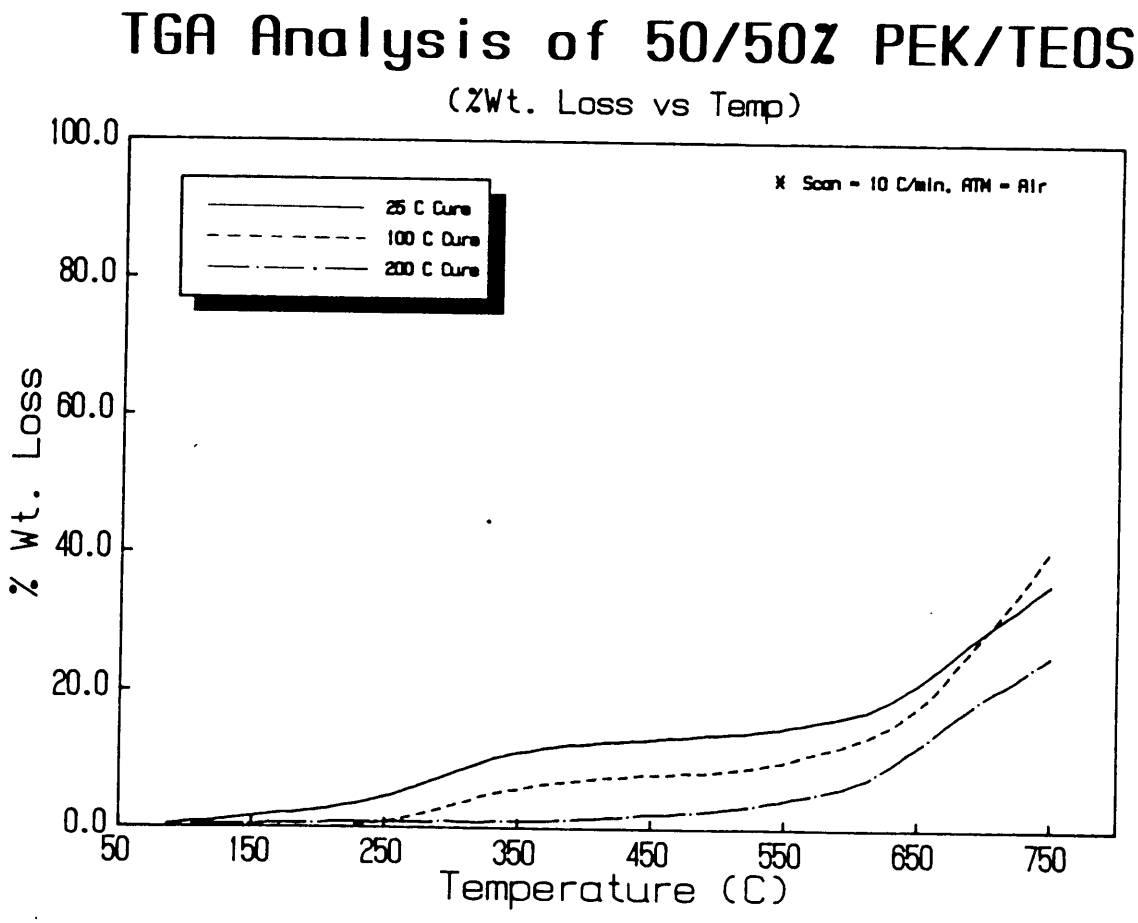

Figure 57. TGA analysis of 50/50% PETE as a function of cure temperature.

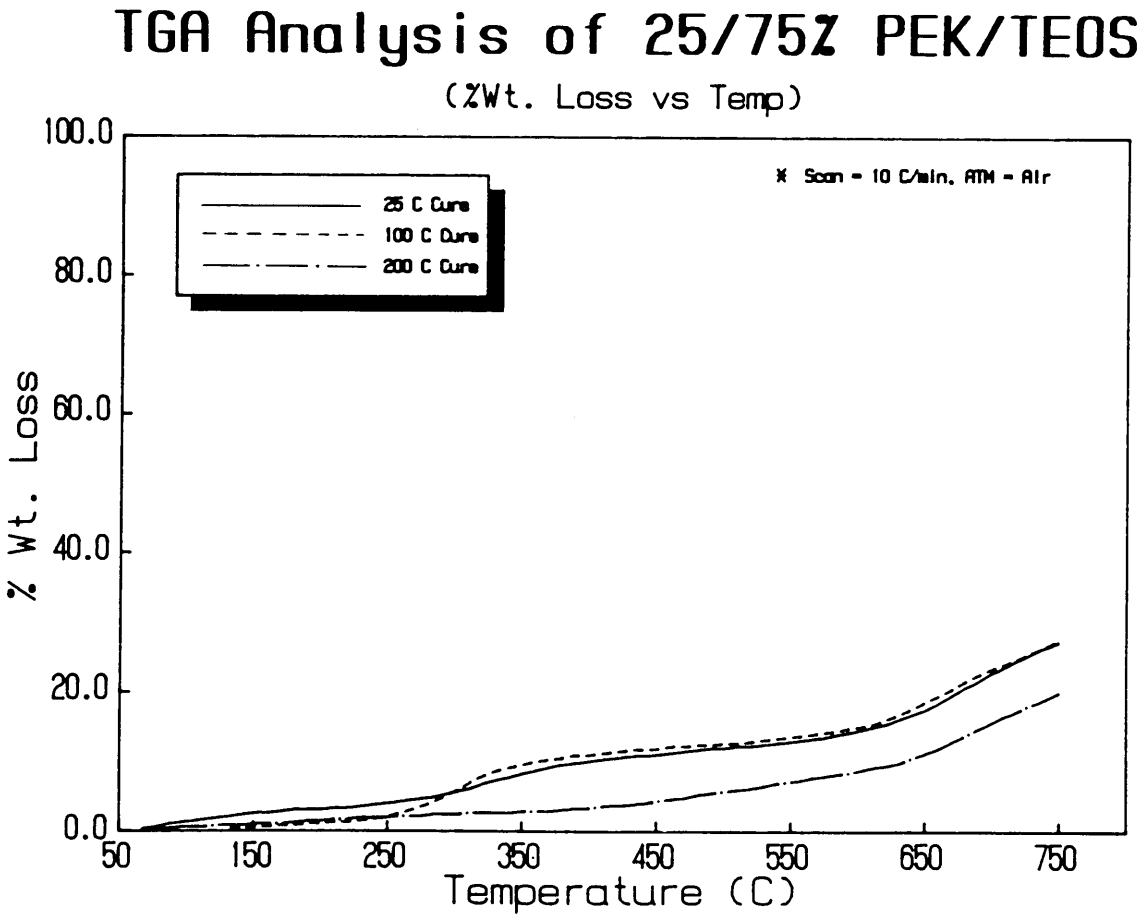

Figure 58. TGA analysis of 25/75% PETE as a function of cure temperature.

In the final experimental set, stagewise DSC T_g measurements were performed to additionally substantiate the earlier observed kinetic behavior found in the stepwise DSC technique. The experimental method first utilizes isothermal heating stages to introduce the designated sample thermal history, and then determines the effect of this treatment on the pomosil T_g Thus, if this experimental method is carried out using a limited selection of the stepwise DSC Tmax's, the stagewise DSC measurements of the PETE glasses should reflect a T_g consistent with the earlier stepwise DSC experiments. In addition to this analysis, the hold time at which the material remains during the thermal treatment is investigated to provide an indication of the curing rates (rate of crosslinking) of the pomosils under these different temperature conditions.

On the whole, the T_g's found by the stagewise DSC measurements are not consistent with those T_g measurements determined by the stepwise DSC technique. Specifically, the PETE T_g's found by this method are higher for the 100/0% , 75/25% , and 50/50% compositions, and lower for the 25/75% glass (see Figures 59-62). Even though these values by comparison are somewhat different, the relative magnitudes of the T_g lie within the experimental error ($\pm 7^{\circ}C$), and typically reflect the same temperature sensitivity as the TEOS content of the PETE is increased. In view of the curing kinetics, it appears that nearly all of the additional crosslinking occurs within the first 5 minutes of the thermal treatment. After this time, the rate of crosslinking slows considerably and assumes a linear relationship, which is especially evident in the higher temperature thermal treatments.

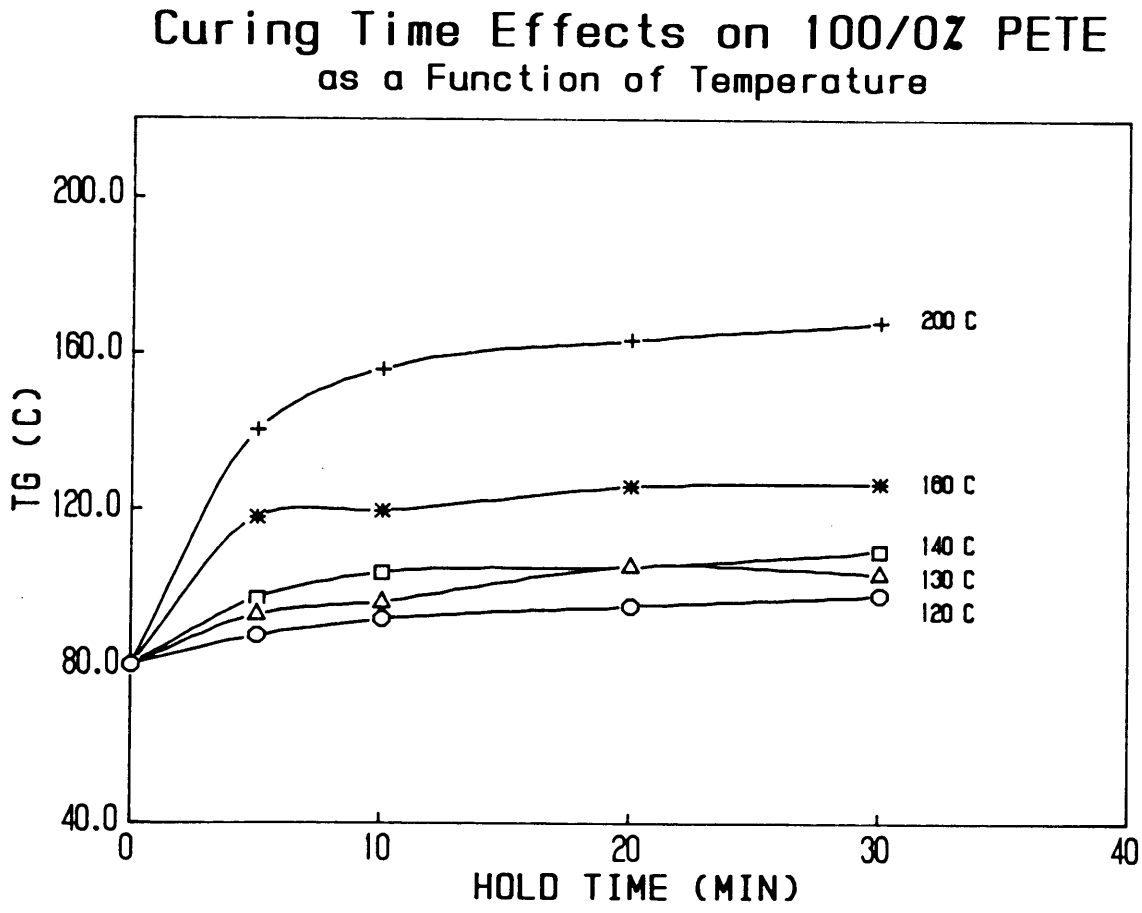

Figure 59. **Stagewise DSC results of 100/0% PETE as a function of curing** temperature and hold time.

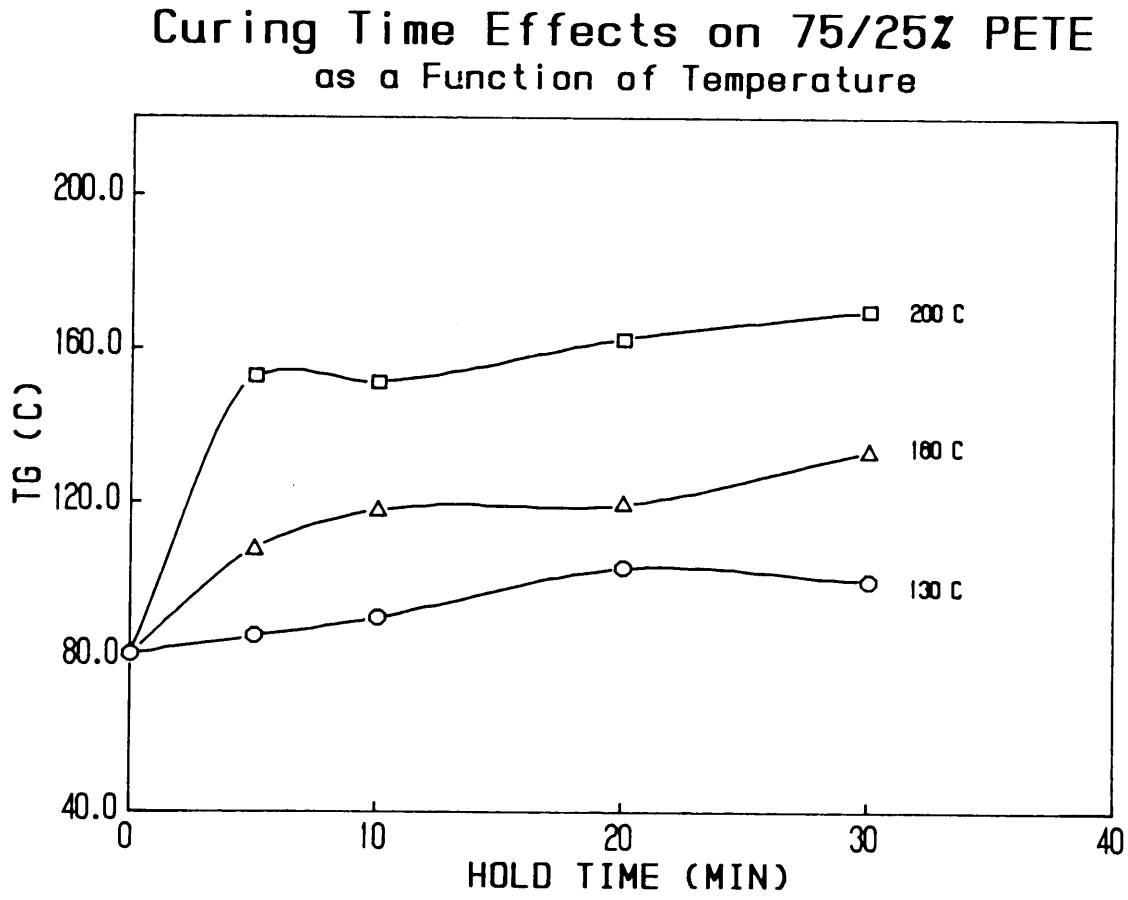

Figure 60. **Stagewise DSC results of 75/25% PETE as a function of curing** temperature and hold time.

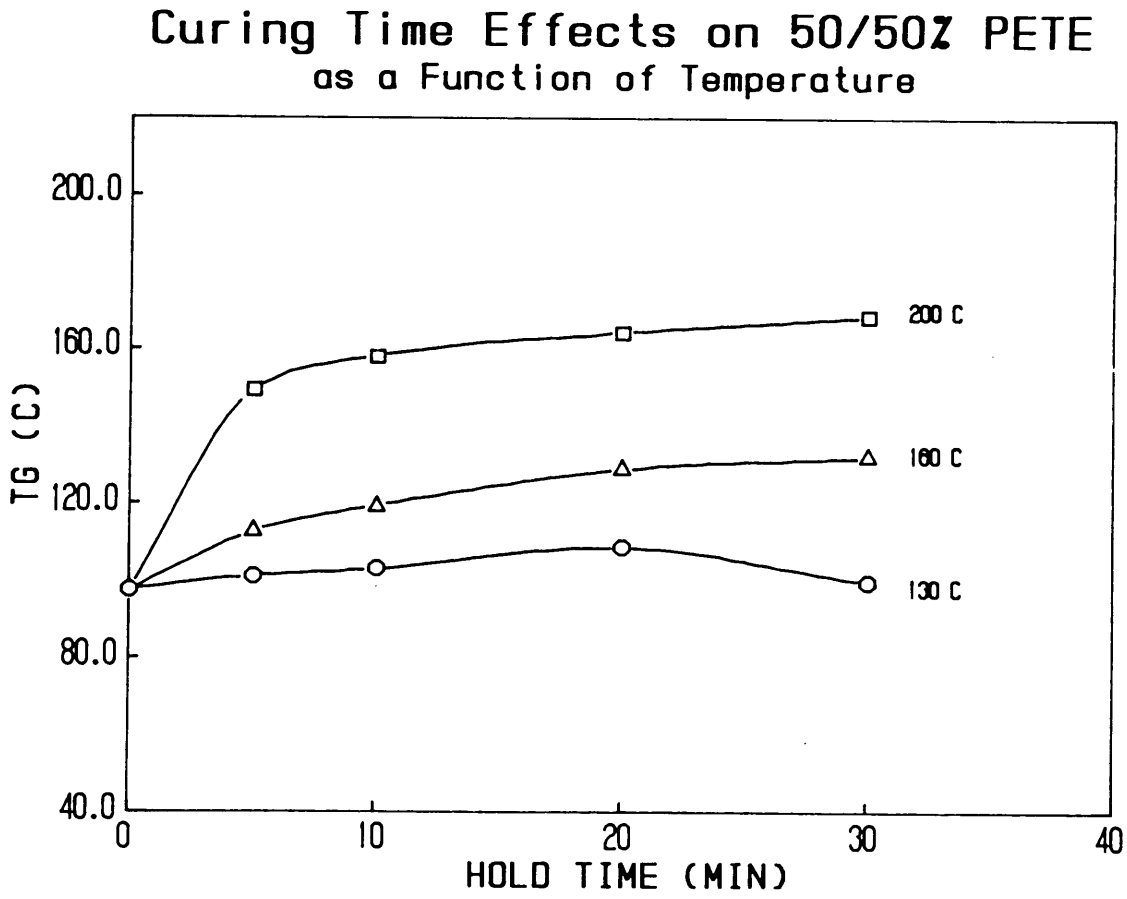

Figure 61. **Stagewise DSC results of 50/50% PETE as a function of curing** temperature and hold time.

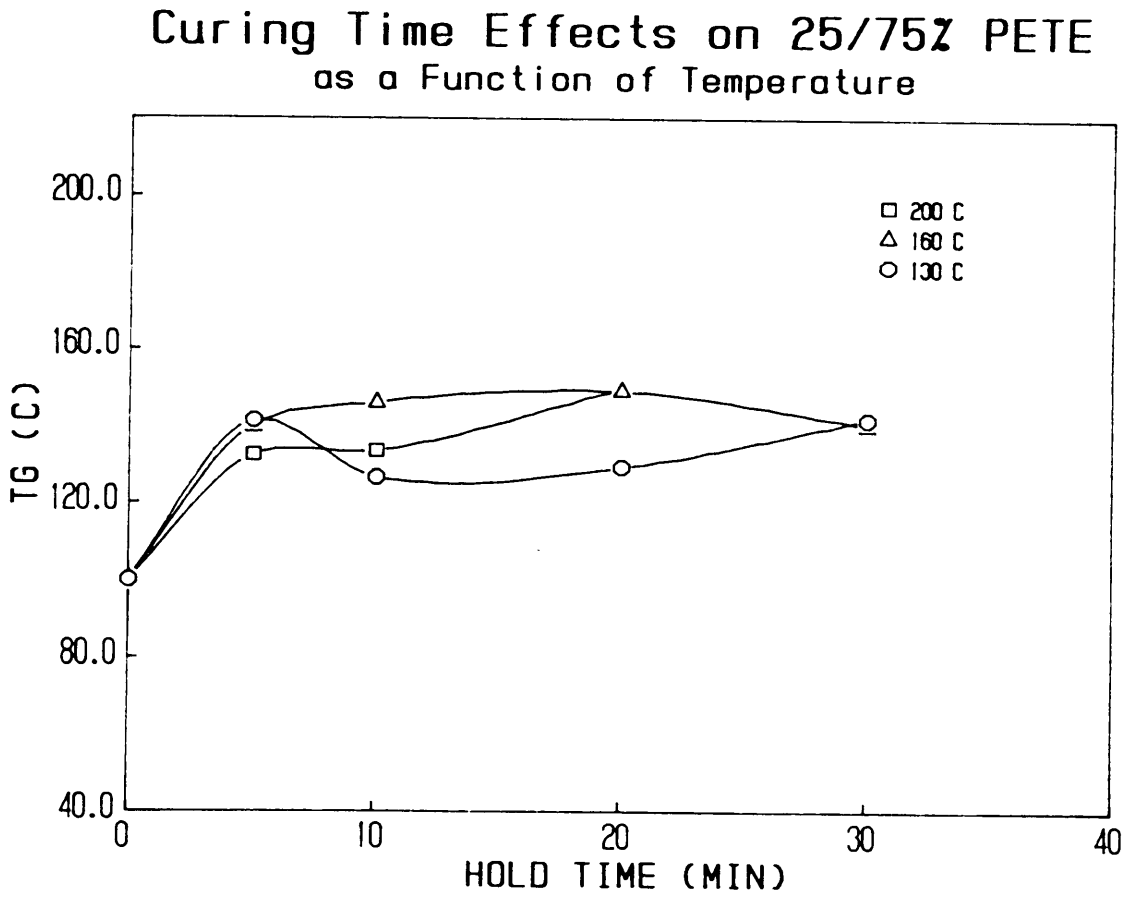

Figure 62. **Stagewise DSC results of 25/75% PETE as a function of curing** temperature and hold time.

5.0 Conclusions

In summary, the development of pomosil glasses with an inorganic-organic matrix structure has been successfully achieved using the endcapped PEK oligomer and TEOS starting components, and the outlined sol-gel reaction procedures. These experimental methods have been shown to form monolithic and crack free materials with variable physical properties depending on the TEOS content employed in the initial reaction mixture. Furthermore, thermally treating the PETE glasses at 100°C and 200°C results in a substantial change in the mechanical and structural nature of these materials.

The first important point that should be recognized concerns the isocyanate endcapping reaction chemistry. This synthesis scheme has been proven to be a viable method of reactively functionalizing the PEK oligomer for use as an organic precursor in the inorganic sol-gel reaction. The newly formed urea linkages, whose stability is questionable at times, has remained unaffected by the acidic hydrolysis medium and the thermal treatments. Thus, the relatively weak inorganic-organic covalent interface has served adequately in the development of the PETE pomosil glasses. Additionally, this technique has been shown to be quite versatile in its ability to prepare organically reactive sol-gel starting materials. Both elastomeric (20-22) and glassy polymeric materials have been successfully incorporated into TEOS based networks by this method.

In the sol-gel reaction involving the PEK oligomer, it has been found that a vitrification problem exists, especially in the lower TEOS content compositions, which limits the degree of network formation attained. This last artifact has been attributed to the diffusional and/or kinetic restrictions imposed on the alkoxy endgroups by the glassy state of the PEK oligomer.

By subjecting the pomosils to 100°C and 200°C thermal treatments, the majority of these barriers are overcome, and the sol-gel reaction proceeds to form a more complete network structure. DSC measurements have indicated this continuing network development by revealing an orderly increase in the PETE T_g. Other methods such as dynamic mechanical, IR, TGA, mechanical, and SAXS techniques have also confirmed this behavior. In short, the implementation of the thermal treatments has been a necessity in establishing a well constructed inorganic-organic network using the glassy PEK polymer.

From a kinetic viewpoint, the extent and rate of chemical curing occurring (network formation) in the PETE pomosils has been found to be significantly influenced by the amount of TEOS present and the temperature of the thermal treatment applied. Typically, the higher the glass content of the PETE glass and the higher the temperature of the thermal treatment, the greater the level of network formation in the final glass structure. Furthermore as the TEOS content is increased, the temperature sensitivity of the chemical curing is increased. In other words, the higher glass content pomosils require a lower temperature of thermal treatment to achieve a satisfactory degree of network formation. Also, much of the sol-gel reaction occurring during the thermal treatments has been shown to develop quite rapidly (i.e., within the first 5 minutes).

In conclusion, the experimental procedure utilized has been found to form monolithic bulk materials that have combined organic and inorganic components to produce a hybrid network structure. To my knowledge, this is one of the first studies undertaken to actually try to incorporate a polymer that is below its T_g at ambient into a sol-gel derived matrix. The benefit of using the glassy PEK in the PETE material is that this pomosil has unique physical and mechanical properties that may be of commercial interests. As a thin film coating cast on a certain substrate (i.e., glass, wood, metal, etc.), the PETE glass may find use as a protective coating that may provide good weather, abrasion, and scratch resistance.

6.0 Recomendations for Future Study

One important aspect in this research that has been mentioned repeatedly, but no quantitative data has been presented deals with the extent of the reaction of the sol-gel mechanism. In all the work thus far, the extent has been qualitatively described as increasing with the cure temperature by following measurable properties associated with the furthering of the network formation. Only the IR technique has shown from a molecular standpoint that the degree or extent of the sol-gel reaction has increased relatively with respect to the temperature of thermal treatment, but still these measurements have no quantitative bearing on the actual extent of reaction. In order to get a handle on this problem, Raman and Si-NMR (solid state and solution) spectroscopies would most likely have to be utilized. Both of the techniques can focus on the silicon alkoxide unreacted functional groups and can monitor their disappearance during the course of the sol-gel reaction and after the thermal treatments. Also, these methods can follow the development of the ≡Si-O-Si≡ matrix and predict the degree of substitution of the silicon matrix site, which then can be directly correlated to the extent of the sol-gel reaction.

Two other points of interest that could be further investigated, but may be of minor importance, is the affect of the PETE molecular weight and the chemical aging of the pomosil glasses with time. Since only one molecular weight has been studied, a selection of different chain length oligomers, preferably low molecular weight materials, may reflect some new mechanical and structural trends. Furthermore with the lower molecular weight PEK, the sol-gel reaction parameters, such as the acid and water content, may have a more significant effect on the final properties of the glass. In the present system, the reaction variables play

a minor role because of the low concentration of the alkoxy silane endgroups in comparison with the mass of the PEK oligomer. In addition to this investigation, the chemical aging could be recorded to ascertain any significant changes in the mechanical and structural properties can be noted. Already in Wilkes et al.'s work with the TEOS/PTMO systems (22), this aging phenomena has been shown to have considerable effect on the mechanical behavior of these materials. From a commercial and industrial standpoint, this type of long term experimentation would ultimately determine whether the pomosil glass is suitable for certain application areas.

Finally on a broad scale, other endcapping routes and organic starting materials could be used to prepare a variety of pomosil glasses with desirable mechanical properties. One particular endcapping procedure that has been previously employed by Mark et al. (14) involves the hydrosilylation addition of trialkoxysilane to a vinyl terminated monomer or oligomer to form the organically reactive sol-gel precursors. A shortcoming of this method is that the experimental synthesis method requires careful direction and a specially prepared platinum based catalyst to successfully achieve a desirable extent of reaction. Even though this technique has inherent problems, it does offer improved chemical and thermal stability over the isocyanate reaction procedure, since this reaction constructs an inorganic-organic covalent interface with a strong silicon carbide bond. One class of materials that may be endcapped by this technique is the Sartomer diacrylates produced by ARCO. A few of these materials have already been used in some instances as transparent scratch and abrasion resistant coatings. Thus, if the mechanical nature of the coatings can be improved by the addition of the TEOS through the sol-gel mechanism (i.e., better scratch resistance and optical properties), then these new hybrid material may have commercial potential as glazing compounds.

References

1. S. Sakka, ***Journal of Non Crystalline Solids*** , 73 (1985), 660.
2. S. Sakka, ***Journal of Non Crystalline Solids***, 48 (1982), 31.
3. S. Sakka, K. Kamiya, ***Journal of Non Crystalline Solids***, 42 (1980), 403.
4. B.E. Yoldas, ***Journal of Non Crystalline Solids***, 83 (1986), 375.
5. B.E. Yoldas, ***Journal of Non Crystalline Solids***, 61 (1982), 105.
6. B.E. Yoldas, ***Journal of Non Crystalline Solids***, 63 (1984), 145.
7. B.E. Yoldas, ***Journal of Non Crystalline Solids***, 82 (1986), 11.
8. R. Aelion, A Loebel, F. Eirich, ***Journal of American Chemical Society***, 72 (1950), 5705.
9. C.J. Brinker, K.D. Keefer, D.W. Schaefer, R.A. Assink, B.D. Kay, C.S. Asheley,***Journal of Non Crystalline Solids***, 63 (1984), 45.
10. C.J. Brinker, K.D. Deefer, D.W. Schaefer, C.S. Ashely, ***Journal of Non Crystalline Solids***, 48(1982), 47.
11. J.C. Pouxviel, J.P. Boilot, J.C. Beloeil, J.Y. Lallemand, ***Journal of Non Crystalline Solids***, 89 (1987), 245.
12. J.E. Mark, ***Markromol. Chem.***, 185 (1984), 2609.
13. M.Y. Tang, J.E. Mark, ***Macromolecules***, 17 (1984), 2616.
14. G.S. Sur, J.E. Mark ***Eur. Polym. J.***, 21 (1985), 1051.
15. J.E. Mark, S.-J. Pan, ***Makromol. Chem. Rapid Commun.***, 3 (1982) 681.
16. G. Philipp, H. Schmidt, ***Journal of Non Crystalline Solids***, 63 (1984), 283.
17. H. Schmidt, ***Journal of Non Crystalline Solids***, 73 (1985), 681.
18. G. Philipp, H. Schmidt, ***Journal of Non Crystalline Solids***, 82 (1986), 31.
19. H. Schmidt, H. Scholze, G. Tunker, ***Journal of Non Crystalline Solids***, 80 (1986), 557.
20. G.L Wilkes, B. Orler, H. Huang, ***Polym. Prep.***, 26 (1985), 300.
21. H. Huang, B. Orler, G.L. Wilkes, ***Polym. Prep.***, 14 (1985) , 557.
22. H. Huang, R.H. Glaser, G.L. Wilkers, to be published.

23. L.V. Kelts, N.J. Effinger, S.M. Mel Polder, ***Journal of Non Crystalline Solids***, 83 (1986), 353.

24. D.W. Schaefer, K.D. Keefer, in "Better Ceramics Through Chemistry," Materials Research Society Symposi Proceedings, Vol 32, edited by C.J. Brinker, D.E. Clark, D.R. Ulrich (North-Holland : New York), 1986.

25. A. Craievich, ***Journal of Non Crystalline Solids***, 86 (1986), 394.

26. P. Meakin, ***Phys. Rev. Lett.***, 51 (1983), 119.

27. M. Kolb, R. Jullien, ***Phys. Rev. Lett.***, 51 (1983), 1123.

28. C. Okkerse, in "Physical and Chemical Aspects of Adsorbents and Catalysts", edited by G.G. Linsen (Academic Press : New York), 1970.

29. Ralph K. Iler, "The Chemistry of Silica", (John Wiley & Sons : New York), 1979.

30. T.W. Zerda, I. Artaki, J. Jonas, ***Journal of Non Crystalline Solids***, 81 (1986), 365.

31. A. Duran, C. Serna, V. Fornes, J.M. Fernandaz Navarro, ***Journal of Non Crystalline Solids***, 82 (1986), 69.

32. I. Artaki, T.W. Zerda, J. Jonas, ***Journal of Non Crystalline Solids***, 81 (1986), 381.

33. L.L. Hench, in "Better Ceramics Through Chemistry", Material Research Society Symposia Proceedings, Vol. 32, edited by C.J. Brinker, D.E. Clark, D.R. Ulrich (North-Holland : New York), 1986.

34. A. Bertoluzza, C. Fagnano, M. Morrelli, ***Journal of Non Crystalline Solids***, 48 (1982), 197.

35. V. Gottardi, M. Guglielmi, ***Journal of Non Crystalline Solids***, 63 (1984), 71.

36. H. Dislich, ***Journal of Non Crystalline Solids***, 73 (1985), 599.

37. H. Schmidt, ***Mate. Res. Soc. Symp.***, 32 (1984), 327.

38. H. Schmidt, O.v. Stetten, G. Kellermann, H. Patzelt, W. Naegele, Proc. Radioimmunoassay and Related Procedures in Medicine, Vienna (1982), p. 111.

39. C.S. Parkhurst, W.F. Doyle, L.A. Silverman, S. Singh, M.P. Anderson, D. McClurg, G.E. Wnek, D.R. Uhlmann, ***Mate. Res. Soc. Symp. Proc.*** 73 (1986), 769.

40. J.S. Riffle, J.E. Mcgrath, J.P. Pullockaren, S. Kilic, C.S. Elsbernd, to be published.

41. G. Wilkinson, F.G.A. Stone, E.W. Abel, "Comprehensive Organometallic Chemistry" 1st ed., (Pergamon Press : New York), 1982.

42. C. Hepburn, "Polyurethane Elastomers", (Applied Science Publishers : New York), 1982.

43. J.E. McGrath, D.K. Mohanty, S. Kilic, to be published.

44. J.K. Gillham, ***Polym. Engr. and Science***, 16 (1976), 353.

45. A.L Smith, "Analysis of Silicones", (Robert E. Krieger Publishing Co. : Florida), 1983.

46. J.W. Van Bogart, "Structure-Property Relationships in Segmented Elastomers: Small Angle X-ray Scattering, Thermal, and Mechanical Studies", (University Microfilms International : Ann Arbor, MI), 1981.

47. T.E. Attwood, et.al., ***Polymer***, 22 (1981), 1096.

48. D.R. Rueda, et.al., ***Polym. Comm.***, 24 (1983), 258.

Appendix A. Calculation of PEK End to End Length

PEK (endcapped with isocyanatopropyltriethoxysilane)

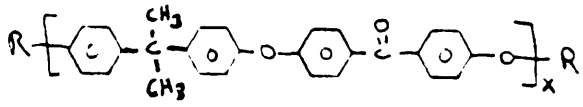

$Mn \cong 4{,}370.8$

where

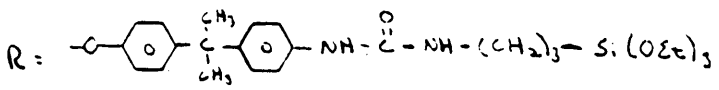

$Mn/_{repeat} = 406.4$

$Mn/_{R} = 461.6$

$$x = \frac{4{,}708.8 - [461.6 - 445.6]}{406.4}$$

$x \cong 8.5$

Assumptions

1. Bond angles

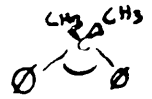

= 110°

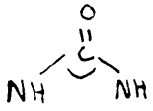

= 120°

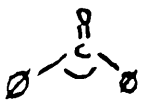

= 124° (47)

= 124° (47)

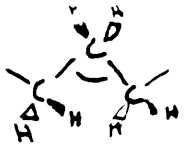

= 110°

2. Bond lengths

φ—O = 1.36Å[48]

φ—C=O = 1.47Å[48]

φ—C = 1.54Å

C—N = 1.47Å

C—C = 1.54Å

C—Si = 1.54 Å

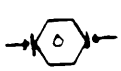

= 2.83Å[48]

3. PEK in the fully extended form should have a trans-planar configuration. However, due to the even number of molecules in the repeat, the chain may have a pseudo trans-helical form and not a trans-planar one. According to this assumption, some bonds would not be in the trans position, but for this approximation all bond configurations are taken as trans for simplifying purposes.

4. The bond angles of the repeat unit are assumed to be approximately be 124° except for the bisphenol-A linkage which has a bond angle of 110° According to this, the 110° angle of the the bis-A unit will be dominant bond angle in the repeat unit, and it will be chosen as the reference angle that projects the chain length along the z axis.

Outline of Calculation

1. Calculate the length of the repeat unit.

2. Project the repeat unit along the z axis to find the total length.

3. Find the length of the endgroups along the z axis and add to the total length found in step 2.

1. Calculation of repeat unit distance along reference axis

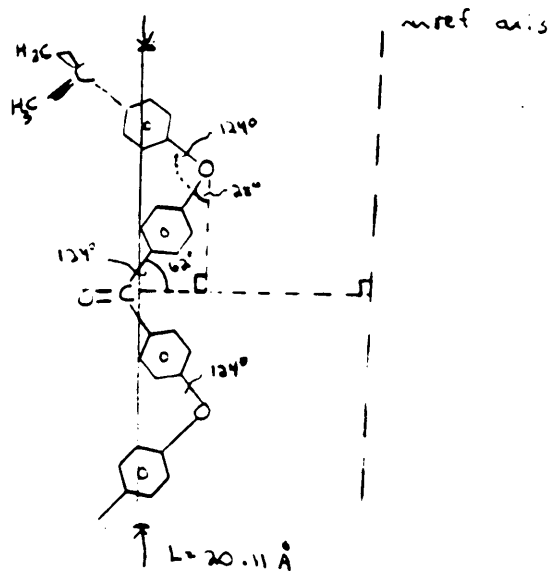

$$L_{repeat} = \cos 28^{\circ}[2(1.54) + 4(2.83) + 4(1.36) + 2(1.47)] = 20.11\text{Å}$$

2. Projection of repeat units along the z axis (not planar configuration)

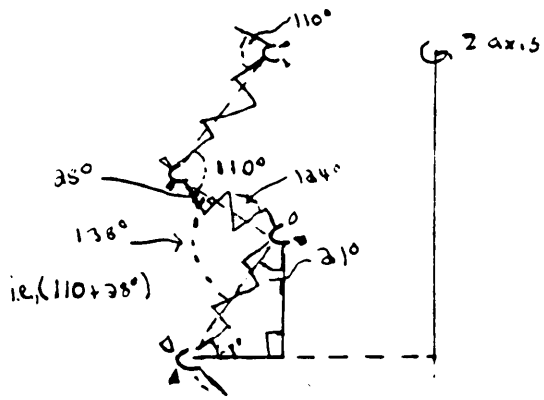

$$L_{repeat} = cos21°(20.11Å) = 18.78Å$$

$$\text{Total } L_{repeat} = 8.5(18.78Å) = 159.63Å$$

3. Calculation of the lengths of the end groups projected along the z axis

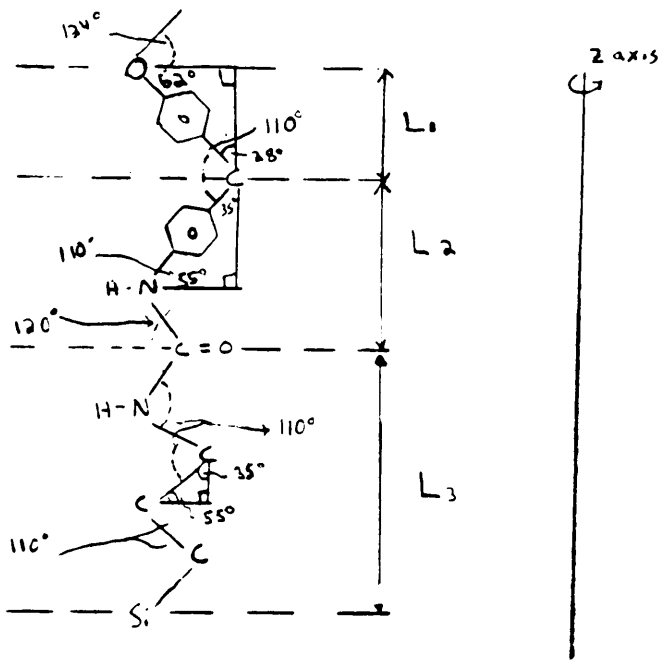

$$L_1 = cos21°[cos28°(1.36 + 2.83 + 1.54)] = 4.72Å$$

$$L_2 = cos35^{\circ}[1.54 + 2.83 + 2(1.47)] = 5.99\text{Å}$$

$$L_3 = cos25^{\circ}[cos35^{\circ}(2(1.47) + 3(1.54))] = 5.61\text{Å}$$

$$L_{end} = L_1 + L_2 + L_3 = (4.72 + 5.99 + 5.61)\text{Å} = 16.32\text{Å}$$

Since one endgroup has one less φ-O bond at the beginning, the total length of the endgroup is found by the following manipulation.

$$\text{Total } L_{end} = 2L_{end} - cos21^{\circ}[cos28^{\circ}(1.36)] = 31.52\text{Å}$$

The final extended chain length is now just the sum of the repeat unit's length plus the endgroups' length.

$$\underset{extended}{\text{Total } L} = \text{Total } L_{end} + \text{Total } L_{repeat} = 31.52\text{Å} + 159.63\text{Å} = 191.15\text{Å}$$

NOTE: Remember that this calculation is only a crude approximation at best, but still it can give a general idea of the order of the length of the endcapped PEK chain is a somewhat extended form.

The vita has been removed from the scanned document